RESOURCE ALLOCATION AND OPTIMIZATION OF MULTI USER COMMUNICATION FOR NEXT GENERATION NETWORK

MUHAMMAD HUSSAIN

02-281151-001

A thesis submitted in fulfillment of the requirements for the award of the degree of Doctor of Philosophy (Electrical Engineering)

DEPARTMENT OF ELECTRICAL ENGINEERING

BAHRIA UNIVERSITY, KARACHI

JANUARY 2023

Approval for Examination

Scholar's Name: Muhammad Hussain Registration No.: 02-281151-001 Program of Study: Doctor of Philosophy (Electrical Engineering) Thesis Title: "Resource Allocation and Optimization of Multiuser Communication for Next Generation Network."

It is to certify that the above scholar's thesis has been completed to my satisfaction and, to my belief, its standard is appropriate for submission for examination. I have also conducted plagiarism test of this thesis using HEC prescribed software and found similarity index 17% that is within the permissible limit set by the HEC for the PhD degree thesis. I have also found the thesis in a format recognized by the BU for the PhD thesis.

Principal Supervisor's Signature:_____ Date: _____

Name: Prof. Dr. Haroon Rasheed

Author's Declaration

I, Muhammad Hussain hereby state that my PhD thesis titled "Resource Allocation and Optimization of Multiuser Communication for Next Generation Network" is my own work and has not been submitted previously by me for taking any degree from this university Bahria University or anywhere else in the country/world.

At any time if my statement is found to be incorrect even after my graduation, the University has the right to withdraw/cancel my PhD degree.

Name of scholar: Muhammad Hussain

Date: _____

Plagiarism Undertaking

I, solemnly declare that research work presented in the thesis titled "Resource Allocation and Optimization of Multiuser Communication for Next Generation Network" is solely my research work with no significant contribution from any other person. Small contribution/help wherever taken has been duly acknowledged and that complete thesis has been written by me.

I understand the zero tolerance policy of the HEC and Bahria University towards plagiarism. Therefore I as an Author of the above titled thesis declare that no portion of my thesis has been plagiarized and any material used as reference is properly referred/cited.

I undertake that if I am found guilty of any formal plagiarism in the above titled thesis even after award of PhD degree, the university reserves the right to withdraw/revoke my PhD degree and that HEC and the University has the right to publish my name on the HEC/University website on which names of scholars are placed who submitted plagiarized thesis.

Scholar/Author's Sign: _____

Name of the Scholar: Muhammad Hussain

Acknowledgment

In the name of Allah, the Most Gracious and the Most Merciful

All praises to Allah, He gave me the strength and courage to complete this thesis. Pursuing a Ph.D. degree is a great learning experience and it would not have been possible without the support of many people. First and foremost, I am extremely thankful to my supervisor Prof. Dr. Haroon Rasheed. His encouraging words and detailed feedback have been very important to me. He welcomed me as his Ph.D. student despite his assiduous and busy life. His brilliant, skillful supervision enriched this study higher than my expectations.

I would like to express my deepest gratitude to the internal thesis defense committee members, foreign evaluators, and final thesis defense committee members for providing me their valuable suggestions and indicating problem areas in my research. I take this opportunity to thank the examiners for their reviews and suggestions. Their knowledge and expertise are something I will always keep aspiring to.

I would also like to thank Bahria University (Karachi Campus) for providing me a perfect environment and technical support whenever needed which made the whole process a lot easier.

Most importantly, I am grateful for my friends and family's unconditional, unequivocal, and loving support throughout the entire thesis process and every day. They are the most valuable people in my life and I dedicate this dissertation to them.

Abstract

Existing wireless networks use orthogonal access that serves users as per the number of available resources. On the other hand, Next Generation Networks (NGNs) use the concept of non-orthogonality that serves multiple users on a single resource which consequently enhances device connectivity and spectral efficiency. Non-Orthogonal Multiple Access (NOMA) scheme employs power division multiple access which is sensitive to interferences and noises. This research presents a composite multiple access scheme that is developed by a combination of Power Domain NOMA (PD-NOMA) and Orthogonal Beamforming (OBF) to improve the spectral efficiency and reduce the interference between beams in the presence of Impulse Noise (IN). Furthermore, a novel IN mitigation and classification technique is presented using deep learning methods which efficiently minimizes the harmful effects of IN from PD-NOMA-based communication systems. This research can be divided into three phases.

The first phase of the research encompasses a new composite multiple access scheme based on PD-NOMA and OBF for exchanging information between smart grid, smart meters (SMs), and other communication units in the presence of IN. In the proposed scheme a cell is divided into sectors and OBF is implemented between sectors to reduce inter beams interference using orthogonalization. Within these sectors, the PD-NOMA scheme is implemented to utilize maximum bandwidth with the help of the successive interference cancellation scheme. According to the simulation and numerical findings, the proposed scheme offers a 3 Mbit/sec higher data rate and 0.24 Mbit/joule greater energy efficiency than the traditional orthogonal frequency division multiple access scheme, leading to better system performance in

the case of 10 SMs/users in a sector of a cell. Another significant achievement of the proposed scheme is that it does not cause inter beam interference and provides 17 Mbit/sec higher data rate by using OBF compared to conventional beamforming in the case of 60 SMs/users in 12 sectors of a cell.

The second phase deals with the analysis of performance degradation of the link due to the IN-contaminated wireless channel. Statistical formation i.e. the Probability Density Function (PDF) and Cumulative Distribution Function (CDF) is formulated for the channel to estimate the effect of IN. Moreover, two closed-form expressions are derived i.e. instantaneous Signal to Noise Ratio (SNR) by using the PDF and CDF for IN-contaminated wireless channel and Bit Error Rate (BER) by using instantaneous SNR for IN-contaminated PD-NOMA-based system.

Finally, in the last phase of the research, a novel IN mitigation and classification technique is presented using deep learning methods for PD-NOMA-based communication systems. The IN detection is performed by first identifying the IN occurrences using a Deep Neural Network (DNN) that learns statistical traits of noisy samples, followed by removal of the harmful effect of IN in the detected occurrences. Compared to the existing IN detection methods, the proposed DNN provided an enhanced BER performance. The proposed method is further tested for high and low IN and weak and strong IN occurrence probabilities. The proposed DNN method detected approximately 0.1 Mbits more true symbols out of 1 Mbits compared to conventional methods. The DNN identified high IN in the incoming noisy PD-NOMA symbols with an accuracy of 99% and low impulses with an accuracy of 87% respectively.

Table of Contents

List of Figures

List of Tables

List of Abbreviations

AMI	Advanced Metering Infrastructure
A-SIC	Advanced Successive Interference Cancellation
AWGN	Additive White Gaussian Noise
BAN	Building Area Networks
BER	Bit Error Rate
BS	Base Station
CBF	Conventional Beamforming
CDF	Cumulative Distribution Function
CDMA	Code Division Multiple Access
CD-NOMA	Code Domain NOMA
Co-PDMA	Cooperative PDMA
Co-PD-NOMA	Cooperative PD-NOMA
CR-NOMA	Cognitive Radio NOMA
CS	Constellation Scrambling
CSI	Channel State Information
D2D	Device-to-Device
DNN	Deep Neural Network
DOA	Direction of Arrival
FDMA	Frequency Division Multiple Access
FPA	Fractional Power Allocation
HAN	Home Area Networks

HDM	High-Dimensional Modulation
HetNet	Heterogeneous Network
HSPA	High Speed Packet Access
IDD	Iterative Detection and Decoding
IN	Impulse Noise
JPPA	Assignment and Power Allocation
LCQ-ML	Low Complexity Quasi-ML
LDS	Low Density Spreading
LTE	Long Term Evolution
LTE-A	Long Term Evolution Advanced
MAI	Multiple Access Interference
MCCD	Multicode Complex Domain
MCMC	Monte Carlo Markov Chain
MDM	Multidimensional Modulation
MIMO	Multiple Input Multiple Output
MMSE	Minimum Mean Square Error
MP-WFRFT	Multiple Parameter Weighted Fractional Fourier Transform
MU-MIMO	Multi User Multiple Input Multiple Output
MUSA	Multiuser Shared Access
NAN	Neighborhood Area Networks
NB-PLC	Narrowband PLC
NGN	Next Generation Network
NIST	National Institute of Standard and Technology
NOMA	Non-orthogonal Multiple Access
OBF	Orthogonal Beamforming

OFDM	Orthogonal Frequency Division Multiplexing
OFDMA	Orthogonal Frequency Division Multiple Access
OMA	Orthogonal Multiple Access
OPA	Optimum Power Allocation
PAIN	Periodic Asynchronous Impulsive Noise
PAPR	Peak to Average Power Ratio
PDF	Probability Density Function
PDM	Power Domain Multiple Access
PDMA	Pattern Division Multiple Access
PD-NOMA	Power Domain NOMA
PD-SCMA	Power Domain SCMA
PLC	Power Line Communication
PSIN	Periodic Synchronous Impulsive Noise
QoS	Quality of Service
RE	Resource Element
ROAD	Rank Ordered Absolute Differences
SCA	Successive Convex Approximation
SCMA	Sparse Code Multiple Access
SE-EE	Spectral Efficiency and Energy Efficiency
SG	Smart Grid
SIC	Successive Interference Cancellation
SIC/PIC-MMSE	Successive/Parallel Interference Cancellation with Minimum Mean Square Error
SM	Smart Meter
SNR	Signal to Noise Ratio
SS	Spreading Sequences

SU-MIMO	Single User Multiple Input Multiple Output
TDMA	Time Division Multiple Access
UE	User Equipment
WAN	Wide Area Networks
WLAN	Wireless Local Area Network
WCDMA	Wideband Code Division Multiple Access

List of Symbols

af	Activation Function
b	Bernoulli Random Sequence
B	Total Bandwidth
$B_{k,l}$	Fraction Bandwidth of l_{th} User in k_{th} beam
dr	Disturbance Ratio
E	Transmitted Signal Energy
f	Subcarrier Index
h	Channel Gain Coefficient
M	Length of the SCMA Codeword
m	m_{th} moment
n	Complex Noise Sample/Level of Gaussian Noise
n_0	Number of Bit Samples
n_1	Neurons in Layers 1
n_2	Neurons in Layers 2
n_3	Neurons in Layers 3
N	AWGN Noise Power
N_0	AWGN Noise Density
N_b	Number of Resource Blocks
n_G	AWGN Noise Level without Impulse
N_G	AWGN Noise Power without Impulse
n_I	AWGN Noise Level with Impulse

N_I	AWGN Noise Power with Impulse
N_r	Number of Receive Antennas
N_t	Number of Transmit Antennas
O	Number of the Nonzero Elements
p	Impulse Probability
P	Total Power
P_C	Constant Power Consumption of Circuit
$P_{k,l}$	Fraction Power of l_{th} User k_{th} in Beam
P_{SIC}	SIC Power Consumption for One Iteration
P_t	Actual Consumed Transmitting Power
R	Distance of User from BS
$R_{Composite}$	Sum-Rate of Composite System
R_{NOMA}	Sum-Rate of NOMA System
R_{OFDMA}	Sum-Rate of OFDMA System
s	User Symbols Vector
T_1 & T_2	Blanking/Clipping Thresholds
T_B	Blanking Threshold
T_C	Clipping Threshold
T_{Tol}	Total Number of Impulses
t_w	Width of the Impulse
w	Weight Vector
x	User Data Vector
α	Power Allocation Coefficient
β	Bandwidth Allocation Coefficient
$\bar{\gamma}$	Average SNR
γ	Instantaneous SNR

θ	Angle of Arrival
λ_{Avg}	Average Impulse Rate
λ	Regularization Parameter
η	Learning Rate
ξ	Combined Noise Level (Additive White Gaussian Noise and Impulsive Noise)
ξ_0	Combined Noise Power (Additive White Gaussian Noise and Noise)
σ	AWGN Variance
χ	Inter-cell Interference Level
χ_0	Inter-cell Interference Power
ψ	Precoding Vector
ω	Weighting Coefficient

CHAPTER 1

INTRODUCTION

Enabling wireless communication is a core component of envisioned Next Generation Networks (NGN) that enable network access across the globe. Through NGN, users will have more data rates especially in emergency vehicles, high-definition medical image transmission services, and other special conditions. NGN will propose adaptable and scalable services, as it is accepted to provide a faster, smarter, and more efficient network. It will also offer remote access to many real-time services and ultra high definition multimedia experience [1, 2].

A huge number of the new connected devices is becoming part of the new emerging networks such as Smart Grids (SGs), smart homes, and the Internet of Things (IoT). Since the existing wireless networks are seriously restricted by limited network resources and robustness against noises and interferences, therefore, there is a dire need for improvement. Furthermore, impulsive electromagnetic interference, also known as Impulse Noise (IN), degrades the signal quality to the point of reception failure and also increases bit errors, causing system reliability to decrease. IN is a problem for existing networks and can also be a threat to NGNs [3, 4].

Frequency Division Multiple Access (FDMA) and Time Division Multiple Access (TDMA) are restricted due to exclusive allocation of frequency and time. Contrarily, there is no restriction on time and frequency in Code Division Multiple Access (CDMA). All users can use the entire bandwidth at any time, however, users are identified by the limited number of orthogonal codes [5]. Orthogonal Frequency

Division Multiple Access (OFDMA) shows better spectral efficiency however due to the limited number of orthogonal subbands only a limited number of users can be served. Hence, none of the networks from 1G to 4G can serve more users from available resources [6]. Furthermore, the idea of beamforming has been used to improve spectral efficiency by offering the highest gain in the preferred direction. However, when it is put on to multiuser communication it increases interference [7].

IN is one of the main problems in many devices which operate in the field. Impulsive interference degrades the performance of the wireless link to the point of connection loss. Little research has been done on the effect of IN in the wireless channel. Before providing the solution to the problem of IN, it is important to analyze the desired information reliability under the circumstance of random IN with different intensity levels. It helps the designer to predict the channel behavior and error in systems [3, 8].

Comparison of different analog domain processing techniques for IN mitigation such as blanking, clipping, and blanking/clipping reveals that selection of threshold value is the key parameter to improve performance. However, a change in threshold in response to channel condition results in the model mismatch. As an implication, the performance of all the conventional threshold-based methods degrades in harsh impulsive environments [9].

Despite the large number of efforts carried out so far in respect to the above-mentioned issues, there is still room for performance improvement of resource allocation.

1.1 Motivation

The new emerging networks such as smart grids, smart homes, and the Internet of Things provide network access to users across the globe. The new connection requirement is increasing exponentially with time because existing wireless networks are seriously constrained by limited network resources such as time, frequency, and power. Existing wireless networks use orthogonal access that serves users as per the number of available resources. Furthermore, NGN applications operate in fields

where popular Gaussian approximation is not sufficient as it does not contemplate the impulsive behavior of the channel. Therefore, there is a need for the analysis of IN for developed efficient mitigation.

1.1.1 Orthogonal and Non-Orthogonal Resource Allocation

Multiple access schemes have been a revolutionary technology from 1G to 4G for the growth of mobile communications. From the design aspect, these multiple access technologies are mostly from the Orthogonal Multiple Access (OMA) category, they are in the time domain, code domain, frequency domain, and time-frequency domain. OMA can easily detect the user information signal by utilizing a simple receiver. However, the entire number of users that the system can accommodate is firmly restricted by the number of available orthogonal resources. Also, the system requirements for synchronization are highly restricted in order to guarantee the orthogonality of resource allocation among users. Therefore, it is very difficult for OMA to meet the data rate and other requirements of NGN. For this reason, NGN demands an innovative multiple access scheme. Non-Orthogonal Multiple Access (NOMA) that may be combined with upcoming wireless communication systems to achieve the requirements, such as massive connectivity, high spectral and energy efficiency, significant achievable data rate, low latency, exceptional user fairness, large throughput, ultrahigh reliability, and upholding the different Quality of Services (QoS) [10]. NOMA can be valued as a reliable and efficient scheme for NGNs such as fifth-generation mobile communication, SG communication, IoT, etc. [11, 12]

1.1.2 Next Generation Network Challenges and Requirements

SG considered as Next Generation Power Grid allows and controls bi-directional energy flow. SG is the integration of automation, information technology, and communication network. SG communication network is not only a massive but also an exceptionally complex network of vast number of sub-networks. There are some big challenges, to ensure the communication requirements of the SG; (i) Complex network having multi subsystem interconnection, multidisciplinary users, and dynamic and reconfigurable model. (ii) Large number of connected SMs and other devices.

(iii) Requirement of energy efficient communication technology. (iv) Scalable data rate in normal/emergency condition. (v) Transmission over noisy channels. (vi) Information security of users, and reliability [13].

Existing wired and wireless communication technologies are quite sufficient to counter the challenges of the SG network but the network requirement is increasing exponentially with time. Therefore, the SG network needs exceptional communication infrastructure. It seems that the latest fifth-generation technology, NOMA can fulfill these requirements with; (i) Dynamic deployment of complex networks by allowing dynamic power allocation schemes. (ii) High spectral efficiency by permitting multiple users on the same frequency. (iii) Massive connectivity by allowing more users simultaneously at the same time. (iv) Showing a better tradeoff between Spectral Efficiency and Energy Efficiency (SE-EE). (v) Proving scalable capacity through a non-orthogonal structure. (vi) Utilizing Successive Interference Cancellation (SIC) scheme for interference cancellation. (vii) Increasing cell-edge throughput, lower latency, and better QoS [13].

1.1.3 Noise and Interference

The NGN such as SGs, smart homes, and IoT have enabled devices accessibility across the globe. Furthermore, these devices which include smart meters (SMs), sensors, actuators, etc. suffer from IN while operating with power systems. Impulsive interference degrades the performance of the wireless link to the point of connection loss. The noise contamination of a communication channel may result in erroneous information about the resources in the field - resulting in complete obstruction of the information. The performances of other communication units and SMs are degraded by IN extant in the power system, produced by electromagnetic disturbances.

In addition, the Power Domain NOMA (PD-NOMA) scheme utilizes Power Domain Multiple Access (PDM) which is found to be susceptible to IN. The classical IN detection approaches perform blanking and clipping by setting an optimum threshold - which is susceptible to vary in response to channel condition - resulting in model mismatch. Any change in the detection threshold of impulses in traditional

methods can cause ambiguity in the receiver threshold of signal detection, thus deteriorating the performance of NOMA. Based on the aforementioned IN intervention and its degrading effects on communication applications, novel mechanisms are desired to mitigate and classify the IN induced in the received signal.

Following are the challenges that are being faced while developing efficient resource allocation plan for NGN:

1. The inability of existing schemes to serve more users from available resources.
2. Interference among users due to simultaneous resource allocation in multiuser communications.
3. Degradation of spectral efficiency due to interference between main lobes in Conventional Beamforming (CBF).
4. Lack of appropriate information regarding the random nature of IN.
5. Insufficiency of classical IN mitigation approaches to find the optimum threshold in variant channel condition.

1.2 Research Problem Formulation

NGNs have some major challenges such as ensuring a good performance level, improving bandwidth utilization, as well as error-free transmission. In the light of these challenges, the research problem of developing efficient bandwidth utilization and error-free transmission for NGN has been formulated that can be addressed by carrying out research in the following sub-domains of resource allocation:

1. For NGNs, appropriate resource allocation and investigation of interference are crucial to compete with the increasing demand for services and the limited number of resources.
2. The desired information reliability should be attained in the presence of IN with different intensity levels to improve the reliability of the wireless link.
3. For error-free transmission, new computational approaches should be developed to address the problem of optimum threshold in classical IN elimination methods.

1.3 Aims and Objectives of the Research

Motivated by the aforementioned grounds, the researcher aimed to achieve the following objectives.

1. Design a composite model for multiuser wireless communication using NOMA and beamforming as well as minimize interference between beams for large number of users.
2. Analyze the effect of IN to develop a statistical model for IN and measure the performance of the proposed scheme in presence of IN.
3. Provide a solution for performance degradation of IN-affected wireless channels due to threshold-based nonlinear approach.

1.4 Scope, Assumptions and Limitations

The purpose of this research is to achieve the objectives by utilizing the following assumption and constraints.

1. Perfect Channel State Information (CSI) is assumed to be available at the receiver in some cases.
2. While, noise is assumed to be white Gaussian with zero mean and variance σ^2 in all cases, Rayleigh fading channel is assumed in some cases.
3. The User Equipment (UE) is assumed to be operational in a bursty impulsive environment in some cases.
4. Wireless channel is modeled as quasi-static channel.
5. Power, data rate, and fairness are considered as constraints of optimization problems.

Where perfect CSI is used to avoid hindering the practical implementation of interference alignment. Rayleigh fading is suitable for the urban region. The wireless channel is modeled as a quasi-static channel for "block-wise" time-invariant communication. Power, data rate, and fairness are the resources of the network therefore these are considered as constraints of optimization problems.

1.5 Work Flow of Experimental Research

The workflow of experimental research is demonstrated in Fig. 1.1. The proposed research has been carried out in three phases. In the first phase, to improve the bandwidth utilization a composite scheme has been formulated based on PD-NOMA and OBF. The proposed scheme takes user location as input which is based on the geographical distance between mobile user and the Base Station (BS). Later on, this input is used in algorithm 1 and algorithm 2 to allocate particular beam and power among users. To reduce inter-beam interference, the Gram-Schmidt process takes a set of linearly independent vectors and constructs orthonormal basis vectors. The theoretical analyses have been verified by performing Monte Carlo simulations via Matlab. The simulation of the sum-rate capacity is done by first generating random inputs i.e. distances of the users from BS and sorting the distances of the users in descending order. Moreover, the distances between users are compared with each other to find a sufficient difference between users. Then Rayleigh fading coefficients with zero mean and unit variance are generated for all users. By Multiplying each user's fading coefficient with the square root of the variance, the channel gain for each user is finally estimated. Average IN noise is considered in the initial simulation, then randomly generated IN is convolved with AWGN. After all the runs, the average achievable sum-rate is obtained.

In the second phase, a closed-form of expression for BER is derived and verified through Mathematica to estimate the loss due to IN. Further verification of theoretical BER in the IN-contaminated Rayleigh fading channel is done by simulation. 1 Mbits are considered as input for BPSK transmission and reception. By initializing the random function, 10^6 bits are generated with an equal probability of 0 and 1. BPSK modulation technique for input bits is selected for computational convenience. Coefficients of AWGN (with zero mean and variance) and Rayleigh channel are generated. The coefficient of AWGN is multiplied by the range of Eb/No and the coefficient of Rayleigh fading is multiplied by BPSK symbols. Finally randomly generated IN is added to the input vector before the reception. At receiving end, equalization is achieved for receive symbols by Rayleigh fading equalizer.

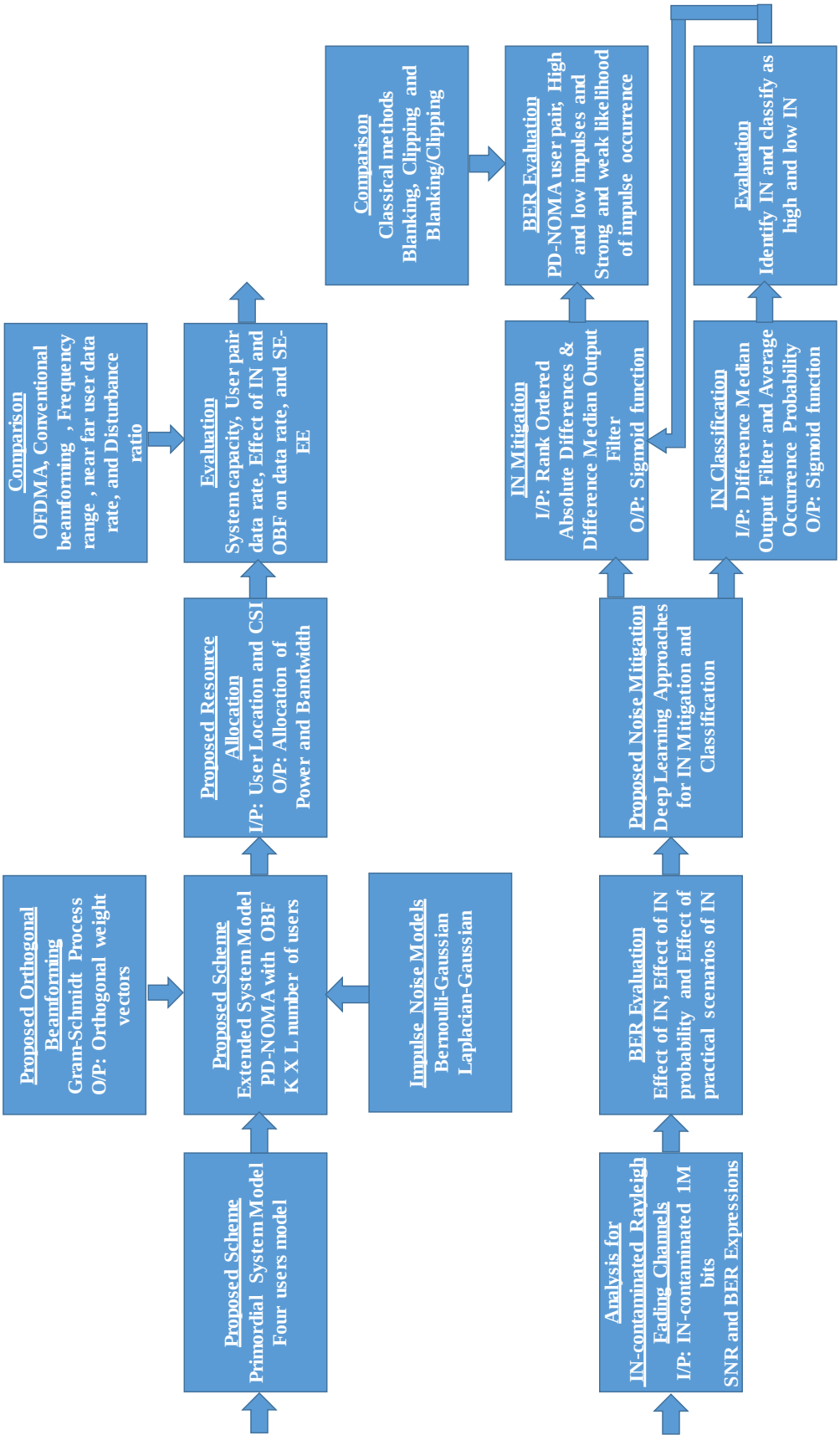

Figure 1.1:: Work flow of experimental research.

Afterward, hard decoding is done by taking the real value of the output of the equalizer. All output values greater than 0.5 are considered 1 rest are 0. Lastly, the errors are counted by comparing the output of the hard decoder with input symbols.

In the last phase, for IN mitigation and classification, the layout of the proposed DNN, its input and output features, and signal detection approaches have been developed. The proposed DNN has been designed with three fully connected hidden layers. The number of neurons in these layers is set as $n_1 = 20,\ n_2 = 20$, and $n_3 = 10$. The input for IN mitigation to the DNN is a set of three features i.e. incoming sample value, difference median output feature, and Rank Ordered Absolute Differences (ROAD) statistic feature. Moreover, the input for IN classification to the DNN also contains three features i.e. incoming sample value, difference median output feature, and average occurrence probability output. An activation function (af) at each layer enables connection from the preceding layer to the following layer using parameter matrix and bias vector. The parameter matrix W and bias vector q connect the hidden layers with each other and to the output layer using the number of neurons (n_r) selected for the R_{th} layer. The output is represented by o/p' and has one layer which generates a binary sequence of 0 or 1.

1.6 Research Contribution from the Dissertation

This section deals with the research contributions made in this dissertation. Additionally, the research publications that have resulted out of the discussed contributions are mentioned by their references.

1.6.1 First Contribution

This research presents a composite multiple access scheme that is developed by a combination of Power Domain NOMA (PD-NOMA) and Orthogonal Beamforming (OBF) to improve the spectral efficiency and reduce the interference between beams in the presence of Impulse Noise (IN). Furthermore, a novel IN mitigation and classification technique is presented using deep learning methods which efficiently minimizes the harmful effects of IN from PD-NOMA-based communication systems.

This research can be divided into three phases.

Firstly a new composite multiple access scheme based on NOMA and Orthogonal Beamforming (OBF) has been presented for exchanging information between SG, SMs, and other communication units in the presence of IN. OBF has been implemented between sectors to reduce inter beams interference. Power division multiple access has been implemented within the sectors to utilize maximum bandwidth with the help of the SIC scheme. Moreover, orthogonal beams are proposed which are generated by Gram-Schmidt orthogonalization process. The effect of IN on power spectral density has been investigated [14]. By investigating noise models for IN, appropriate models i.e. Bernoulli-Gaussian and Laplacian-Gaussian have been analyzed to find the effect of IN on the proposed scheme [15, 16].

Furthermore, the first algorithm has been proposed for the user ordering strategy for the PD-NOMA downlink system. Also, optimization of power and bandwidth has been presented, under ergodic user-rate constraints and total transmission power constraints. The second algorithm has been proposed for optimum power allocation. It has also been discovered that the optimum power scheme ensures that each user gets a minimum fair data rate [17]. Moreover, the maximum possible number of users - who can employ simultaneously on the PD-NOMA scheme - has been determined [15].

1.6.2 Second Contribution

Secondly, the statistical information has been provided through formulating the PDF and CDF for estimation of the channel. Moreover, two closed-form expressions have been derived i.e. instantaneous Signal to Noise Ratio (SNR) by using the PDF and CDF for IN-contaminated wireless channel and Bit Error Rate (BER) by using instantaneous SNR for IN-contaminated PD-NOMA-based system. Using impulse rate and disturbance ratio, the actual loss of bits has been calculated during impulses in different IN practical scenarios [18, 19].

1.6.3 Third Contribution

Finally, a novel IN mitigation and classification technique has been presented using deep learning approaches for PD-NOMA-based communication systems. A deep learning approach has been proposed in this research work to efficiently remove the harmful effect of IN from the noise-contaminated PD-NOMA symbols. The proposed approach has been further tested for high and low IN and weak and strong IN occurrence probabilities. Moreover, another deep learning approach has been proposed in this research work to effectively distinguish between high IN and low IN in the noise-contaminated PD-NOMA symbols which can help to improve the performance of IN detection models [18].

1.7 Thesis Organization

Chapter 1 introduces the motivation, formulation of research problem, research aims and objectives, and authors' contributions.

Chapter 2 presents the background theory and literature review necessary for contiguous research work. Firstly, existing multiuser communication technologies are discussed that are based on OMA schemes such as CDMA, OFDMA, MIMO, Beamforming, etc. NOMA and its popular categories are comprehensively reviewed and compared in terms of working principle, design feature, user-rate, system capacity, and BER. Furthermore, an overview of emerging NGNs such as IoT, VANET, SG, and mobile networks is presented, as well as challenges in their implementation and analyzed how NOMA may meet these criteria? The fundamental concepts and sources of IN along with a comprehensive literature review on IN mitigation techniques are presented. In last, the performance comparison between different IN mitigation techniques, and the performance of popular NOMA schemes are presented in presence of IN. A state-of-the-art review of popular categories of NOMA, IN mitigation, and SG-assisted wireless technologies is presented in their respective sections.

Chapter 3 presents one of the main contributions of this research i.e. four-user composite multiple access model based on a combination of orthogonal and non-orthogonal schemes. An extended version of the composite multiple access model is presented that is based on PD-NOMA and OBF for exchanging information between SG, SMs, and other communication units in the presence of IN. Considering the noisy channel condition of the SG, appropriate noise models i.e. the Bernoulli-Gaussian and Laplacian-Gaussian are used in the proposed scheme. Mathematical justifications are provided for system capacity, system capacity with beamforming, spectral and energy efficiency, and spectral and energy efficiency with SIC of the proposed scheme in presence of IN. Secondly, different practical scenarios of impulsive noise are considered to evaluate the field performance of the proposed scheme in the presence of IN. The overall performance of the proposed scheme is compared with traditional OFDMA in terms of the number of users, system capacity, nearer and farther user data rate, effect OBF on data rate, spectral and energy efficiency, and actual loss of bits.

Chapter 4 deals with the algorithms and optimization schemes. Algorithms-1 is proposed for selecting an access method for users based on the user ordering strategy in the downlink PD-NOMA system. Under the constraints of ergodic user-rate and total transmission power, optimization of power and bandwidth is formulated. On the basis of the optimization results, algorithm-2 is presented for the optimum power allocation. The maximum possible number of users is determined - who can employ simultaneously on the PD-NOMA scheme without degrading the sum-rate over IN-contaminated Rayleigh fading channel.

Chapter 5 presents the IN mitigation scheme and its BER performance. In addition, the effect of IN is analyzed by determining PDF and CDF. Two closed-form expressions are derived i.e. instantaneous SNR by using the PDF and CDF for IN-contaminated wireless channel and BER by using instantaneous SNR for IN-contaminated PD-NOMA-based system.

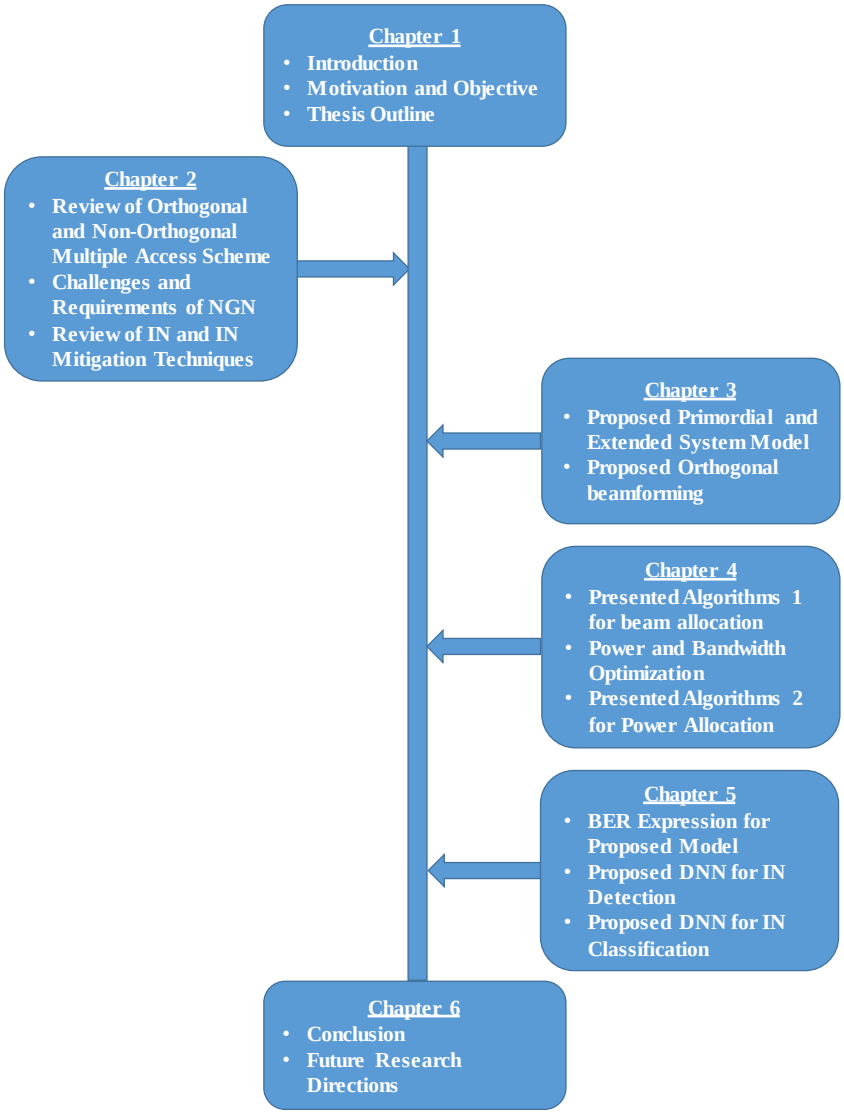

Figure 1.2:: Thesis organization.

DNN based approach is presented for mitigation and classification of IN. The proposed method is further tested for high and low IN and weak and strong IN occurrence probabilities. Lastly, through another DNN, the distinction between the high IN and low IN is tested in the noise-contaminated PD-NOMA symbols.

Chapter 6 presents the conclusions of the dissertation and future directions of the research.

1.8 List of Research Articles

1. Muhammad Hussain, Hina Shakir and Haroon Rasheed, "Deep Learning Approaches for Impulse Noise Mitigation and Classification in NOMA-based Systems," in IEEE Access, vol. 9, pp. 143836-143846, 2021, (IF=3.367) doi: 10.1109/ACCESS.2021.3121533.

2. Muhammad Hussain, Haroon Rasheed, "Non-orthogonal Multiple Access for Next-Generation Mobile Networks: A Technical Aspect for Research Direction," Wireless Communications and Mobile Computing, vol. 2020, Article ID 8845371, 17 pages, 2020. (IF=2.336) https://doi.org/10.1155/2020/8845371

3. Muhammad Hussain and Haroon Rasheed, "Performance of Orthogonal Beamforming with NOMA for Smart Grid Communication in the Presence of Impulsive Noise," Arabian Journal for Science and Engineering (2020). (IF=2.334) https://doi.org/ 10.1007/s13369-020-04457-y

4. Muhammad Hussain and Haroon Rasheed, "Communication Infrastructure for Stationary and Organized Distributed Smart Meters," 2019 2nd International Conference on Communication, Computing and Digital systems (C-CODE), Islamabad, Pakistan, 2019, pp. 17-22, doi: 10.1109/C-CODE.2019.8681020.

5. Muhammad Hussain and Haroon Rasheed, "A Computational Power Allocation Scheme for Fair NOMA Downlink System," Journal of Information Communication Technologies and Robotic Applications, pp. 73-79, Jun. 2018. (HEC X-Category)

6. Muhammad Hussain, Haroon Rasheed, Naveed Ali and Najamus Saqib, "Roadside Infrastructure Transmission of VANET Using Power Line Communication," CCODE 2017 (International Conference on Communication, Computing and Digital Systems) IEEE, Paper No 432, page no. 139-143, March 8-9, 2017.

7. Muhammad Hussain and Haroon Rasheed, "Two Deep Learning Approach for Impulse Noise Mitigation in NOMA-enable Smart Energy Meter," submitted in Transactions on Emerging Telecommunications Technologies, Wiley.

CHAPTER 2

BACKGROUND

This chapter presents, the background theory and literature review on the orthogonal and non-orthogonal schemes which are closely related to the proposed scheme. The chapter also highlights the core issues in the implementation of NGNs such as bandwidth limitation and interference and noise which is related to the application of the proposed scheme. Finally, the background theory and literature review on IN mitigation techniques are presented which help in noise analysis and proposed mitigation technique.

2.1 Multiuser Communication

Multiuser communication systems have been recognized as one of the key technology for realizing next-generation wireless networks. Despite this, multiuser communication confronts several obstacles, including increasing number of users, higher spectral efficiency, reduction in signal interference, and noise occurrence among users. Next generation multiuser wireless communication offers several benefits, which include extremely low latency, very high data rates, significant improvement in the number of users, increased capacity, and perceived QoS. This may be achieved at the cost of an increased receiver complexity by non-orthogonal access with the spatial diversity of users.

NOMA is one of the capable contenders to achieve the vision of next-generation

wireless communications. One of the key features of NOMA is that it supports a higher number of users from available orthogonal resources. On the other hand in OMA, the number of users is restricted by available resources. A variety of research have evaluated the capability of wireless communication for NGN, discussed in detail below. The research suggested that higher data rate can be achieved via non-orthogonal multiuser communication which is essential in the implementation of NGN.

2.1.1 Orthogonal Access Schemes

Orthogonal schemes can attain a good system performance without increasing the complexity of the receivers and mutual interference between users. However, due to the exclusive allocation of resources, orthogonal schemes lack the capability to resolve the developing challenges due to the high requirement of NGN. A summary of different multiple access schemes and techniques is as follows.

2.1.1.1 Point to Point Communication

Point to point transmission between a single user terminal and a BS is known as single user communication such as FDMA or TDMA. In these systems, BS transfers data to a single user with a given frequency or at a specific time [20]. The SNR and data rate of the k_{th} user for such a system can be expressed as:

$$SNR_k = \frac{P_k|h_k|^2}{N_0 B_k} \tag{2.1}$$

$$R_k = B_k \log_2\left(1 + \frac{P_k|h_k|^2}{N_0 B_k}\right) \tag{2.2}$$

where R_k is the achievable data rate for the k_{th} user, h_k is the channel gain coefficient, P_k is the average signal power, N_0 is the noise density, $N(N = N_0 B)$ is the noise power and B_k is the fraction of the total bandwidth B.

In comparison to FDMA and TDMA, there is no restriction on time and frequency in CDMA as shown in Fig. 2.1. All users can use the entire bandwidth at any time, however, they are identified by codes. One major limitation in CDMA is that the system can not have more than K orthogonal codes [5]. The SNR and

data rate of the k_{th} user for the CDMA system can be expressed as:

$$SNR_k = \frac{P_k|h_k|^2}{N_0B + (K-1)P_k} \tag{2.3}$$

$$R_k = B\log_2\left(1 + \frac{P_k|h_k|^2}{N_0B + (K-1)P_k}\right) \tag{2.4}$$

where K is the number of users employed on the CDMA system.

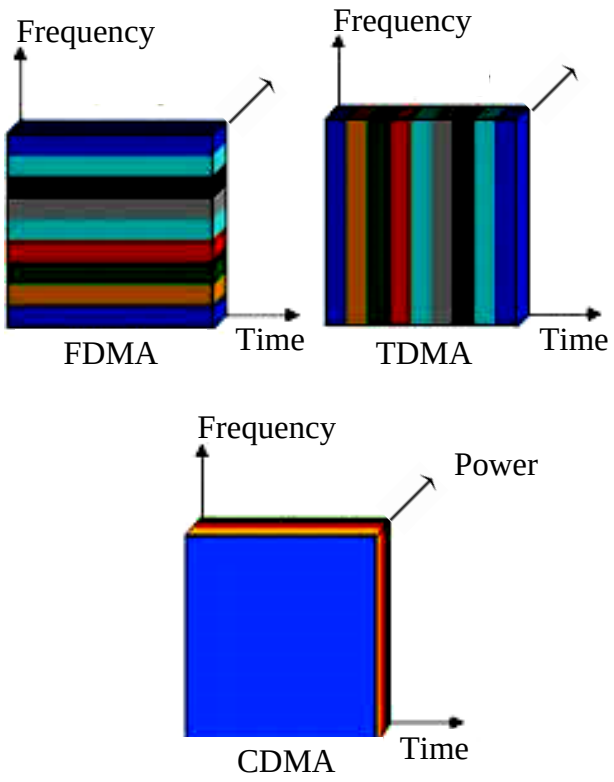

Figure 2.1:: Frequency, time, and code domain multiple access schemes.

The Orthogonal Frequency Division Multiplexing (OFDM) technique is a digital modulation scheme while the OFDMA technique is a multiuser access scheme. In OFDMA, multiple access is accomplished by allocating the different subsets of subcarriers to different users. The difference between an OFDMA and an OFDM is that in the OFDMA the users are allocated by both time and frequency domains while in the OFDM the users are allocated only by the time domain [6]. The SNR and data rate of the k_{th} user for the OFDMA system can be expressed as:

$$SNR_k = \frac{P_k|h_k|^2}{N_0B_k} \tag{2.5}$$

$$R_k = B_k \log_2 \left(1 + \frac{P_k |h_k|^2}{N_0 B_k}\right) \tag{2.6}$$

where R_k is the achievable data rate for the k_{th} user, h_k is the channel gain coefficient, P_k is the average signal power.

2.1.1.2 Multiple Antenna System

In recent times, multiple antenna schemes such as Multiple Input Multiple Output (MIMO) has been implemented to support communication systems to maximize their coverage area and improve their gain. The antennas are generally added at the BS. In multiple antenna system, the transmission speed is comparatively low than expected because the BS cannot transmit data to all of its users at the same time. Therefore, the SNR and data rate of the k_{th} user for the Single User MIMO (SU-MIMO) system can be written as:

$$SNR_{k\,(SU-MIMO)} = \frac{|h_1^2 + h_1^2 + \cdots + h_r^2|}{r} \frac{P_k}{N_0 B_k} \tag{2.7}$$

$$R_{k\,(SU-MIMO)} = NtB_k \log_2 \left(1 + \frac{|h_1^2 + h_1^2 + \cdots + h_r^2|}{r} \frac{P_k}{N_0 B_k}\right) \tag{2.8}$$

where $\frac{|h_1^2 + h_1^2 + \cdots + h_r^2|}{r}$ is diversity gain and Nt is number of antennas used for MIMO system.

If all users occupy separate individual frequencies but utilize the same time slot as a result user congestion takes place. The advantage of these communication schemes is that the co-channel interference is not very prominent and the systems are simple. On the other hand, the drawbacks of these schemes are that throughput and transmission speed is not improved as expected [21].

Apart from the speedy development of wireless communication, countless efforts have been made to increase the data rate, system throughput, and channel capacity by allowing multiple users to communicate using the same frequency at the same time slot, known as multiuser communication [20]. The SNR and data rate of the k_{th} user for the Multiuser MIMO (MU-MIMO) system [22] can be written as:

$$SNR_{k\,(MU-MIMO)} = \frac{P_k \left(\psi_k h_k\right) \left|\psi_k h_k^T\right|^2}{\sum_{i \neq k}^{K} P_k \left(\psi_i h_i\right) \left|\psi_i h_i^T\right|^2 + N_0 B} \tag{2.9}$$

$$R_{k\,(MU-MIMO)} = NtB\log_2\left(1 + \frac{P_k\left(\psi_k h_k\right)\left|\psi_k h_k^T\right|^2}{\sum_{i\neq k}^{K} P_k\left(\psi_i h_i\right)\left|\psi_i h_i^T\right|^2 + N_0 B}\right) \tag{2.10}$$

where ψ_i and ψ_k are precoding vectors for the i_{th} and k_{th} users' P_k is the power for the k_{th} user and h_i and h_k are the coefficients of communication channel and Nt is the number of antennas used for MIMO system.

Regardless of the complexity in implementation of multiple antennas at user's terminals, users attain increased data transmission speed and efficient use of frequency spectrum as shown in Fig. 2.2 [20].

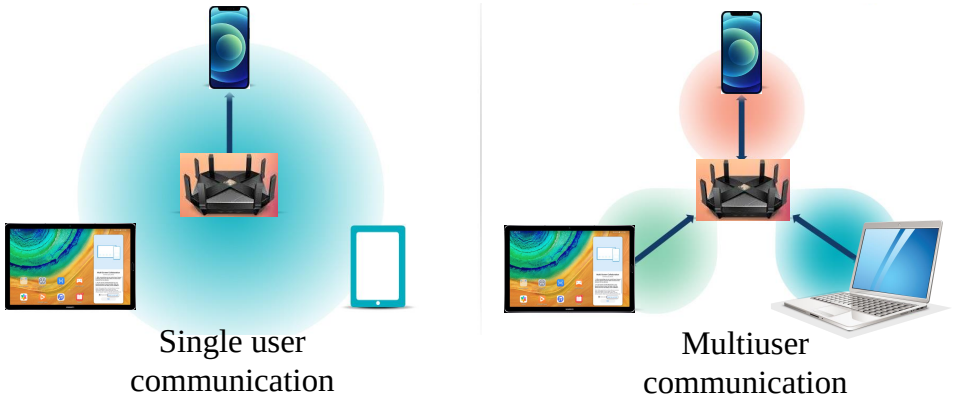

Figure 2.2:: Single user MIMO and multiuser MIMO.

Various studies have evaluated system efficiency regarding multiuser and single user communication. On the basis of multiuser communication advantages, they are considered more realistic in many wireless communication standards, for example, 4-Generation (IMT Advance), 5-Generation (WIMAX)/802.16m, 802.11af, 802.11ac, and 802.11ad [20].

2.1.1.3 Beamforming

The idea of using multiple antennas to offer the highest gain in the preferred direction while providing a lesser gain in other directions is known as beamforming. The current beamforming scheme requires feedback information or a feedback channel to fulfill system necessities such as achieving great system throughput and low BER. The method to achieve correct feedback information is quite difficult and utilizes a

substantial amount of power. One of the major drawbacks is that when it is put on to multiuser communication it increases interference. In essence, several users employ at the same frequency and same time, thus users produce interference among themselves, and therefore throughput and the signal to interference plus noise ratio are comparatively low.

The research studies suggested in [23] that the employment of multiple antenna scheme enhances the data rate, coverage area, SNR, and throughput. Moreover, the research suggested a low cost and a less complicated scheme to decrease signal interference of other users, in order to improve the Signal to Interference ratio (SIR). Additionally, researchers have also identified in [24] a multiple antenna scheme with a limited frequency spectrum, capable to provide effective utilization of the spectrum. Currently, the multiple antenna scheme requires channel feedback or information channel from users like Per User Unitary Rate Control (PURC), which is the advanced multiuser MIMO technique. Furthermore, researchers have presented opportunistic beamforming [25] and distributed beamforming [26] schemes, both methods use feedback information to increase system quality. Feedback data and CSI are implemented to synchronize the receiver and transmitter. Therefore, the receiver and transmitter can communicate with error-free data. The major advantages of the above bi-directional feedback methods include less errors and improved data transmission. Regardless of processing techniques are comparatively difficult and require a substantial amount of power when transmitting the feedback data. The feedback data might be inaccurate because the communication channel remains constantly random. In [7] researcher presented a composite scheme with a combination of OMA scheme and CBF. In order to increase the system throughput and decrease the entire system power consumption at the same time for the multiuser MIMO-OFDM downlink systems, authors have suggested a resource sharing technique. To optimize joint data rate and power, authors converted the actual problem into a convex dual scenario and to solve the problem used Lagrange dual decomposition method.

One of the beamforming techniques that keep away from feedback information by utilizing the estimation of Direction of Arrival (DOA). The beamforming scheme conserves a required signal through steering the main beam in the required

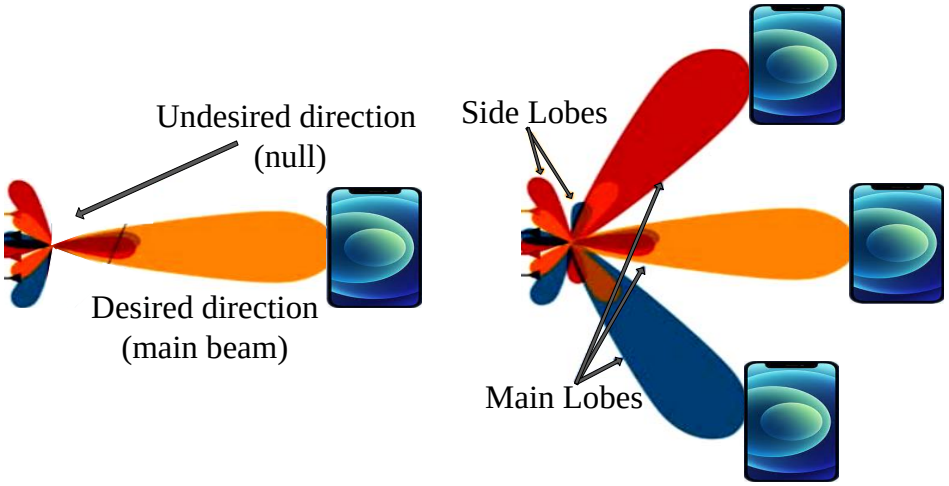

Figure 2.3:: Single user beamforming and multiuser beamforming.

direction whereas removing interference signals by producing side lobes or else nulls in other directions as shown in Fig. 2.3. This scheme offers several benefits such as improved link quality/ reliability, a reduction in energy consumption, and increased coverage area. This type of beamforming is known as CBF. Generally, the weighting constants can be easily determined for CBF from the information of the location of the users [27, 28].

In multiuser communications, all of the users occupy the same frequency and the same time slot, as a result, users face interference between themselves therefore conventional beam formation cannot be realistic for multiuser communication. The side lobes of other beams interfere with the main lobe of the given beam, which results in low system throughput and low SNR. The SNR and data rate of such a system for the k_{th} user can be expressed as:

$$SNR_{k\,(BFM)} = \frac{P_k h_k |x_k^2|}{\sum_{i \neq k}^{K} P_k h_i |x_i|^2 + N_0 B_k} \tag{2.11}$$

$$R_{k\,(BFM)} = B_k \log_2 \left(1 + \frac{P_k h_k |x_k^2|}{\sum_{i \neq k}^{K} P_k h_i |x_i|^2 + N_0 B_k}\right) \tag{2.12}$$

where P_k is the power of k_{th} user, h_i and h_k are the coefficients of communication channel and x_i and x_k are the signal vectors containing the user data vectors for the i_{th} and k_{th} users. $\sum_{i \neq k}^{M} P_k h_j |x_j|^2$ are the inter-beam interference in which minor lobes of beam interfere with main lobe.

$$SNR_{k\,(OBFM)} = \frac{P_k\left(\omega_k h_k\right) h_k \omega_k |x_k^2|}{\sum_{i\neq k}^{K} P_k\left(\omega_k h_i\right) h_i \omega_k |x_i|^2 + N_0 B_k} \tag{2.13}$$

$$R_{k\,(OBFM)} = B_k \log_2\left(1 + \frac{P_k\left(\omega_k h_k\right) h_k \omega_k |x_k^2|}{\sum_{i\neq k}^{K} P_k\left(\omega_k h_i\right) h_i \omega_k |x_i|^2 + N_0 B_k}\right) \tag{2.14}$$

where ω_k known as weighting coefficient at the BS according to the DOA, P_k is the power of k_{th} user in predefined direction, h_i and h_k are communication channel and x_i and x_k are signal vectors containing the user data vectors for i_{th} and k_{th} users. All users are employed on orthogonal carrier and $i \neq k$, if equal it is null.

Due to the vast number of connected devices and their huge data, available wireless communication technologies of the current era cannot meet the requirements of next generation wireless networks. There is a need for an advanced technology capable of efficiently satisfying the continuously increasing demand-response of NGN.

2.1.2 Non-Orthogonal Multiple Access Scheme

Within the common physical layer using the code domain or power domain multiple access, NOMA permits numerous users to utilize frequency and time resources [29]. In recent times, various NOMA topologies have received a lot of attention due to their attractive features. Generally, NOMA is categorized into two types. These types are Code Domain NOMA (CD-NOMA) and the PD-NOMA [19]. NOMA achieved its goals by a combination of multiple access techniques like Sparse Code Multiple Access (SCMA) [30], Multiuser Shared Access (MUSA) [31] with Low Density Spreading (LDS) [32], and Pattern Division Multiple Access (PDMA) [33].

In the third generation mobile system, the Wideband CDMA (WCDMA) scheme was launched. As a result, users were able to transmit moving pictures (videos) through the improved speed of data communication. Furthermore, 3G presented an improved technology, i.e., High-Speed Packet Access (HSPA) and HSPA+ (3.5G), through which the user data experience was improved. However, in comparison to Wi-Fi and Wireless Local Area Network (WLAN), high data rate applications like streaming of moving images were slower in 3G. Today, network operators provide services of 4G networks based on Long Term Evolution (LTE). The achievable communication speed rises up to 5 to 6 times in comparison to 3G, and data throughput is also expressively enhanced in LTE than HSPA+. In LTE-Advanced (LTE-A), the

available bandwidth is twice as LTE; therefore, several 4G network service providers are also transferred to LTE-A (4.5G). With LTE and LTE-A, communication technology has improved, at a level close to Wi-Fi with respect to user data experience. 4G network and LTE and LTE-A technology are saturated in terms of further improvement. The wireless data requirement is increasing day by day. Therefore, there is a need for new technology to speed up data access. However, for wireless communication, improvement in the data capacity and the data transmission rate is essential. Therefore, for the mobile Internet extension and modernization, researchers all over the world started investigating ways to improve data capacity and data transfer rates.

In addition, from the beginning of digital communications in the 1990s, cellular phone technology has made great progress by focusing on increased data rate and capacity. Today, communication trends, mobile Internet, and video calls have become a reality. Hence, a new version has been launched, i.e., 5G mobile communication. Now, at any emergency condition such as online medical imaging or smart vehicles in congestion, more data needs to be delivered to the specific user. Thus, 5G networks will respond accordingly. Researchers also recognize 5G as an opportunity to redefine not only the networks capable to connect a wide variety of new devices but also the networks that realize exceptional data rates. The next version of 5G wireless mobile technology is 6G, which means 6th generation wireless mobile technology [11, 34]. Satellite networks to wireless communications and mobile computing for global coverage will be efficiently used in 6G which was not used before [35]. The 6G wireless mobile technology maximizes data throughput and improves system performance. The 6G technology is responsible for enhancing data transfer and data security. It also increases data configuration choices. In 6G technology, devices connected to the Internet by using wireless broadband receive 10 GB or even more data speed. 6G is a satellite-based network; roaming and handover from one satellite to another satellite is still an issue that will be solved soon. The combination of fiber optics and the latest radio technology is used in 6G, to provide a very high data rate. The 6G wireless mobile technology will change the way of thinking and will perform beyond the expectation of the users [35]. Moreover, this performance depends on technology use in NGN.

Numerous proposals have been presented by researchers to establish the performance of NOMA in both downlink and uplink. The basic principle of downlink NOMA is presented in [36], power division is used for multiple user access at BS, and SIC is used for signal detection at the receiver. In [37], researchers proposed a two-user model for NOMA. Researchers presented link-level simulations and system-level simulations for the NOMA downlink system. Results provided in [37] showed that NOMA performance is better than OMA in terms of overall system throughput and individual user throughputs. The authors in [37] derived the closed-form expressions for outage probability and ergodic sum-rate for the NOMA downlink system. To find the effect of user pairing for the two-user model of the NOMA system, the authors employed statistically allocated transmit powers among NOMA users [38]. Moreover, the authors proposed fixed and opportunistic user pairing schemes. In [17, 39], the authors considered the consequence of power allocation on fairness. To ensure that users are getting an equal share of system resources, the fairness index should be close to 1. The authors proposed a power allocation scheme to maintain the fairness index. In [40], the authors used the concept of user pairing; the authors paired strong channel users along with weak channel users for the cooperative NOMA system through imperfect CSI and perfect CSI feedback. The authors in [41] presented NOMA-aided precoded spatial modulation in which researchers combined NOMA with MIMO. Researchers also presented a comparison with OMA in terms of implementation cost, multiuser interference, spectral efficiency, and performance gain of the system. In [42], the authors proposed full-duplex NOMA relaying based Device-to-Device (D2D) communication. The authors in [42] proposed the solution for the D2D power allocating problem by presenting a linear fractional programming-based power allocation scheme.

The basic principle of uplink NOMA is presented in [43], the SIC signal detection scheme is utilized at BS, and the power control scheme is used at the user side. The authors investigated the challenges of joint power allocation and subcarrier assignment and the authors designed a suboptimal solution to increase the sum-rate of the NOMA cluster. In [44], the researchers derived the closed-form expressions for outage probability and system capacity for the two-user model of the NOMA uplink system. The researchers investigated the static power allocation for multiple users and recognized that a user could be in outage without proper selection of the

required data rate. In [45], for the uplink NOMA system, the authors presented an adaptive power control scheme which is based on evolutionary game theory. To enhance users' throughput or payoffs, the proposed power control scheme allows users to adaptively adjust their transmit power level. SIC is used for signal detection at the receiver. In [46], researchers provided the advantages and challenges of NOMA as a contender scheme in dense networks. The authors compared the performance of NOMA in uplink systems. To compare the performance of WSMA-based NOMA and multiuser MIMO, researchers presented link-level evaluation results. In [47], the authors provided a foundation to investigate multicell uplink NOMA systems. The authors considered the coverage probability of a NOMA user with high interference at the BS due to a large number of co-channel NOMA transmitting users. The authors in [47] provided closed-form expression of the rate of coverage by characterizing the Laplace transform of the intercluster interference in different SIC scenarios. Afterward, the authors characterized the Laplace transform of the intercluster interference through distance distribution from geometric probability. To evaluate the benefits of NOMA, in 2018, 3GPP considered NOMA as a research icon and provided guidelines to support NOMA, in comparison to the OMA [48]. Table 2.1 summarizes the review of NOMA.

Table 2.1:: A state-of-the-art review of NOMA.

Ref.	**Objective**	**Solution Approach**	**Category**	**Tech.**
[49]	Improvement in reliable detection, maximum diversity gain, and reduced system complexity.	The highest diversity gain with minimum outage probability is achieved by Cooperative PD-NOMA (Co-PD-NOMA). User pairing is used as a promising solution to reduce system complexity.	Single carrier Power Domain	Co-PD-NOMA

[5]	Achieve fairness performance of the NOMA scheme better than TDMA under perfect and average CSI.	Investigated power allocation techniques that ensure fairness by formulating the research problems as nonconvex optimization.	Single carrier Power Domain	PD-NOMA
[50]	Further improvement of the outage performance of MIMO-NOMA.	Improvement is achieved by implementing detection and precoding matrices for MIMO-NOMA.	Single carrier Power Domain	MIMO-NOMA
[51]	Design resource allocation algorithm for multicarrier NOMA systems. To ensure that full-duplex BS simultaneously serves multiple half-duplex uplink and downlink users.	An algorithm is designed in which the solution of a nonconvex optimization problem is used as weighted sum system throughput maximization for multiple half-duplex uplink and downlink users simultaneously served by a full-duplex BS.	Multi-carrier Power Domain	MC-NOMA
[52]	Optimize power allocation and subchannel assignment to increase energy efficiency for the downlink NOMA system.	For subchannel multiplexed users, a low-complexity suboptimal algorithm is presented, which comprises of power proportional factor determination and energy-efficient subchannel assignment.	Single carrier Power Domain	PD-NOMA
[53]	Improve the link-level performance of SCMA in highly overloaded scenarios.	Proposed an iterative multiuser SCMA receiver by employing channel coding which uses the coding gain and diversity gain.	Multi-carrier Code Domain	SCMA

[54]	Maximize the mutual information in SCMA.	The mutual information is maximized between continuous output and discrete input using an iterative codebook optimization algorithm.	Multi-carrier Code Domain	SCMA
[55]	Substantially minimize the hurdles of the Message Passing Algorithm (MPA) scheme.	For uplink SCMA systems, a Shuffled-MPA (S-MPA) scheme is proposed, based on a serial message update strategy.	Multi-carrier Code Domain	S-MPA
[56]	Reduce the decoding hurdles of the current MPA.	Based on list sphere decoding, a low-complexity decoding algorithm is proposed. The LSD only works with signals inside a hypersphere by evading the extensive search for all possible hypotheses.	Multi-carrier Code Domain	LDS
[57]	Minimize the hurdles of the SCMA decoding.	Proposed a Monte Carlo Markov Chain based SCMA (MCMC-SCMA) decoder which gets benefited from the linearly increasing complexity of the MCMC method.	Multi-carrier Code Domain	MCMC
[58]	Maximize the sum-rate subject to QoS and system-level constraints like power constraint.	Sum-rate is increased by multiple users utilizing the same SCMA codebook. The PD-NOMA scheme is utilized for user signal non-orthogonality.	Power & Code Domain	PD-SCMA

[59]	For random signature selection, allow grant-free transmission to achieve high overloading.	Introduced a blind multiple user detection for MUSA systems by using a special blind detection algorithm.	Single carrier Code Domain	MUSA
[60]	For the paired users, optimize the modulated symbol mapping.	MUSA is considered in relation to SIC by using mirror constellation BER.	Single carrier Code Domain	MUSA
[61]	To permit a simple multiuser interference cancellation by using family of short length complex sequences.	Successive/Parallel Interference Cancellation with Minimum Mean Square Error (SIC/PIC-MMSE) is proposed for appropriate MUSA receivers.	Single carrier Code Domain	SIC/ PIC-MMSE
[62]	Increase user overloading and decrease multiuser interference.	The pool of the Spreading Sequences (SS) is enlarged by using non-orthogonal dense SS to increase user overloading and reduce multiuser interference.	Single carrier Code Domain	MUSA
[63]	To further enlarge the coverage area and improve transmission reliability.	With forward relay and half-duplex decode, an uplink Cooperative PDMA (Co-PDMA) scheme is utilized.	Single carrier Code Domain	Co-PDMA
[64]	Increase the performance of PDMA uplink system by using diversity gains and coding potentials.	By using diversity gains and coding potentials, an Iterative Detection and Decoding (IDD) algorithm is developed for an advanced PDMA receiver.	Single carrier Code Domain	IDD

[65]	Avoid error propagation by using the cyclic redundancy check.	Based on the Minimum Mean Square Error (MMSE) channel decoding and detection, a novel iterative decoding and detection algorithm is proposed which is known as the SIC iterative processing algorithm.	Single carrier Code Domain	SIC-MMSE
[66]	Propose power allocation and pattern assignment in the downlink PDMA system.	To optimize the overall throughput of total users - based on the optimum Iterative Water-Filling (IWF) algorithm - a Joint Pattern Assignment and Power Allocation (JPPA) scheme is presented.	Single carrier Code Domain	JPPA & IWF
[67]	Improve security by changing the signal's identity.	Physical layer security system is presented based on Constellation Scrambling (CS) and Multiple Parameter Weighted Fractional Fourier Transform (MP-WFRFT).	Single carrier Code Domain	MP-WFRFT

NOMA is a diverse multiple user access scheme as compared to other established and existing multiple access schemes such as OMA. At the transmitter side, NOMA deliberately introduces intercell and/or intracell interference; thus, it can utilize non-orthogonal transmission. At the receiver side, the SIC technique is used to decode the desired signal. In comparison with OMA, the complexity of the receiver is increased in NOMA along with better spectral efficiency. Hence, the fundamental concept of non-orthogonal access is to achieve high spectral efficiency at the cost of receiver complexity. Therefore, this enhancement in chip processing technology makes the non-orthogonal access scheme possible.

2.1.2.1 Power Domain Non-orthogonal Multiple Access

The NOMA scheme consists of two key technologies. One is PD-NOMA, and the other is CD-NOMA. PD-NOMA efficiently utilizes the SIC scheme to perform multiuser detection. SIC is a famous physical layer interference cancellation scheme used to receive two or more users' signals simultaneously [19]. SIC performs efficiently in comparison to the existing scheme which causes degradation of the signal. In the SIC scheme, the strongest signals are subtracted from the received combined signal one after another by the SIC receiver; finally, the SIC receiver extracts the desired signal. It is a gradual interference elimination strategy, shown in Fig. 2.4.

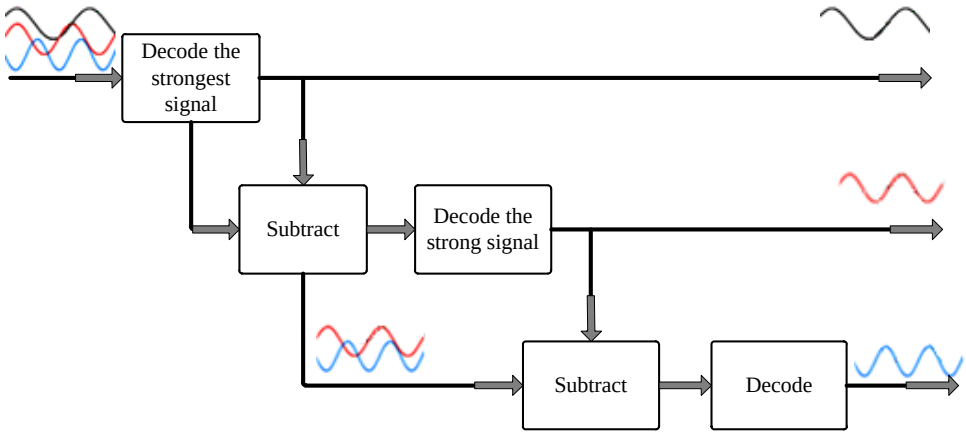

Figure 2.4:: SIC scheme.

SIC scheme is also used in CDMA to eliminate Multiple Access Interference (MAI). First, the MAI introduced by the user could be eliminated with the help of a signal amplitude recovery process by subtracting the individual user's amplitude one at a time from the received signal. The same process is carried out repetitively to subtract remaining users and to decode the desired signal [68]. Secondly, the PD-NOMA scheme uses the power domain technology i.e., PDM, which was not used efficiently in previous schemes as used in the PD-NOMA. In the PD-NOMA, non-orthogonality is deliberately introduced. In fact, power dissimilarity among paired users and implementation of SIC within the power domain ensures that user detection is concurrent. PD-NOMA is different from the other common methods used previously to control power. Also, an algorithm is needed to be used for power

distribution at the BS [69].

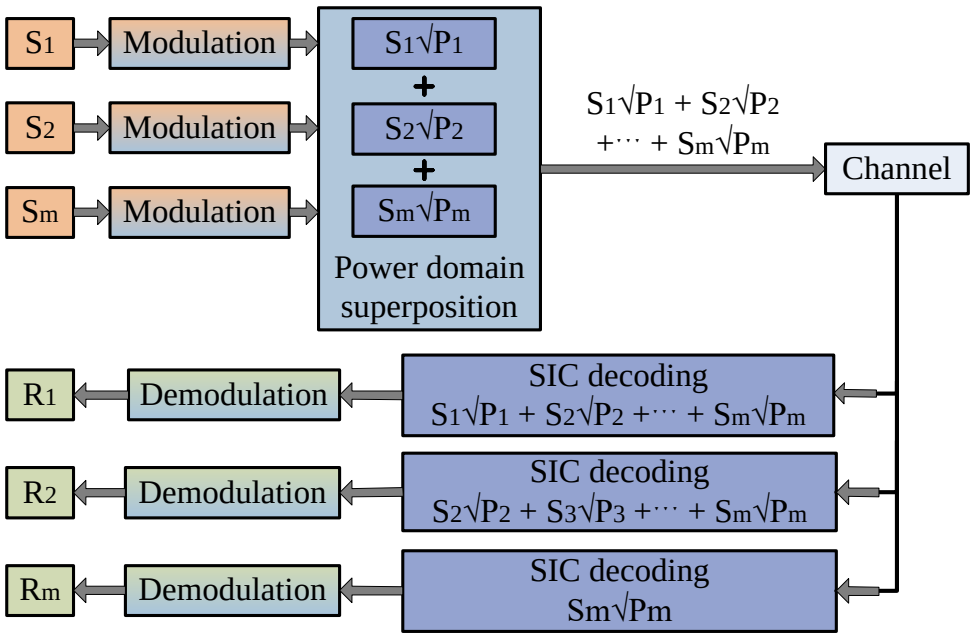

Figure 2.5:: PD-NOMA system with SIC.

Fig. 2.5 illustrates the PD-NOMA system with a SIC computation unit. Users are uniformly distributed in among every cell. With different transmission powers of multiple users in each subband, the BS simultaneously performs downlink transmission for multiple users.

Several single users can be scheduled at the same time for the same subband by implementing the proportional fair scheduling scheme at BS in the PD-NOMA system. The scheduling procedures for users are described in Fig. 2.6 [70]. First, the BS selects sets of users known as the NOMA candidate user set, in which total users cannot exceed N_{max}. The selected user set is prepared by using the total number of possible combinations of users within one single cell. Secondly, for every user set, BS allocates the transmission power by using a power allocation scheme. The scheduling matrix for the corresponding user set is estimated on behalf of power assignment ratios. Thirdly, with the help of the maximum scheduling matrix, the scheduler decides the candidate user sets on each subband for data transmission. Finally, for every allocated subband, the scheduler estimates equivalent SNRs for every single scheduled user. The coding and modulation scheme determines the SNR for each user [70].

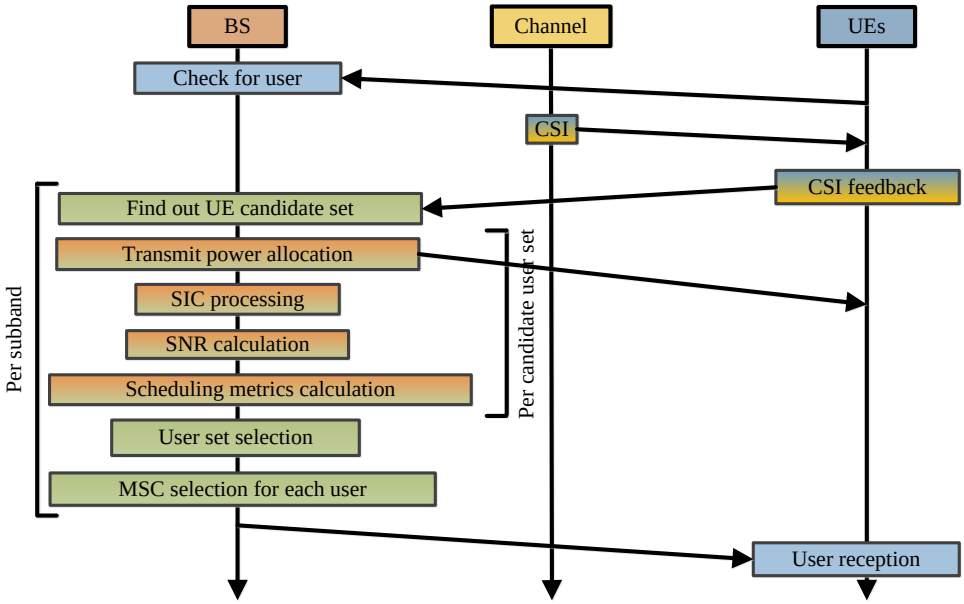

Figure 2.6:: Scheduling algorithm for PD-NOMA.

In PD-NOMA, the total transmitted power P is divided among multiple users. Let a group of k UEs be located under the same BS. Therefore, the fraction of power allocated to the k_{th} user by BS is P_k, where $P_k + \sum_{k-1}^{i=1} P_i = P$. A typical NOMA system model is shown in Fig. 2.5. The received signal at the k_{th} receiver can be written as:

$$y_k = s_k\sqrt{P_k}h_k + \sum_{k-1}^{i=1}\sqrt{P_i}h_i \tag{2.15}$$

where $s_k\sqrt{P_k}h_k$ is the received vector for the k_{th} user and $\sum_{k-1}^{i=1}\sqrt{P_i}h_i$ is the interference due to other users. For the PD-NOMA downlink system [71], the SNR of the k_{th} user can be written as:

$$SNR_k = \frac{P_k|h_k|^2}{\sum_{k-1}^{i=1} P_i|h_k|^2 + N_0B} \tag{2.16}$$

Also, throughput for the k_{th} user can be written as:

$$R_k = B\log_2\left(1 + \frac{P_k|h_k|^2}{\sum_{k-1}^{i=1} P_i|h_k|^2 + N_0B}\right) \tag{2.17}$$

where P_k and P_i are power allocated to the k_{th} and i_{th} users, h_k is the channel gain coefficient for the k_{th} user, N_0 is the noise density, and B is the bandwidth.

2.1.2.2 Sparse Code Multiple Access

By means of a typical NOMA technology, SCMA is considered as the most promising next-generation multiple access scheme for communication networks. SCMA combines LDS and Multidimensional Modulation (MDM) through the SCMA encoding process [72]. In MDM, the number of propagating modes is scaled to the number of available carrier dimensions, which is known as coded modulation. For a small set of subcarriers, each user spreads its data via a distinguished LDS. In this way, more than one user can share each subcarrier as there is no exclusivity in the subcarrier allocation. At every subcarrier, a user can have a relatively small number of interferences as compared to the total number of users. In SCMA uplink scenarios, codebook sets are assigned to every user and each user selects the random codewords from the dedicated codebook sets. All of the users' codewords are multiplexed and shared at the same orthogonal medium i.e., the OFDM subcarrier, illustrated in Fig. 2.7 [73]. On that account, the multidimensional codebook plays a crucial role in SCMA systems.

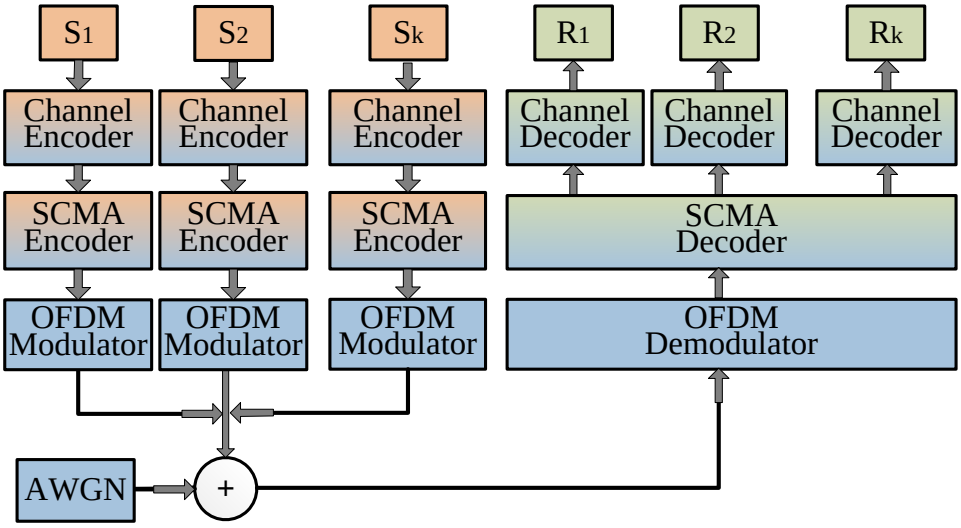

Figure 2.7:: SCMA uplink system with k users.

In the SCMA system, a map is defined as an SCMA encoder in which from $\log_2(K)$ to K bits of M-dimensional complex codebooks are available. M represents the spreading factor of the system, which is the length of an SCMA codeword. Sparse

vectors are equal to $N(N < M)$ which are the nonzero entries of M-dimensional complex codewords from the codebook. If $N = 2$, two-dimension constellation points can be mapped over $m > 2$ resources. A user could be configured with a codebook by using a contention-based multiple access scheme for uplink transmission [74]. An M-dimensional codeword is carefully chosen from the codebook to be is used for mapping a user's data bits for transmission on M radio resources (Fig. 2.8 [75]) which are subcarriers of the OFDMA scheme. Each block of SCMA is transmitted over M number of OFDMA tones.

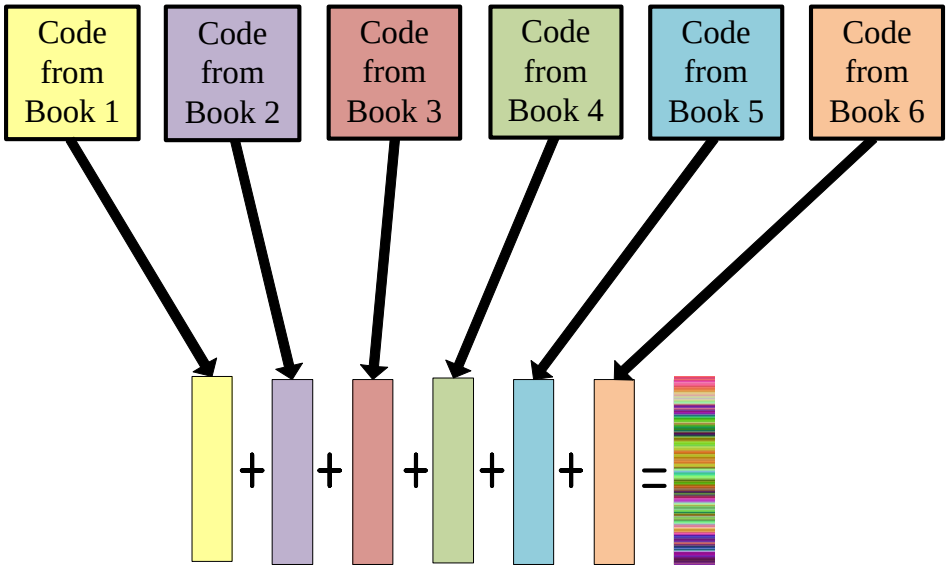

Figure 2.8:: SCMA code multiplexing.

Let an SCMA uplink system with K numbers of users or codebooks, where M is the length of the codeword and O is the number of the nonzero elements present in each codeword. d_k is the distance between k_{th} user U_k and BS. K number of users are multiplexed over M subcarriers. The received signal from all subcarriers $y = [y_1, y_2, y_3, \cdots, y_m]^T$ at BS can be written as:

$$y = \sum_{k=1}^{K} \sqrt{\frac{P_k}{O}} \text{diag}(f_k)\text{diag}(h_k) + N \tag{2.18}$$

where P_k is the transmission power of user U_k. $x_k = [x_{k1}, x_{k2}, x_{k2}, \cdots, x_{km}]^T$ are the codewords or transmitted symbols of user U_k. The channel coefficient vector for user U_k is $h_k = [h_{k1}, h_{k2}, h_{k3}, \cdots, h_{km}]^T$.

For the SCMA uplink system [76], the average SNR can be written as:

$$SNR = \sum_{k=1}^{K} \frac{f_{km} P_k |h_{km}|^2}{O d_k^{\alpha}} \tag{2.19}$$

For the SCMA uplink system [76], the average sum-rate can be written as:

$$R = \sum_{m=M}^{K} E\left(\log_2\left(1 + \sum_{k=1}^{K} \frac{f_{km} P_k |h_{km}|^2}{O d_k^{\alpha}}\right)\right) \tag{2.20}$$

where α is the path loss exponent, E is the transmitted signal energy, h_{km} is the channel gain for the k_{th} user on the m_{th} subcarrier, f_{km} is the subcarrier index, and P_k is the power for the k_{th} user.

2.1.2.3 Multiuser Shared Access

MUSA uses the Advanced-SIC (A-SIC) scheme and good criterion SS. In SS, the data bit sequence is encoded per codeword. Moreover, the same number of codewords could be encoded by utilizing the encoder at the same time. Afterwards, the coded bits are permuted (arranged in all possible ways) through random interleaving patterns. If a large number of interleaving patterns are used, the permuted sequence would be statistically independent. The coded sequence is distributed to each subcarrier after modulation on the quadrature amplitude modulation scheme [77].

MUSA uses special SS, for spreading multiple users' individual data. After that, the user's spread data is overlapped and transmitted. For recovering and demodulating the data of individual users at reception, MUSA uses an A-SIC receiver. The basic idea is illustrated in Fig. 2.9 [78]. To allow grant-free transmission and maintain a higher overloading factor of users, the nonbinary complex spreading codes at the SIC receiver can be used.

The SIC algorithm is utilized by the SIC receiver to achieve non-orthogonality among users. It is designed to reduce the power, delay, and complexity - in case a requirement arises by short spreading codes and large user overloading. A good choice is to use one of the types of Multicode Complex Domain (MCCD). Due to the design flexibility with the imaginary part and real part, the length of multi-MCCD

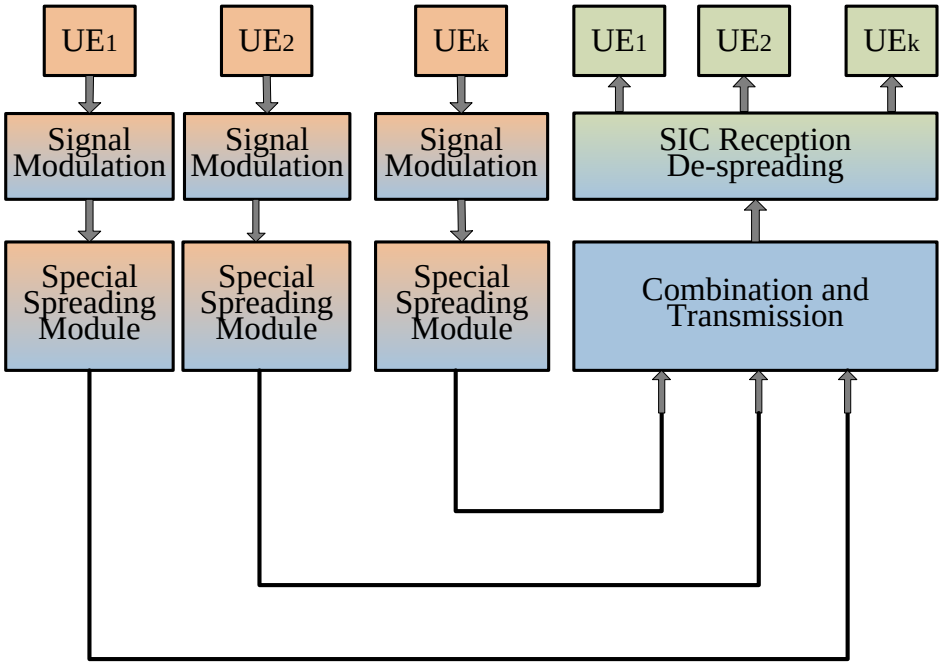

Figure 2.9:: Multiuser shared access.

could be shortened. The sequence with component ± 1 is a type of complex spreading code that might be created as shown in Fig. 2.10 [78]. Moreover, Fig. 2.10 shows the real and imaginary parts of the code for $M = 2$ and $M = 3$. Therefore, before normalization, all elements of the complex spreading codes are just elements of the set $\{1 - i, -1 - i, -1 + i, 1 + i\}$ because the values of the imaginary part and real part contain 1 and -1. The maximum number of existing codes is 4^L for the code length L. In the current scenario, the maximum existing code is 256 for the code length of 4, which is not sufficient. Therefore, the existing elements of the set which include the imaginary part and real part need to increase, to improve the number of existing codes, which should be M-ary with $M > 2$.

Preferred value of M is 3; the sequence with components 0 and $\pm 1$is a type of complex spreading code that might be created as shown in Fig. 2.10. Therefore, before normalization, all elements of the complex spreading codes are just elements of the set $\{-1 + i, -1 + 0i, -1 - i, 0 - i, 1 - i, 0 + 0i, 1 + 0i, 1 + i, 0 + i\}$ because the values of the imaginary part and real part contain $0, 1$, and -1, that is, a 3-ary [78]. With the help of the new set, 9^L codes could be created to ensure significant improvement in the number of user access.

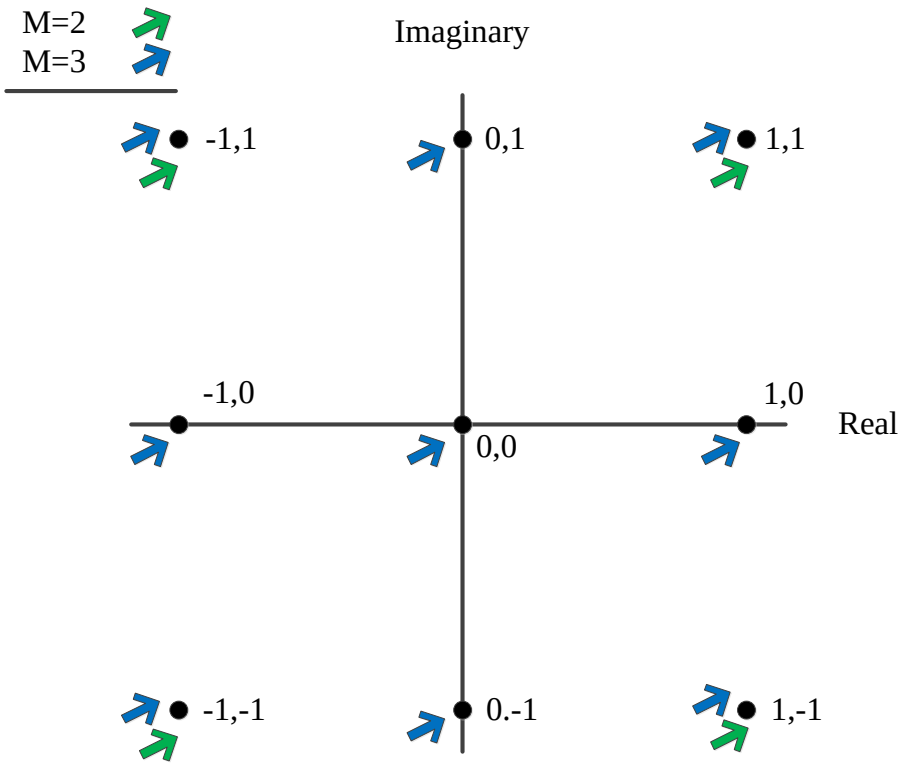

Figure 2.10:: Complex spreading code.

For multiuser detection at the receiver, SIC is used in MUSA. Linear conjunction of the received signal detects symbols of multiple users. For the linear system, MMSE is used for detecting users. The received signal can be written as:

$$y = hx + n \tag{2.21}$$

$$\tilde{x} = h^{-1}y - \tilde{n} \tag{2.22}$$

where x is the composite transmitted signal, h is the channel coefficient matrix, and n is a complex noise sample of Gaussian noise with zero mean and variance σ.

In MUSA, to detect the signal of each user at the receiver, the system computes the inverse of channel matrix h^{-1}. Through this inverse, the estimated signal $\tilde{x}$ is can be achieved. The MMSE weight matrix can be written as:

$$W_{MMSE} = \left(h^H h + \sigma^2 I\right)^{-1} h^H \tag{2.23}$$

where I is the identity matrix. Now, the estimated signal can be written as:

$$\tilde{x} = W_{MMSE}\, y \tag{2.24}$$

The SNR at the Nt_{th} antenna of the MUSA uplink system [79] can be formulated as:

$$SNR_{nt} = \frac{E_x |w_{nt} h_{nt}|^2}{E_x \sum_{t \neq nt} |w_{nt} h_t|^2 + N_0 |w_{nt}|^2} \tag{2.25}$$

Also, throughput at the Nt_{th} antenna can be written as:

$$R_{nt} = \log_2 \left(1 + \frac{E_x |w_{nt} h_{nt}|^2}{E_x \sum_{t \neq nt} |w_{nt} h_t|^2 + N_0 |w_{nt}|^2} \right) \tag{2.26}$$

where E_x is the transmitted signal energy, N_0 is the Additive White Gaussian Noise (AWGN) density, Nt is the number of transmitted antennas, h_{nt} is the Nt_{th} column of the channel matrix, and w_{nt} is the Nt_{th} row of the weight matrix. The weight matrix is constructed by using MMSE technique.

2.1.2.4 Pattern Division Multiple Access

PDMA is an emerging NOMA technique based on SIC Amenable Multiple Access (SAMA) technology [80]. PDMA utilizes Low Complexity Quasi-ML (LCQ-ML) SIC detection [81] at the reception and holistic/combined scheme of SIC Amenable (SIC-A) pattern at the transmission side. An example of the PDMA pattern with resource mapping is shown in Fig. 2.11 [82].

On four Resource Elements (REs), six users are multiplexed. First of all, a single PDMA pattern is allotted to a single user. All four REs in the cluster are used for data mapping of user 1, the first three REs are used for user 2, the first and third REs are used for user 3, the second and fourth REs are used for user 4, the third RE is used for user 5, and the fourth RE is used for user 6. For all six users, the order of transmission diversity is $4, 3, 2, 2, 1$, and 1 [82].

Different users in PDMA are separated at the transmitter through a non-orthogonal character of pattern with various domains, for example, code, space, and power domain. Particularly, at the receiver side, multiple users consist of an irregular diversity degree in order to perform SIC amenable detection. After SIC

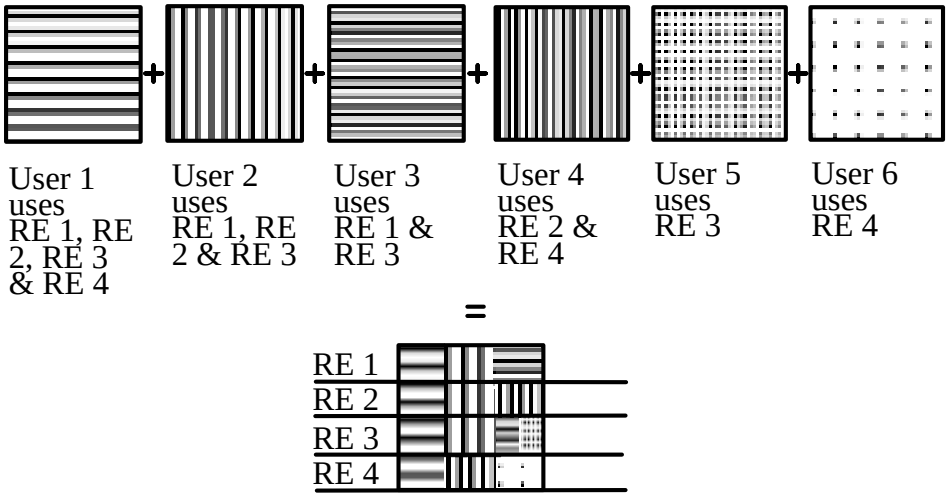

Figure 2.11:: PDMA pattern for 4 REs, used by 6 users.

amenable detection, users can acquire an equivalent diversity degree (Fig. 2.12 [82]). Ultimately, the steadiness between multiplexing and diversity degree can be achieved in PDMA [82].

At the receiver side, Nr indicates the number of receiving antennas and Nb is the number of available resource blocks. BS receives the signal of Nb resource blocks. The received signal at the Nr_{th} antenna of BS is $y_{nr} = [x_{1,Nr}, x_{2,Nr}, x_{3,Nr}, \cdots, x_{Nb,Nr}]^T$. At the Nr_{th} antenna, the received signal of the Nb_{th} resource block can be written as:

$$y_{nb,nr} = \sum_{k=1}^{K} H_{PDMA}(nb, nr) h_{nbk,nr} \sqrt{p_{nbk}} x_k + n_{nb,nr} \tag{2.27}$$

where H_{PDMA} is the $PDMA$ pattern matrix, P_{nbk} is the transmitted power of the k_{th} user at the Nb_{th} resource block, and x_k is the transmitted signal from the k_{th} user to BS. $n_{nb,nr}$ is complex AWGN in Nb_{th} resource block at the Nr_{th} receiving antenna. Using [83], the SNR at the Nr_{th} receiving antenna in Nb_{th} resource block of the k_{th} user for the PDMA system can be written as:

$$SNR_{nbk,nr} = \frac{p_{nbk} H_{PDMA(nbk)} |h_{nbk,nr}|^2}{\sum_{j \neq k}^{K} p_{nbj} H_{PDMA(nbj)} |h_{nbj,nr}|^2 + N_0} \tag{2.28}$$

Also, throughput for k_{th} user can be written as:

$$R_{nbk,nr} = \sum_{r=1}^{Nr} \sum_{b=1}^{Nb} \left(1 + \frac{p_{nbk} H_{PDMA(nbk)} |h_{nbk,nr}|^2}{\sum_{j \neq k}^{K} p_{nbj} H_{PDMA(nbj)} |h_{nbj,nr}|^2 + N_0} \right) \tag{2.29}$$

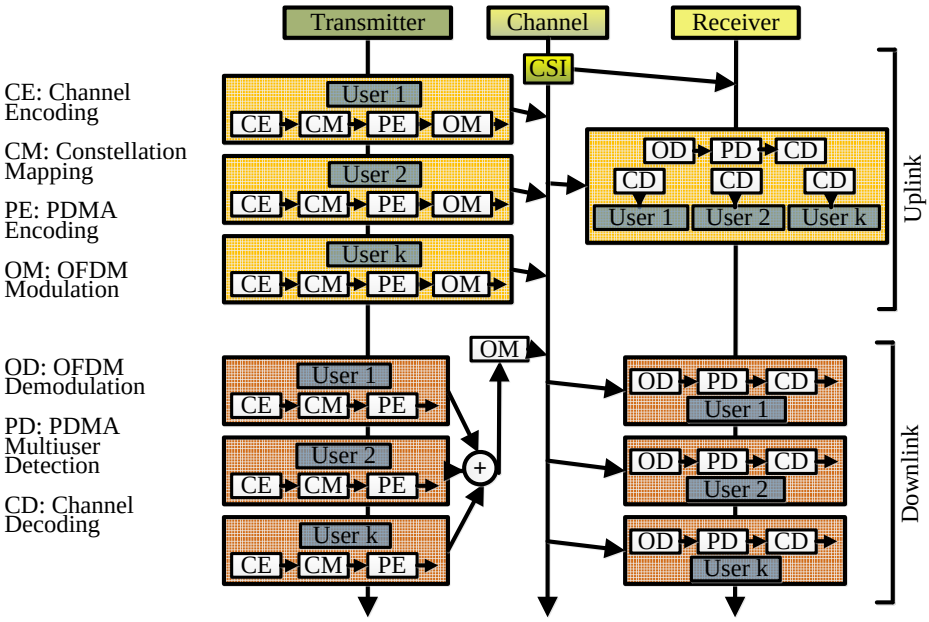

Figure 2.12:: PDMA system model.

where $h_{nbk,nr}$ is the channel gain coefficient, and N_0 is the AWGN density. Moreover, Table 2.2 highlighted the key features, advantages, and disadvantages of major categories of NOMA schemes.

Table 2.2:: Feature of different NOMA schemes

Type	Advantage	Disadvantage	Key feature
PD-NOMA	(i) Unaffected by apparent near-far. (ii) 20% increased uplink spectral efficiency. (iii) 30% increased downlink throughput [84].	(i) Improvement in chip technology is required due to the high complexity of the receiver. (ii) PDM is in the research phase. (iii) SIC increases the system signaling overhead.	(i) PD-NOMA utilizes PDM for multiple user access. (ii) SIC scheme is used at the receiver. (iii) PD-NOMA takes advantage of different channel conditions.

SCMA	(i) 3 times increased spectral efficiency. (ii) 2.8 times increased uplink system capacity. (iii) 8% and 5% increased coverage gain and downlink throughput respectively [84].	(i) Difficult process of optimization and code design. (ii) Increased interference among users. (iii) High-Dimensional Modulation (HDM) is required.	(i) Sparse SS based on LDS-OFDM is utilized. (ii) Spreading with low-density signatures and bit-to-constellation mapping are combined. (iii) Users' codewords are taken from codebooks that are created by multidimensional constellation.
MUSA	(i) Reduced Block error rate. (ii) Provides support to a huge number of users. (iii) 1.5 times increased spectral efficiency [84].	(i) Increased interuser interference. (ii) Complex spread symbol design.	(i) MUSA is an upgraded scheme of CDMA via code domain multiplexing. (ii) MUSA achieves higher overloading through low-correlation SS at the transmitter side. (iii) MUSA utilizes SIC to decode superimposed symbols at the receiver.

PDMA	(i) 2-3 times increased uplink system capacity. (ii) 1.5 times increased spectral efficiency for the downlink system.	(i) Complex design and pattern optimization. (ii) Increased interference among users.	(i) Non-orthogonal patterns are used in PDMA. (ii) Multiplexing is achieved in the space, power, code, and composite domain. (iii) Code domain multiplexing is similar to SCMA. (iv) LCQ-ML SIC detection is utilized in PDMA.

In addition, technologies used in different types of non-orthogonal access schemes are presented in Table 2.3.

Table 2.3:: Technology used by NOMA.

Type	**PD-NOMA**	**SCMA**	**MUSA**	**PDMA**
PDM	•			
SIC	•		•	•
LDS		•		
HDM		•		
MPA		•		
MCCD			•	
MLD				•

As per the studies, PD-NOMA utilizes non-orthogonal transmission among the users as compared to CDMA and OFDMA. PD-NOMA has no apparent near-far problem compared to 3G. Similarly, the MAI complications are not challenging in PD-NOMA. PD-NOMA provides a simple way to respond to multiple links and

changing conditions of the link by applying adaptive modulation and coding particularly in high-speed mobile environments [85]. Therefore, it is unnecessary to use a highly accurate feedback signal or CSI from the user end in PD-NOMA. In contrast to 4G, PD-NOMA users share the same channel leading to increased spectral efficiency at the unchanged transmission [86, 87]. Besides, from a technical implementation aspect, PD-NOMA still faces several challenges. Firstly, implementation needs enhancement in chip technology in respect to signal processing as the non-orthogonal decoder is complex in design. Furthermore, the PDM scheme is under the research phase and has a long way to go [84].

As an innovative multiple-access modulation technique, SCMA offerers several improvements, for example, multidimensional constellation shaping gain along with benefits of CDMA and LDS. The link-level performance of SCMA in highly overloaded scenarios can be achieved by employing channel coding which uses the coding gain and diversity gain. Although the structure of the code is well defined, optimization and design of the code can be problematic [84]. To reduce the decoding hurdles of the MPA, LSD-based a low-complexity decoding algorithm is used in SCMA, in which the LSD only works with signals inside a hypersphere by evading the extensive search for all possible hypotheses.

Uplink access in MUSA utilizes an advanced complex multidomain code structure and multiuser decoding on the basis of SIC. In order to confirm unlimited reliable access at the same frequency-time slot for multiple users, MUSA makes the procedure of resource allocation simpler in the access scheme. This is done to cuts the access time, making the system implementation simpler and minimizing energy utilization. MUSA downlink access utilizes superposition symbol expansion and superposition coding scheme, to offer better capacity as compared to downlink transmission provided by the OMA. Additionally, uplink access in MUSA helps to decrease the energy consumption and make the implementation of user terminal simpler which is the same as MUSA downlink [84].

PDMA has the capacity to increase the performance of the spectrum utilization for the downlink system by 1.5 times and increases capacity in the uplink system by 2-3 times [15]. To improve the security in the PDMA system, CS with MP-WFRFT is utilized. To avoid error propagation, MMSE channel decoding and

detection-based SIC iterative processing are used in the PDMA system. Co-PDMA is used in connection with forward relay and half-duplex decode in order to further enlarge the coverage area and improve transmission reliability. However, PDMA needs to cater to some important challenges in future applications. These include designing simpler receivers, designing patterns at the transmission end to discriminate users without difficulty, and combining MIMO with PDMA in order to develop space domain coding design, etc.

2.1.2.5 Recent Development

The race for developing 5G technology has integrated NOMA with different communication technologies, such as NOMA-based communication for the Tactile Internet, NOMA for D2D communication, Cognitive Radio NOMA (CR-NOMA), and SWIPT-NOMA-based communication is discussed further. A brief review of recent developments in NOMA is as follows. The authors in [88] presented NOMA-based application for specific communication such as the Tactile Internet, through which heterogeneity can be achieved in 5G networks. Tactile Internet allows non-orthogonal resource sharing from a pool of massive machine-type communications, ultra-reliable low latency communications, enhanced mobile broadband, and critical machine-type communication devices from the same BS. The authors in [88] summarized many different types of NOMA and their appropriateness for low latency Tactile Internet-based applications. Additionally, the authors in [88] presented a sample case of a health-care based network and explained how in the health care domain NOMA-based architecture can be utilized for low latency networks.

In [89], the authors used NOMA at the D2D transmitter to improve the spectral efficiency of the network. The authors proposed in [89] the Tactile Internet driven delay assessment for D2D communication scheme to resolve the issue of interference and delay from the neighboring nodes in two-hop transmission. In the first phase at relays (intermediate nodes), full-duplex communication is used for the first and second hop transmission at the same time. Afterward, at D2D transmitter, transmission rate is improved using Tactile Internet-based communication. In the second phase, to reduce the cochannel interference and increase the throughput of

the cell edge users, pricing-based 3D matching is proposed by the authors. Furthermore, authors in [89] used Successive Convex Approximation (SCA) with less complexity in order to optimize the power of the D2D transmitter. SCA converts the nonconvex optimization problem of power control and subchannel allocation into the convex problem.

In [90], to improve the sum-rate of the femtocell users, researchers proposed a joint power control and channel allocation algorithm by utilizing CR-NOMA at the femtobase station. The authors used the channel gain difference among weak and strong user pairs in the proposed algorithm. This reduced the interference between NOMA users and improved channel utilization. Furthermore, to provide the QoS for weak users, the authors differentiated the odd and even numbers of users in a femtocell. The aforementioned scheme, OMA, is utilized to obtain a preset data rate by a greedy channel allocation algorithm.

The authors in [91] presented a subchannel assignment scheme for SWIPT-NOMA-based Heterogeneous Networks (HetNets) with imperfect CSI for the downlink system. Furthermore, the many-to-many matching theory is presented by authors to formulate the subchannel assignment. Considering imperfect CSI, the authors in [91] presented the energy-efficient subchannel assignment as a nonconvex probabilistic optimization problem. The many-to-many matching theory is utilized by authors to deal with this problem. The authors used SWIPT and NOMA with macrousers and pico/femtobase station, in which multiple users served by NOMA simultaneously and SWIPT harvest energy from the radio frequency signals. Both techniques increase the energy efficiency of the network.

In [92], to maximize the sum-rate and spectral efficiency of femtousers with guaranteed QoS, the authors investigated the NOMA transmission with 5G enabled cognitive femtocell. To reduce the NOMA interference among multiple femtousers, a pairing algorithm between weak and strong users was presented. Moreover, the sum-rate for an even/odd number of femtousers in order to achieve a higher data rate was calculated.

2.1.2.6 Research Challenges

This section presents challenges faced by the major categories of NOMA, contributions of NOMA in enabling the 5G network, integration with different communication technologies, and recent research trends. However, several challenges still need to be catered to in future research. Following some are significant challenges of NOMA.

Imperfect SIC Cancellation In practical circumstances during SIC processing, some residual interference remains in the system which makes the SIC scheme is imperfect. Therefore, in theoretical analysis, need to consider this imperfect cancellation aspect. Furthermore, error propagation in SIC is also a major problem. This indicates that when the higher-order user decodes erroneously, the error will sequentially propagate to lower-order users.

Imperfect CSI The analysis of the recent work on NOMA reveals that researchers assumed a perfect CSI to implement multiuser interference cancellation at the user receiver or resource allocation at BS. However, perfect CSI is impossible in practical scenarios. Therefore, real-time NOMA systems work with channel estimation errors. For this reason, in the theoretical analysis of NOMA, it is imperative to consider channel estimation errors and imperfect CSI.

Design of Spreading Sequences or Codebooks In SCMA, codebook design is still an issue particularly, for outsized higher-dimensional codebooks. For further performance improvement of SCMA, the joint design of the factor graph matrix and constellation construction is required - which can be achieved by advance multidimension constellation. Furthermore, to improve link adaptation, the design scheme - for the case of all the overloaded users having different codebook sizes (transmission rate) - needs to be investigated. Moreover, to determine the performance and capacity under practical scenarios, researchers have to consider error propagation in codebook allocation in theoretical analysis.

Receiver Complexity Contrary to OMA schemes, in NOMA, SIC needs additional implementation complexity, because the SIC receiver must detect and cancel other users' signals prior to detecting its own signal. Moreover, as the number of users in the cell increases, the receiving complexity also increases. Thus, a high-performance nonlinear detection algorithm is required at each stage of SIC for error-free propagation.

Heterogeneous Networks A wireless network containing nodes with different coverage sizes and transmission powers is known as a HetNet. The HetNet helps in increasing coverage and capacity with reduced energy consumption for future wireless networks. Real-time NOMA allows sharing of resources for different types of networks. To improve the system throughput of HetNets, heterogeneous collaborative communication schemes with NOMA should be investigated.

Other Challenges Several other challenges of NOMA systems must be addressed, including signal design and channel estimation, maintaining system scalability, the reduction of the Peak to Average Power Ratio (PAPR) for multicarrier NOMA, the difficulties of channel-quality feedback design, and flexible configuration of multiple access schemes. Researchers believe that by addressing these challenges NOMA can further improve.

2.1.2.7 Future Trends

NOMA has received huge attention in modern developments, therefore, researchers prefer NOMA for future networks. Some future research trends are NOMA in large-scale HetNets, full/half-duplex user relaying in NOMA systems, NOMA for wireless powered IoT networks, NOMA-based massive MTC networks, adaptive NOMA/OMA mode-switching, NOMA systems over $k-\mu$ shadowed fading channels, in large-scale underlay cognitive radio networks, and NOMA with spatial modulation [93].

In-depth review of NOMA, non-orthogonality is introduced deliberately either in code, frequency, or time. NOMA systems can be categorized into two cate-

gories; CD-NOMA and PD-NOMA. In PD-NOMA, on the basis of the large power difference between the users, PD-NOMA differentiates signals at the receiver by using the SIC scheme. All users utilize the same time-frequency. In PD-NOMA downlink, farther users get more power than nearby users and nearby users perform more SIC than the farther user. For the uplink, to extract the signal of different users, the SIC scheme is used at BS. In code-domain multiuser access, CD-NOMA allocates different codes to users and multiplexed over the same time-frequency. On the other hand, in OMA the total bandwidth is divided into multiple small sub-band, each user utilizes a dedicated sub-band. This sub-band is mathematically orthogonal and referred to as a subcarrier. [68, 94, 94].

The BER performance of CD-NOMA and PD-NOMA degrade in the presence of IN. At higher SNR, PD-NOMA provides better results as compared to CD-NOMA. Higher transmitted power reduces the effect of lower amplitude of IN. Therefore power domain access provides robustness to PD-NOMA against IN. One of the major issues for PD-NOMA is power allocation for the dynamic users which is eliminated in SG due to static users/SMs. Furthermore, in CDMA, complex decoding algorithm is required for decoding non-orthogonal code. Hence, the CD-NOMA receiver is more complex than the PD-NOMA receiver. Under such conditions, the PD-NOMA among all NOMA schemes is expected to be the best candidate for SG.

2.2 Next Generation Networks

The rapid development of connected devices and intelligent terminals (intelligent terminals include memory and processor), is expected in near future. The number of devices supported by the NGN is expected to grow 100 times more than the current generation networks. Thus, the throughput capacity per unit area of NGN (specifically of the busy area) also needs to increase by a factor of 1000 (at least 100 Gbps/km^2 or more). The NGN is expected to manage 10 times more simultaneous connections as compared to the current generation. Through NGN, users will have more data rates especially in emergency vehicles, high-definition medical image transmission services, and other special conditions. NGN is expected to proficiently achieve greater network efficiency and high data rates. NGN will propose adaptable and scalable services, as it will provide a faster, smarter, and more efficient network.

It will also offer remote access to many real-time services and ultra high definition multimedia experience [95].

2.2.1 Internet of Things

In this day and age, IoT has become a popular trend. IoT is a network of interconnected physical things (objects) use to connect and exchange data of these objects with other systems and devices over the Internet with the help of software, sensors, and other technologies.

2.2.1.1 Challenges

Bandwidth limitation: The advancement of IoT devices and their addition into next-generation intelligent systems creates a massive increase in network bandwidth requirements. The bandwidth issue is worsened by another feature of IoT applications: deployment of IoT devices is typically in large numbers, resulting in an inconvenient situation in which many high data rate devices compete for extremely limited network bandwidth within a small coverage area [96].

Energy Harvesting: One of the most significant challenges in implementing IoT is ensuring that IoT devices have constant and sufficient power. Because the majority of IoT devices in the field suffer from energy shortage due to battery power limitations. Recently, a research proposed radio frequency energy harvesting as an alternative to battery for IoT devices. The RF source is more reliable and adjustable in terms of ensuring a certain level of essential energy transfer. Furthermore, RF with beamforming can send power to IoT devices in any direction that are far away from the transmitting side [97].

Noisy Channel: Nevertheless, impulsive electromagnetic interference, also known as IN, is a problem in many IoT systems that require an ultra-high reliability mitigation scheme. Impulsive interference degrades the signal quality to the point of reception failure and also increases bit errors, causing system reliability to decrease.

Therefore, IN degrades overall system performance. For the implementation of reliable communication systems, analysis and mitigation of IN are essential [3].

2.2.2 Vehicular Ad Hoc Networks

Vehicular Ad hoc Network (VANET) is among the NGN that allows vehicles to communicate with each other and with roadside units at a short range of 100 to 300 meters. The primary goal of deploying VANET is to address the issue of accidents. It has a wide range of applications for human safety and for drivers to drive safely on city roadways [14].

2.2.2.1 Challenges

Bandwidth limitation: The IEEE 1609 Wireless Access standard allocates 75 MHz (seven channels with 10-20 MHz) out of 5.9 GHz frequency spectrum for VANET communication [98]. It uses orthogonal modulation for a short range of up to 1000 meters with a maximum data rate of 27 Mbps. More congestion occurs when the number of mobile nodes increases. Communication with other vehicles using limited bandwidth becomes an issue in a high-traffic environment. To avoid this difficulty while maintaining high bandwidth efficiency, a suitable communication infrastructure should be developed [99].

Latency: Considering the dynamic nature of the VANET and the mobility of vehicles, reducing transmission latency is a significant challenge. The majority of existing VANET schemes do not provide low latency transmission via a wireless link to share information between the vehicles and to roadside units. There are two ways to reduce the delay, firstly to decrease delay with the increment of the computation capacity and secondly to reduce execution delay, resulting in a smaller queuing delay [100].

Noisy Channel: For signal transmissions between electronic control units, in-vehicle PLC systems are under consideration. When actuators in vehicles are func-

tioning, a lot of bursty impulsive noises occur. In order to deploy a communication system, it is imperative to analyze communication environments that are primarily characterized by channel propagation and noises. To develop reliable communication systems, measurement and analysis of IN - caused by electromagnetic disturbance - are essential in VANET [101].

2.2.3 Mobile Network

The next generation of wireless communications acts as the backbone of next-generation mobile networks. Next-generation mobile networks is expected to deliver video streaming, voice calls, data services, Internet visits over a transparent network. Ultimately users will able be to get their entertainment, information, and other content data from a number of sources.

2.2.3.1 Challenges

Bandwidth limitation: The main objectives of the next generation of wireless communications include high bandwidth, increase in data rates, a huge number of connected devices, decrease in trip latency, decrease in energy consumption and increase in battery life. Since the number of connected devices increases every day, new low-latency and bandwidth-hungry applications and services are also increasing on a regular basis thus, the requirement of data rate increases twofold every year. These are the primary factors that are affecting the development of new generation networks, such as 5G systems [4].

Noisy Channel: 5G utilizes the frequency spectrum of 3 GHz - 300 GHz with the wavelengths within the range of 100 mm to 1 mm, hence it is called as mmWave. The presence of IN in this frequency band contaminates signals and leads to decreased spectral efficiency and increased BER. Regardless of the high computational complexity the design of the NOMA receiver should capable of dealing with many kinds of noise including impulsive noise [102].

High Mobility: Implementation requirements, challenges, and possible solutions in respect to the 5G mobile communication network in high-mobility scenarios are discussed in [103]. The utmost challenge with fast-moving mobile users is developing a reliable content update mechanism. The reason behind this is the fact that handovers may produce significant network overhead in fast-moving user networks. Consequently, a need emerges for techniques such as the improved version of separation of control and user planes to reduce the number of handovers [104].

2.2.4 Smart Grid

SG is an integrated system that uses a two-way flow of electricity and information to improve the reliability, efficiency, and flexibility of the electricity network. The purpose of using SG is to overcome the problem of energy shortage during peak hours. SG caters to this issue by offering real-time communication between utilities and customers as well as improving power network resilience by incorporating renewable energy sources [105].

The development of SG requires power distribution networks that need flexible, scalable, secure, and end-to-end connectivity. SG intends to emphasize the amount of bandwidth required to efficiently monitor and interact with all the secondary substations of distribution networks. When considering phasor measurement units all over the power system, these concerns become even more crucial. Thus, the latency and bandwidth requirements for the SG are the two significant challenges [106].

Nevertheless, high voltage substations work in harsh environments in which electromagnetic disturbance causes IN. The electromagnetic disturbance is due to electrical switching, transient processes, and partial discharge. It is imperative to consider IN in a high voltage environment because only the analysis of the ambient or thermal noise (usually referred to as Gaussian noise) is insufficient [107].

The SG consists of two parts: bidirectional energy flow and two-way information exchange. The idea of bidirectional energy delivery can be described as energy produced by the power station and supplied to the consumers and/or vice versa. The approach of two-way information exchange can be described as the abil-

ity of power companies and consumers to access instantaneous information, utilize dynamic energy flows, and receive different energy parameters at the same time. Information streams gather and carry the data for observing and supervisory the dynamic power flows.

For the precise operation of multiple subunits of SG, communication infrastructure plays an essential role by exchanging instantaneous information between devices and systems associated with SG. In SG, SMs are placed at the customer side for exchanging information with electric supply utility via Advanced Metering Infrastructure (AMI). The SM provides the facility to collect data with the help of communication infrastructure and control applications by utilizing two-way communication. The SM is also used to manage, monitor, and sense bidirectional power flow. Moreover, SMs are used to support decentralized generation, collect statistics about the utility, inform about the storage of energy devices or systems, and compose the metering units [108].

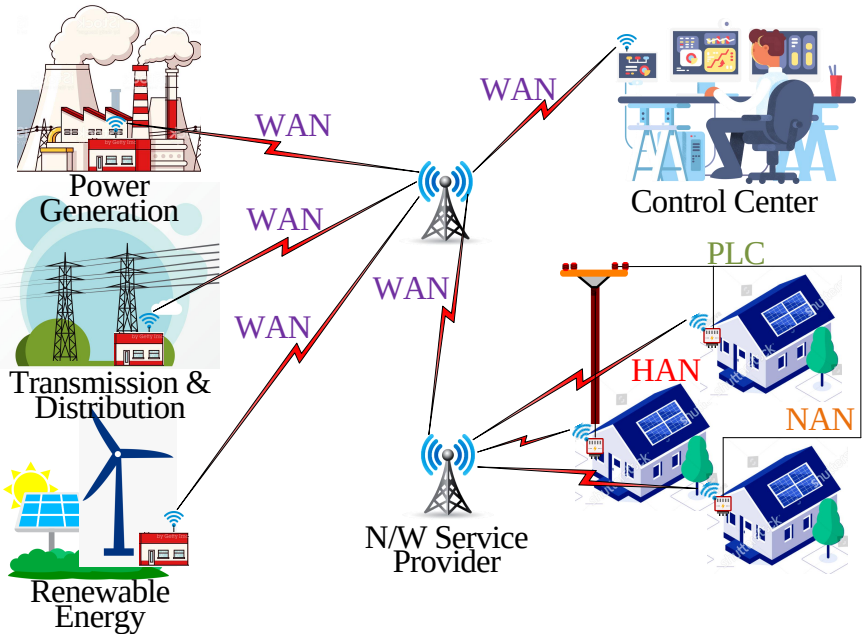

Figure 2.13:: SG communication networks.

To support innovative and self-ruling grid functionalities in Home Area Networks (HANs), Neighborhood Area Networks (NANs), and Wide Area Networks (WANs) of SG, an efficient, reliable, and flexible communication technology is required to transform the conventional power grid into an automated SG as shown in

Fig. 2.13. Communication requirements and capabilities of the different types of networks are characterized in Table 2.4 [109].

Table 2.4:: Communication requirements and capabilities of the different types of networks.

Network	**Coverage Range**	**Data Rate**	**Technologies**
HAN	10 meters	Low data rate is usually required in the control information.	ZigBee, Wi-Fi, Ethernet, PLC
Neighborhood Area Network	100 meters	The average data rate i.e. 2 Kbps is used in node density-dependent network, control, and user information.	ZigBee, Wi-Fi, PLC, cellular
Wide Area Network	kilometers	A few hundred Mbps to a few Gbps for gateway connectivity between the utility and the distribution control system.	Microwave, WiMax, 3G/LTE, fiber optic links

In the existing power grid, communication already exists at a small level to help simple and limited automatic actions. Nevertheless, extensive requirements of communication infrastructure that involve long-distance deployments in all directions, e.g., control systems and wide-area monitoring, still depend on massive human labor involvement. For example, technicians may require to visit the site and monitor the recovery procedures. Therefore there is a dire need to automate monitoring, control, and outage management of power using the bidirectional communication in AMI. Moreover, SMs in HAN communicate with smart home appliances. Whereas in NAN, meter-to-meter communication is required. Therefore, the latest wireless communication technology is mandatory, not only from a commercial point of view but for the robustness of the SG. Wireless technologies are regarded as the main contenders for the implementation of the SG communication network, due to easy implementation and low installation cost [10].

Due to the extensive applications that exist in SG communication, researchers

have to face difficulties in choosing the optimal communication type. They must consider various challenges that may occur during the selection process, such as (i) SG not only a huge but also a composite network of large number of sub-networks. (ii) A large number of connected SMs and other communication devices. (iii) Real-time transmission for operation and control. (iv) Energy-efficient transmission to increase capacity. (v) Energy harvesting wireless sensors and actuators. (vi) High disturbance due to power system noise [13].

2.2.5 Smart Grid Assisted Existing Communication Technology

Converting the conventional power grid into the SG is impossible without appropriate wireless or wired technology. National Institute of Standard and Technology (NIST) U.S. has released the report regarding SG standards by presenting a comprehensive review of numerous wireless and wired communication infrastructures that can be implemented for SG [13]. In consideration of the NIST standard, a summary of available technology contributing to SG communication is itemized in Table 2.5 [110] and details are as follows.

2.2.5.1 Wired Communication for SG

Power line communication Power line communication (PLC) is a much-balanced finding for remote application and monitoring in the framework of SG. It is also suggested that widely available existing power lines infrastructure (named as No New Wired Technology) for SG communication allows ubiquitous, reliable, and secure connections. PLC is currently used in local area networks and automated meter reading (AMR), etc. On the basis of frequency bandwidth, the researchers have classified PLCs into two types; Narrowband PLC (NB-PLC) and Broadband PLC (BB-PLC). For interconnected applications of SG, NB-PLC is suitable for smart metering, in which high data rates are not required. For medium voltage power line networks, PLC has been already deployed for fault location and detection. The combined transmission of wireless channels and PLC which help to increase the reliability in SG are presented in [111, 112].

Table 2.5:: Available technology which contributing in SG communication.

Applications	**Coverage Range**	**Data Rate**	**Technologies**
AMI, HAN User data	30-50 m	250 Kbps	ZigBee
AMI, Fraud Detection	1-3 km	2-3 Mbps	PLC
AMI, Demand Response	10-50 km(LOS) 1-5 km(NLOS)	Up to 75 Mbps	WIMAX
AMI, Demand Response, HAN	1-10 km	384 kbps-2 Mbps	3G
AMI, Demand Response, HAN	1-10 kms	Up to 170 kbps	GPRS
AMI, Demand Response, HAN	1-10 km	UP to 14.4 kbps	GSM

Despite, these advantages PLC also possesses several disadvantages. Due to noise sources such as radio interference, electric motors, and power switches, the PLC channel consists of noisy characteristics. Also, the power lines have extremely time-varying characteristics which degrade the BER performance. Therefore, PLC is not considered a reliable communication medium. Some researchers are concerned about security when the PLC network is used for data communication. The unshielded and untwisted structures of the power cable create electromagnetic interference which might affect the receiving module. To study the dynamic characteristics of the PLC channel [113], researchers have designed a model adaptive to dynamic communication protocol. Still, these models are incapable of representing the frequency selective and time-varying characteristics of the PLC channel. As a result, the standard model for the PLC channel is not yet developed. PLC needs significant input from power utilities and standardization parties for its extensive recognition in the framework of the SG.

Fiber Optic Communication Extensively deployed optical networks already exist for terrestrial communication. This existing optical fiber network can be used

as a backbone communication network in SGs. For single wavelength transmission optical fiber communication can provide transmission rates up to 10 Gbps, even higher transmission rates from 40 Gbps to 1600 Gbps can be achieved by wavelength division multiplexing (WDM). The electromagnetic and radio insusceptibility of optical signals declares optical fiber as a reliable and secure communication network. Moreover, the optoelectronic sensor, actuators, and transducers are more capable for precise measurement of voltage, current, and other parameters. However, the installation cost of a fiber optics network for controlling and monitoring is quite high. This drawback can be minimized by using the existing fiber optics network as backbones in the SG communication networks [114].

2.2.5.2 Low Coverage Wireless Communication for SG

ZigBee In wireless communication technology, ZigBee Standard and ZigBee Smart Energy Profile are described by NIST [13]. In [115], the authors found ZigBee having low power consumption and also has a low data rate. It is thus appropriate for control and automation applications such as remote meter reading, smart lighting control, HAN, etc. The core issue of ZigBee is that it is operated in an unlicensed ISM band network which makes it difficult for commercial use.

Bluetooth The advantages and disadvantages of Bluetooth have been discussed by authors in [116] for SG. The role of Bluetooth is now increasing in SG communication. Bluetooth uses Frequency Hopping Spread Spectrum (FHSS) as an access technique to avoid interference and eavesdropping, therefore, Bluetooth offers reliable and secure communication. But network area coverage by Bluetooth is restricted to 100 m and only a limited number of nodes can be served.

Wireless LAN WLAN (IEEE 802.11) is an available uninterrupted communication technology with a higher data rate [117]. WLAN provides reliable communication over a network with low-cost deployment, simple installation, high device mobility, and high data rates. It is suitable for SG applications such as residential Building Area Networks (BAN) and AMI. Besides this, data security needs robust

encryption techniques because of the important metering data delivered through every access point. Moreover, long distance SG communication requires high coverage wireless infrastructure, as discussed below.

2.2.5.3 High Coverage Wireless Communication for SG

WiMAX Long-distance coverage and high data rate make WiMAX suitable for SG communication. WiMAX network can be utilized for SG applications such as long-distance meter reading, real-time price estimation, and outage detection. For meter reading purposes for SG, the authors analyzed the performance of WIMAX in [118]. For smart metering application performance and comparison of the WiMAX-WLAN and WiMAX standalone network is presented. The capacity of both types of networks, WiMAX-WLAN, and WiMAX standalone is analyzed. For smart metering, to decrease latency according to diverse categories of traffic in the WiMAX network, the authors allocate bandwidth by using the radio resource management algorithm.

Cellular Networks The authors have presented a comprehensive review of multiple companies for SG communication that are using UMTS, WCDMA, CDMA, GPRS, and GSM technologies. Vodafone, China Mobile, Telecom Italia, and Telenor have just started using GSM networks for smart metering. Meanwhile, cellular technologies have already been presented as a well-established infrastructure, so that without the additional cost of deployment they can be effectively utilized for SG communication. Hence, over a broad coverage area GSM (2G), CDMA (2.5G), UTMS (3G), and LTE (4G) can be utilized for smart metering. Authors in [110] discussed significant improvement in network capacity for SG using the OFDMA scheme in LTE. The results confirmed that OFDM offers a significant reduction in interference and an increase in system capacity.

SATCOM The historical fall in the cost of services and equipment and the improvement in efficiency has created satellite communications (SATCOM) a remarkable option for the implementation of SG applications. The authors provided

analytical methods to find the feasibility of satellite systems with different orbit configurations for SG applications. The authors also presented a general idea of how satellite communications can help in remote communications of SG such as emergency management and environmental monitoring applications [119].

Existing technology has the ability to transform the conventional grid into the SG. Table 2.6 presented a state-of-the-art review of the SG-assisted wireless communication technology. Therefore, continuously evolving functionalities and the number of connecting devices in SG require next-generation technology such as NOMA (unconventional multiple access scheme of 5G mobile communication). Potential challenges associated with the implementation of NOMA in SG communication are as follows.

Table 2.6:: A state-of-the-art review of SG-assisted wireless communications.

Ref.	**Objective**	**Solution Approach**	**Tech.**	**User**
[120]	Deployment of SG applications in dense and complex scenarios.	Spectrum reuse technique is used for dense networks and HetNets.	D2D & small cell	Large
[121]	Enable information exchange between SMs and the corresponding gateway.	LTE pilot installation and pilot symbols collection are utilized.	Band-31 (450MHz) LTE-A	Large
[122]	Enhance the physical layer reliability of SG.	Continuous phase modulation mapper is used in an OFDM scheme.	802.11 OFDM	Moderate
[123]	Increase the tolerance against noise and improve the efficiency of SG.	Multipath PLC with the OFDM technique is used. Channel and noise models are presented for the PLC system.	OFDM over PLC	Moderate
[124]	Improve the SM receiving sensitivity in scenarios where the channel estimation is difficult.	The adaptive OFDM-MFSK is used that selects the best M value for minimum BER and higher throughput.	OFDM-MFSK	Moderate

[119]	Deployment in those scenarios in which terrestrial communication infrastructures do not exist.	SATCOM two-way communication systems provide IP services for machine-to-machine communication for extensive coverage and rapid installation.	SAT-COM	Huge
[118]	Enable demand-response applications of AMI.	The uplink performance of the LTE-FDD and LTE-TDD modes is investigated for a large number of devices sending small to medium size AMI packets.	LTE-FDD and LTE-TDD	Large
[125]	Improvement in automated SG infrastructure.	Analytical and simulative traffic engineering models are presented for SG with wireless technology approaches using GPRS, UMTS, and LTE in cellular networks.	GPRS, UMTS and, LTE	Huge
[126]	Implement communication for AMI.	Reengineering principle is applied to access granted and data transmission stages of the GSM.	GSM/ GPRS	Huge
[127]	Enhance interoperability, choice of frame duration, type of service, and scheduling strategies for SG applications.	The simulation-based evaluation recommends a priority-based scheduler as an appropriate solution for scheduling time-critical SG applications.	WiMAX	Large

[128]	Data exchange for monitoring and control applications.	Hybrid mixing of CDMA/IDMA and Optical-CDMA/Optical-IDMA systems over powerline/optical fiber are implemented.	CDMA, IDMA, OCDMA, and OIDMA	Large
[129]	Improve security and privacy.	CDMA-based data aggregation method is provided that allow access to utility in the root node while keeping the smart metering data secure.	CDMA	Large

2.2.6 Potential Challenges Associated with Implementation of PD-NOMA in SG Communication

PD-NOMA is a renowned 5th generation multiple access scheme for wireless communication. Based on power division in contrast to time and frequency. Existing multiple access technique i.e. OFDMA offers lower energy utilization, higher spectrum efficiency, and significantly reduces interference. However, it is still not capable to fulfill the requirements of SG due to limited bandwidth. In PD-NOMA, each user utilizes the total bandwidth of the system at the same time and frequency. A typical PD-NOMA system is illustrated in Fig. 2.14. In PD-NOMA, all users' signals are superimposed and transmitted through the same channel while, at the receiving side each closer user cancels the other farther users' signals by using SIC, and the farthest user considers other users' signals as noise. PD-NOMA characteristics are suitable with the QoS for the SG communication requirements arising in Field Area Network (FAN), NAN, and WAN. On the other, for HAN and BAN existing technology i.e. OFDMA-based Bluetooth, Zigbee, WiFi, etc. can be used. In particular, PD-NOMA offers a great data rate by its high bandwidth efficiency [106]. Therefore PD-NOMA can fulfill the requirements of the diverse services that are essential of SG applications.

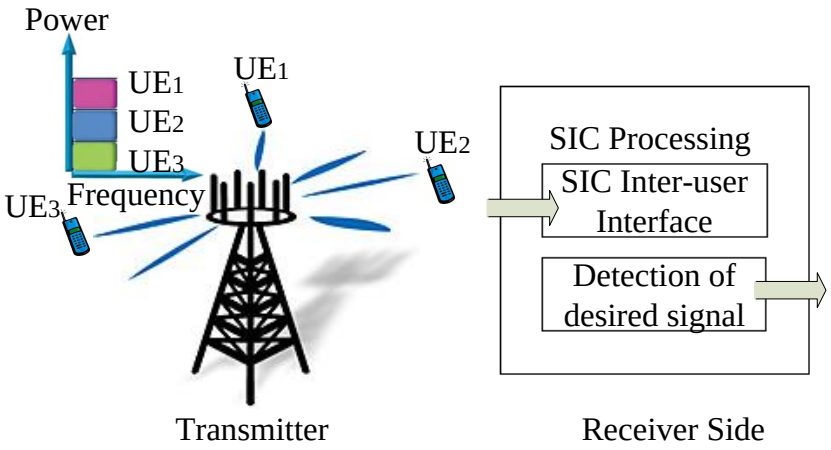

Figure 2.14:: PD-NOMA with SIC.

Existing wireless and wired communication technologies are relatively adequate to respond to the challenges of the SG Network but the exponential evolution of the SG requires extraordinary communication infrastructure. It indicates that the newest 5G PD-NOMA can achieve these requirements with: (i) Dynamic deployment for complex networks by allowing dynamic power allocation schemes. (ii) Massive connectivity by allowing more users simultaneously at the same time. (iii) With a low computational complexity scheme for SIC, PD-NOMA is suitable for real-time transmissions. (iv) Showing a better SE-EE tradeoff. (v) Energy harvesting mechanism of PD-NOMA.

2.2.6.1 Massive Connectivity

The implementation of wireless communication in SG imposes several key challenges in design. Renewable energy sources and sensors generate a huge volume of information data that need a heterogeneous communication system [130]. But there is a deficiency of data rate on the limited wireless spectrum [105]. A typical power supply communication network consists of the following:

- A central high-bandwidth network, which includes a high-speed wireless network.
- An advanced multiple access technique that provides high spectral and energy

efficiency.

- WAN, to make the aggregation of this huge data possible.

The PD-NOMA has the capacity to achieve the above requirements for SG communication. The non-orthogonal division of resources in PD-NOMA specifies that the number of devices or supported users is not restricted by their scheduling granularity or accessible resources. Consequently, PD-NOMA can support more users as compared to OMA by means of non-orthogonal resource sharing[131].

2.2.6.2 Real-Time Operation with SIC Receiver Variations

In SG, information from different devices or user requires to be processed in real-time such as real-time demand and supply, real-time authentication, real-time monitoring, etc. Sometimes information needs to convey at a fast pace such as during disaster scenarios, medical imaging, and traffic congestion for smart vehicles. Although PD-NOMA provides high spectral efficiency it requires SIC in order to differentiate the signals of different users. Conversely, SIC is very useful when the users are at an appropriate distance from BS or consist of different channel conditions. The receiver cancels the other user's signals sequentially or serially. The nearer user performs much more SIC computation than the farther user. As the number of users increases nearer user needs to perform more SIC computation as shown in Fig. 2.15, therefore SIC computation produces more processing delay.

If each stage of SIC cancellation delays one bit, then total $K-1$ bits delay produces by K number of users. Thus, decoding of the desired signal for the farther user is much faster than the nearer user but at the same time propagation delay is higher for the farther user than the nearer user. In this scenario, higher expectations of the performance of real-time operations can not be achievable. Variation at SIC receiver is a big challenge for real-time operation in SG and needs a unified framework to study the variation of SIC in wireless networks with arbitrary propagation and computational delay [132].

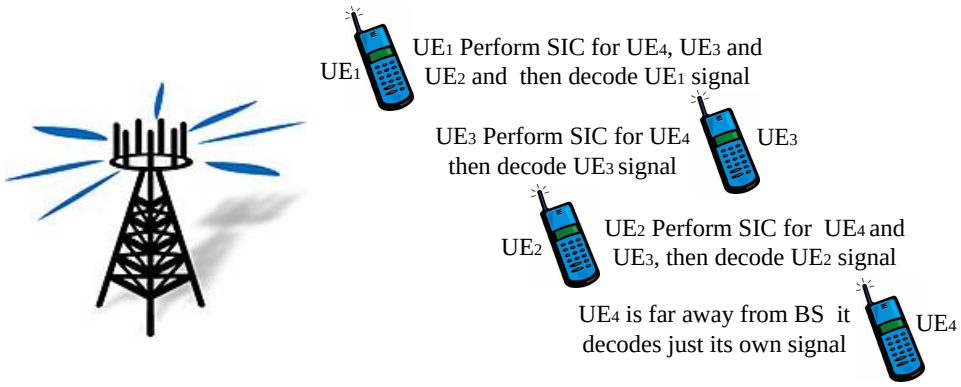

Figure 2.15:: PD-NOMA downlink system.

2.2.6.3 Energy Efficient Transmission

In wireless communications, unit energy consumption versus throughput is considered as one of the key parameters of performance known as SE-EE tradeoff. Here, the throughput may only consider the informative data as the whole transmitted bits that keep out transmission errors, signaling bits, headers, and duplicate packets. Additionally, the majority of the research neglect the circuit power and power required for cooling the device while emphasizing only optimizing transmit power. If all the above-mentioned constrained are considered, energy-efficient transmission can be ensured.

New capable multiple access PD-NOMA offers high spectral efficiency (SE) with a great number of users. Furthermore, the energy efficiency of PD-NOMA system has received recognition since the requirements of energy-efficient communication have increased. Because energy-efficient communication is becoming one of the big economical and technological concerns worldwide. An energy-efficient allocation of power scheme can maximize the energy efficiency. In PD-NOMA, several users are served by power division at the same time, which increases the energy efficiency of the system that's why PD-NOMA has higher energy efficiency than conventional OMA [133].

2.2.6.4 Energy Harvesting

In SG applications, for monitoring purpose Wireless Sensor Networks (WSNs) are used on the crucial part of power distribution grids which contain limited battery backup. It is essential to decrease the power utilization of sensor nodes because WSN nodes have energy limitations due to the ruthless transmission characteristics of SG surroundings. A possible approach to decrease power utilization is to use transmitting power as transmitted powers may be modified as per channel conditions. An alternative way is to employ an energy harvesting system to supply more power for nodes by utilizing environmental energy resources. In outside substation environments, electromagnetic and solar energies are potential environmental energy sources. In addition, electromagnetic energy is available at any time, on the other hand, solar power can be effectively used on a bright day. Therefore energy harvesting using radiofrequency is a better solution nowadays [134].

To extend the lifespan of energy reserved for networks and maintain network connectivity, PD-NOMA offered energy harvesting as a promising solution. For PD-NOMA, using radio frequency energy harvesting, researchers have considered time allocation-based wireless energy harvesting along with data rates optimization. The authors proposed combined power transfer and wireless information networks in PD-NOMA. Particularly, nearer PD-NOMA users that are nearby to the energy source react as energy harvesting relays to service farther PD-NOMA users. In end, by correctly selecting the constraints of the system, for example, power dividing factor and transmission rate, system efficiency can be improved even if the users don't utilize their specific batteries.

2.2.6.5 IN in Smart Grid/Smart Meter

SM and most of the other communication devices are part of the power grid system; therefore, the communication channel for these devices becomes noisier. The noise contamination of a communication channel may result in erroneous information about the resources in the field - resulting in complete obstruction of the information. The performances of other communication units and SMs are degraded by IN extant in the power system, produced by electromagnetic disturbances. SMs are usually

placed near breakers and transformers for data collection of voltage, current, power, etc., by using sensors that are connected through a wire to the power lines. In case impulse occurs in the power system, it also appears in the wireless transmission unit of SM as shown in Fig. 2.16. For the IN modeling, employed the Bernoulli-Gaussian model and Laplacian-Gaussian model previously used by [135, 136] and [137], respectively, for PLC. Moreover, the aforesaid model was used in [8, 138, 139] for wireless commutation analysis which validates our selection. Investigation of the IN recommends the following three categories.

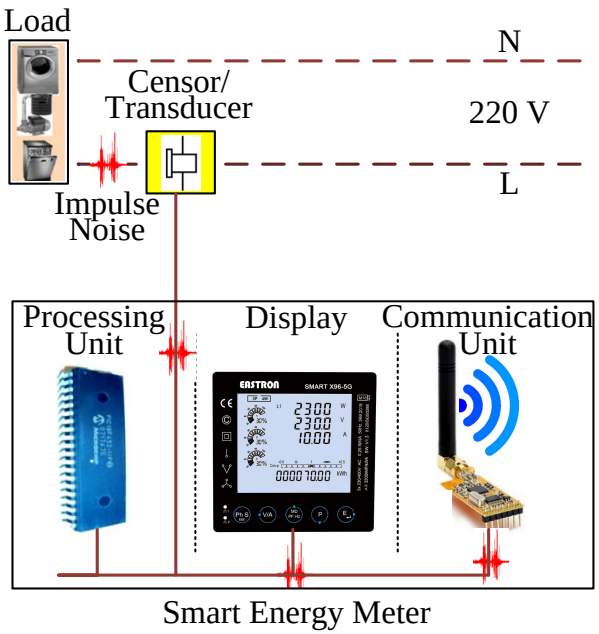

Figure 2.16:: Smart Meter.

Periodic Synchronous IN Periodic Synchronous IN (PSIN) has significant spectral components in the frequency spectrum. PSIN is also known as cyclostationary noise, synchronous with the main AC of 50 Hz/100 Hz. This type of noise is produced by silicon control rectifier diodes present in the electrical systems. PSIN includes high peaks of voltage level that occur for small durations with repeats equal to or double the rate of the mains.

Periodic Asynchronous IN Periodic Asynchronous IN (PAIN) is asynchronous with the mains AC. It is usually formed by periodic impulses with a higher repetition

rate of 50 kHz and 200 kHz. PAIN is unpredictable because of irregular occurrences with the mains AC. This type of noise is created mostly by switching power supplies. Furthermore, with a high repetition rate, PAIN also has a repetition rate, equal to the mains AC. Therefore, PAIN is also classified as a cyclostationary.

Asynchronous IN Asynchronous IN is irregular in nature. It is usually generated due to transients triggered by the connection and disconnection of electrical equipment. This type of noise is produced by the effects of the drills and electrical motors.

2.2.7 Grid Parameters

SG aims to connect all the entities through communication and to improve the performance without using traditional approaches. For controllability, observability, and fast reliable information flow, an efficient communication system is required, which will eventually result in a safe, reliable, and secure power grid. However, the SMs are deployed in the field where the characteristics of the channel are highly noisy. The field comprises large and tricky portions containing IN which degrade the received signal leading to a communication failure. Therefore, two key parameters have been used to analyze the effect of IN. One is the IN parameter for modeling IN which is used in designing a wireless module of SMs for error-free reception. The other is the impulsive environment parameter for characterization of the field which is based on the data collection of an impulsive environment. Based on the actual circumstances, a reliable wireless link can be established between consumer and utility by adjusting the parameter according to the actual situation [140].

2.2.7.1 Impulsive Noise Parameter (ξ_o)

Implementation of wireless communication in the SG experiences different types of noises due to different types of surroundings. IN is composed of short power spikes which increase the level of noise. IN appears as a flat frequency response on the frequency spectrum. Impulse can improve the noise level up to 50 dB but for a very short period of time, typically 50 μsec with average arrival rate of 5 sec^{-1} and

average inter-arrival time of 200 msec. As a result, numerous bits or even burst of errors in communication links may occur in an instant.

In traditional wireless communication, the AWGN model is used for thermal noise. Although AWGN is an accurate model for the SG, in certain outdoor and indoor surroundings communication in the power system can be affected by IN. Several regularly used appliances in daily life such as hair dryers, microwave ovens, photocopiers, printers, etc. are the main reason for the occurrence of IN in wireless channels near the power lines [141]. The presence of IN in the electric power system is the most dominant characteristic of noise. Moreover, opening and closing of circuit breakers may cause a very strong IN in the communication system of the SG. Narrowband noise and colored background noise are the primary noises that establish background noise in SG communication. Variations in amplitudes of these noises are very slow over time. Furthermore, IN is extremely important among the noise varieties present in SG communication networks, generated mostly by electrical appliances. IN is considered to be the leading cause behind the inaccuracy in the data transmission over the SG channels [107]. Therefore, the total noise, combination of AWGN and IN can be expressed as:

$$\xi_o = \sigma_G^2 + p\,\sigma_I^2 \tag{2.30}$$

where n_G and n_I are AWGN with variances σ_G^2 and σ_I^2 along with parameter p (probability) [135, 136].

2.2.7.2 Impulsive Environment Parameter (dr)

To analyze the performance of communication systems in harsh environments, it is essential to develop a statistical model for IN. The analysis of the effect of individual random impulses on the system is quite difficult because the impulses are random in nature. Moreover, Impulses are variant in magnitude and occur for a very short duration. Effect of Impulses can be analyzed by Disturbance Ratio (dr) which considers the actual loss of bits/information. The performance parameter dr is described by the ratio of the length of the specific time window and the sum of the widths of all impulses occurring within this specific window. In addition, actual disturbed time

can be calculated by the dr through which actual loss of bits/information can be estimated.

There are two main issues to consider when analyzing the effects of IN on data transmission i.e. time of impulse occurrence and the strength of impulse. For the first issue, the use of Rectangular Impulse Envelopes allows simple characterization using only a few parameters. Three basic factors, the width of the impulse, the arrival time of impulse, and inter-arrival time, can be used to estimate the time behavior. To find the dr, the rectangular envelope of impulses includes information of the characteristic parameters, the width of the impulse, the amplitude of the impulse, and the arrival time of the impulse. The time between two consecutive occurrences of impulses is known as inter-arrival time. To resolve the second issue, impulse energy, impulse amplitudes, power, and power spectral density [14], can be used.

The total number of impulses that appear in a second is known as the average impulse rate λ_{Avg} and the dr which specifies the real disturbed time (in ratio) is given by:

$$dr = \frac{\sum_{i=1}^{J} t_{w,i}}{T_{Tot}} \tag{2.31}$$

where $t_{w,i}$ is the width of the i_{th} impulse in sec and j is the total number of impulses occurring in time T_{Tot} (sec) [142].

2.2.8 Mitigation Techniques for IN

2.2.8.1 Conventional IN Mitigation Techniques

The classical IN detection approach involves blanking and clipping by setting an optimum threshold that is susceptible to vary in response to channel conditions which eventually causes model mismatch. Any change in the detection threshold of impulses in traditional methods can cause ambiguity in the receiver threshold of signal detection, thus deteriorating the performance of PD-NOMA. The unique traits of PD-NOMA scheme i.e. non-orthogonal resource allocation and subsequent interference cancellation, have additionally increased the user's response to such IN interference [143]. The aforesaid issues demand more research work to evaluate

the impact and suppression strategies of such noise on PD-NOMA-based systems. Moreover, investigation on efficient IN classification methods can significantly help to develop better IN mitigation strategies. A comparison of the proposed DNN with the state-of-the-art methods is presented in Table 2.7.

To mitigate the effects of IN, several methods have been used in previous works. One of them is the threshold-based IN scheme, in which the short duration and the high amplitude of IN are investigated as the key features. The most common method in this kind of mitigation is the memoryless nonlinear approaches for example blanking [144], clipping [145], and blanking/clipping [146]. A threshold optimization is presented in [147] based on Neyman-Pearson criterion in [148]. Moreover, the authors provided an analytical equation for mitigation of IN for the quasi-optimal blanking and clipping thresholds. Analog domain processing is used in [151, 152] in which the IN is considered as broadband and distinguishable. The performance of threshold-based nonlinear solutions is extremely dependent on the selection of thresholds [9]. If the threshold changes in response to channel conditions, the model becomes mismatched. Therefore, the performance of all these conventional methods degrades rapidly in the harsh impulsive environment.

2.2.8.2 DNN-based IN Mitigation Techniques

A DNN is an artificial neural network that has few hidden layers between an input layer and an output layer. These networks have the potential to handle unstructured data, unlabeled data, and non-linearity. DNNs have a hierarchical structure of neurons that resemble the human brain. Based on the information received, the neurons send the signal to other neurons. The output is passed if the signal value is larger than the threshold value, otherwise, it is ignored. The data is transmitted to the input layer, which produces output for the next layer, and so on until it reaches the output layer, which delivers the probability-based prediction as yes or no. A layer is made up of numerous neurons, and each neuron has an Activation Function. The Activation Function serves as a gateway for signal transfer to the next linked neuron. The input weight affects the output of the next neuron and ultimately, the last output layer. Initially, the weights are assigned randomly, but when the network

is trained repeatedly, the weights are tuned to ensure that the network generates accurate predictions.

Table 2.7:: Comparison of proposed DNN with state-of-the-art methods.

Ref.	**Objective**	**Solution Approach**	**Technique**	**Performance**
[144]	Performance improvement of blanking non-linearity element for OFDMA signals in impulsive noise channels.	An iterative interference cancellation scheme with an adaptive blanking threshold for each iteration.	Iterative Blanking	Best performance with only three iterations over fixed blanking threshold.
[145]	Selection clipping threshold with a priori knowledge approximate.	An approximate knowledge of the arrival probability of impulses to render the clipping threshold, for OFDM transmission.	Probabilistic Clipping	Outperformed its conventional method when coupled with a turbo decoder using adapted log-likelihood ratio metric.
[146]	Boost SNR at the OFDMA multicarrier receiver.	A nonlinear estimators based on the multiple thresholding with associated piecewise attenuation, or clipping, of the received signal amplitude.	Multiple-Threshold Blanking/ Clipping	Estimators closely approached the performance of the optimal MMSE Bayesian estimator.
[148]	Calculation of a blanking and a clipping threshold.	Simple methods that obtain quasi optimal thresholds of a blanker and a soft limiter.	Blanking/ Clipping	A blanker and a soft limiter are suitable in strong and moderate impulsive environments.

[153]	IN removal from OFDM-based PLC systems.	A combined Time-domain /Frequency-domain technique for IN removal in OFDM-based PLC systems.	Blanking, Clipping and Blanking/ Clipping	Combined TD/FD technique performs better than practically used non-linearities to significantly reduce the adverse effect of impulsive noise.
[154]	Interference reduction in high density network of independent small BSs.	Distributed power allocation algorithm based on multi-agent Q-learning.	Machine Learning	Optimal joint power allocation for small BS network.
[155]	IN removal from received symbols in OFDM-based Systems.	A two-step technique in which a Deep Neural Network (DNN) identifies the IN samples. The detected IN sample is suppressed in the second step.	DNN	Performs better than the traditional IN mitigation approaches which include blanking and clipping.
[143]	Obtain the optimum threshold of the corresponding PD-NOMA user.	A DNN based approach to estimate the IN parameters (threshold) from the received OFDM symbol for OFDM-based PD-NOMA systems.	DNN	Simultaneously maximized the performance of all the users by threshold optimization.
[18]	IN mitigation in PD-NOMA-based system.	A deep learning approach that detects IN by utilizing the information about randomness of noise and statistical properties of input samples.	DNN	Outperformed the existing IN mitigation techniques. In addition, classifies IN as high IN and low IN which offers a new research direction.

In [156, 157] and [154, 158] the authors used the machine learning popular method of deep learning, in signal and image processing applications and resource allocation in wireless networks, respectively. The ability of DNN to learn from samples and to check the uncertainty makes it suitable for the detection of IN. In this respect, appropriate processing strategies and network structures are required. In the OFDMA system, the performance of the conventional approaches also degrades due to the high PAPR of OFDM signals. Therefore, there is a tradeoff between a false positive and true detection in the conventional threshold-based approaches.

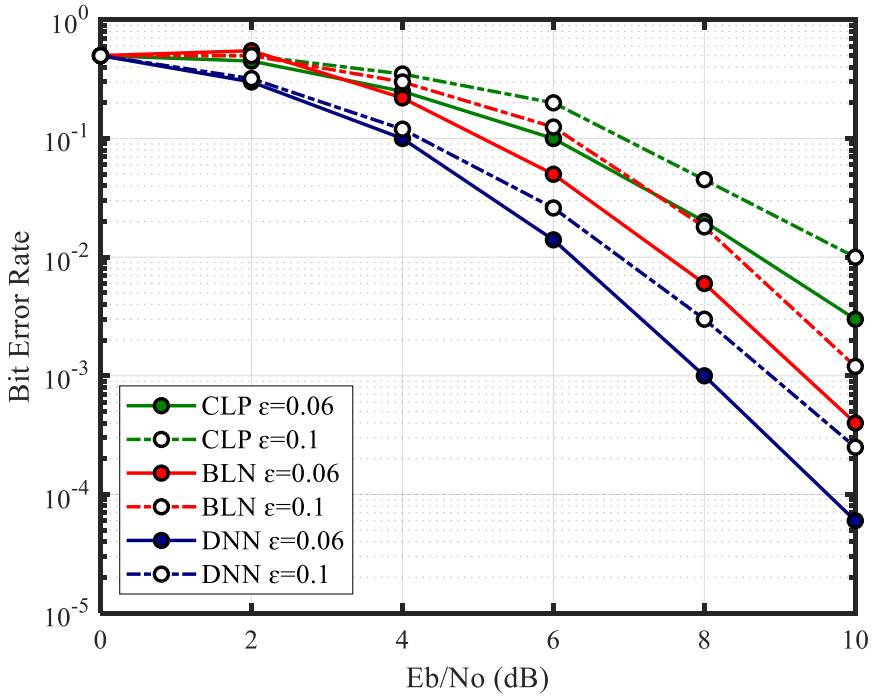

Figure 2.17:: Performance of DNN based IN mitigation technique.

To cater to the above-mentioned drawbacks, in [155] authors proposed a machine learning-based IN mitigation technique for an OFDM system and compared the performance with conventional technique as shown in Fig. 2.17. The proposed IN elimination strategy consist of two parts: (i) IN detection and (ii) IN elimination. In the first part, a DNN is used to identify the IN effected signal instances. In the second part, the identified IN affected signal can be either clipped or blanked. In [159], DNN process the runtime sample value then median deviations filter output

is used. In [160], to identify whether the runtime sample is affected by IN or not, ROAD statistic is used.

2.2.9 Performance Comparison of Major NOMA Category for SG

Comparative analysis of sum-rate performance and the total number of users of PD-NOMA, SCMA, MUSA, and PDMA is illustrated in Fig. 2.18. It has been confirmed by theory and lab tests that SCMA provides a better sum-rate among all major four categories while the complexity of SCMA is bigger than the PD-NOMA due to the code domain. SCMA is capable of achieving coding gains and improved shaping. SCMA allows a fixed number of resource blocks to each user while PDMA allows a changeable number of resource blocks to each user, since, in PDMA, the user data rate is different, which results in degradation of the system sum-rate. Despite the fact that PD-NOMA and MUSA both utilize SIC, PD-NOMA also utilizes PDM and MUSA utilizes a special SS to spread the user's data symbols. Therefore, MUSA offers a better sum-rate than PD-NOMA.

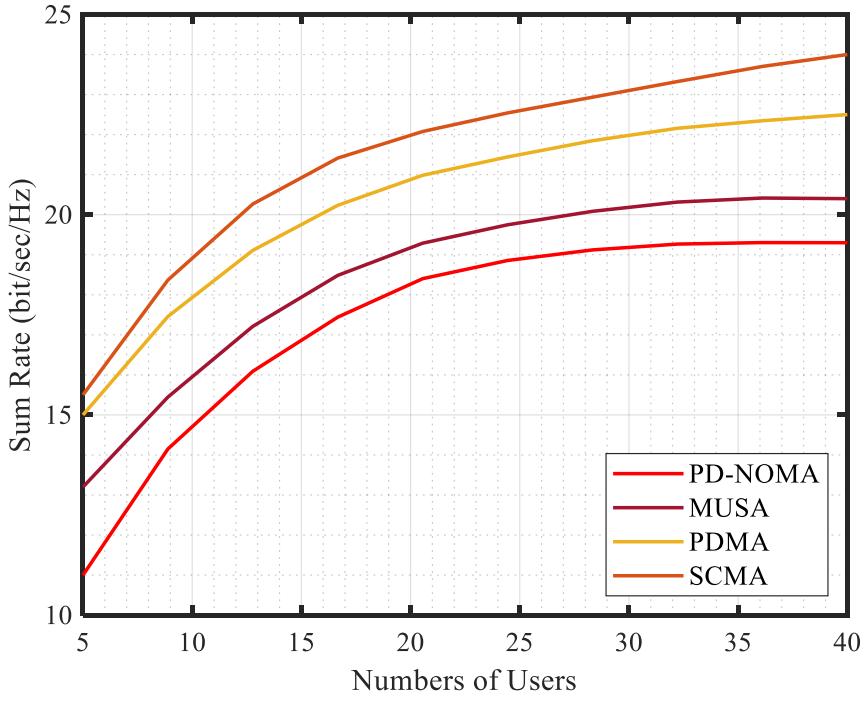

Figure 2.18:: Sum-rate of different non-orthogonal schemes.

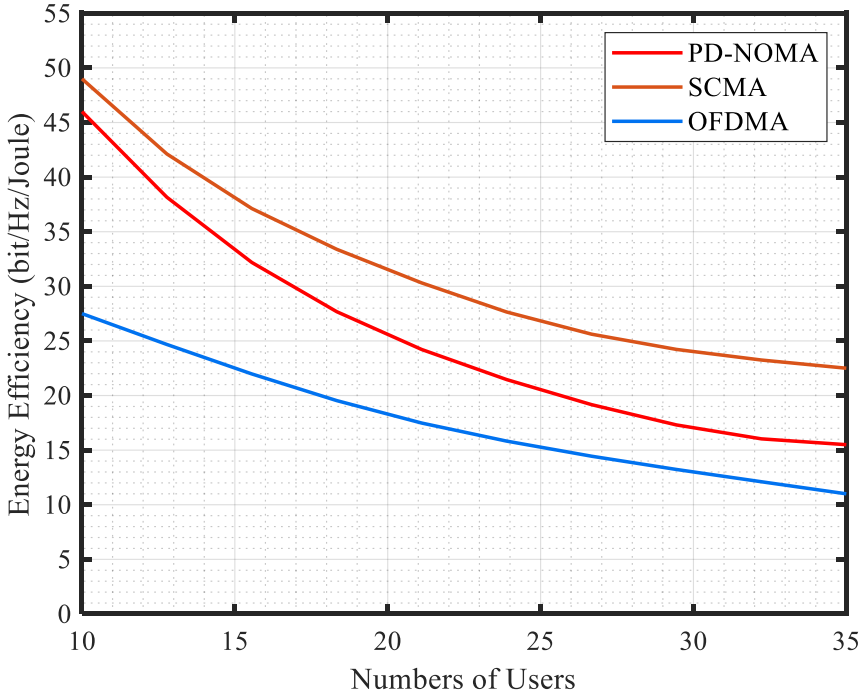

Figure 2.19:: Energy efficiency of different orthogonal and non-orthogonal schemes.

A comparison of the average aggregate energy efficiency of PD-NOMA and SCMA schemes against the number of its users is illustrated in Fig. 2.19. SCMA outperforms its counterparts due to non-orthogonality with high overloading. Therefore, in SCMA, further access of users is achieved with low energy consumption. PD-NOMA also utilizes non-orthogonal access; more users can be employed on less numbers of resources, but due to power domain access, overloading cannot be achieved. On the other hand, OFDMA underperforms because OFDMA is an orthogonal scheme in which users are restricted by orthogonal resources.

Fig. 2.20 illustrates the BER performance of PD-NOMA, SCMA, PDMA, and MUSA uplink systems over Rayleigh fading channel. For performance comparison of the PDMA and SCMA, the same factor graph is used with QPSK modulation. The number of orthogonal resources is 4, and the number of symbols which are transmitted is 6. Therefore, the resulting overloading factor becomes 150%. With the help of [161], the codebooks are designed in SCMA. Pseudorandom sequences whose imaginary and real values are obtained from set {-1, 0, 1} are used to generate SS for MUSA, and non-orthogonal patterns are designed accordingly [162] for PDMA.

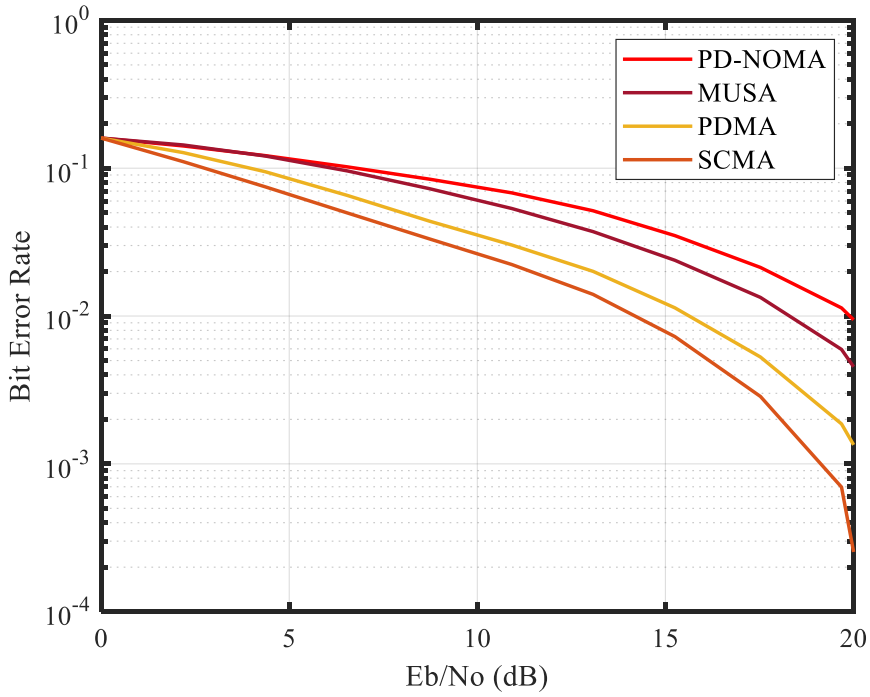

Figure 2.20:: BER performance of different non-orthogonal schemes.

The SCMA uplink system offers high-quality BER performance among all code domains, as shown in Fig. 2.20. However, the BER performance of MUSA and PD-NOMA is very similar and lesser than SCMA and PDMA. The effect of error propagation of the SIC receiver on the system performance is the main reason for the performance degradation of MUSA and PD-NOMA. PDMA utilizes the unchanged factor graph as used in SCMA, however, SCMA still offers better BER performance than PDMA. The reason for this performance improvement is the near-optimal strategy of sparse codewords. The conclusion is that the CD-NOMA scheme achieves a better system sum-rate than the PD-NOMA scheme, therefore, PD-NOMA shows poor performance among all.

For the SG applications, the performance of different NOMA schemes depends on robustness against IN. The BER performance of the different NOMA schemes degrades in the presence of IN in the time domain or in the frequency domain. The signal/information in the frequency domain may seldom be completely corrupted by the time domain crumb. Fig. 2.21 illustrates the BER performance of PD-NOMA, SCMA, PDMA, and MUSA uplink systems over Rayleigh fading channel. However, the channel is contaminated by IN with the PDF, $P_n(x) =$

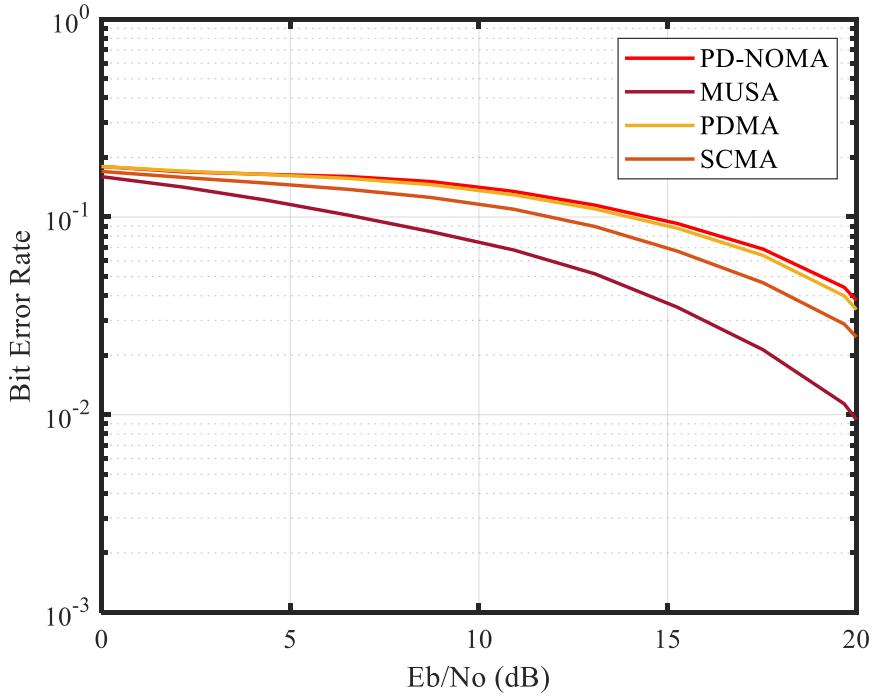

Figure 2.21:: BER performance of different non-orthogonal schemes in the presence IN.

$(1-p)\mathbf{G}(x,0,\sigma_G^2)+p\mathbf{G}(x,0,\sigma_G^2+\sigma_I^2)$. Where $G(x,0,\sigma_G^2)$ is a Gaussian PDF with variance σ_x^2 and mean $\mu_x = 0$. The BER performance degradation in SCMA and PDMA is higher than in MUSA. The reason behind this is that the MMSE-SIC receiver in the MUSA system is less sensitive to non-Gaussianity compared to MPA. The performance degradation in PD-NOMA is comparatively low. The performance of PD-NOMA can further be improved by selecting a better power allocation scheme.

2.3 Generation Partnership Project (3GPP)

The primary objective of the 3rd Generation Partnership Project (3GPP), a joint initiative involving many telecoms groups, is to provide internationally applicable specifications for third-generation (3G) mobile networks. The International Telecommunication Union's (ITU) International Mobile Telecommunications-2000 initiative and the Global System for Mobile Communications (GSM) standards served as the foundation for the project. Since then, the cooperation initiative has extended its scope to cover the upkeep and creation of GSM technical papers.

2.3.1 5G KPIs and 3GPP's Timeline

Members of the 3GPP frequently gather to work together and develop cellular communications standards. The 3GPP is currently developing 5G standards. 3GPP comprises many organizations, each with a distinct area of specialization. The physical (PHY) layer as defined by RAN1, the MAC layer as described by RAN2, and, in certain situations, the PHY layer test as defined by RAN4 are the lower levels that are the focus. Three key performance indicators (KPIs) are the emphasis of the criteria for 5G set out by the International Telecommunication Union (ITU) [163]:

- Peak data rates greater than 10 Gb/s for the enhanced mobile broadband (eMBB)
- More than connections 1 M/km2 for massive machine-type communications (MMTC)
- Latency less than <1 ms for ultra-reliable low-latency communications (URLLC).

It will take significant effort to define a new standard for 5G. 3GPP has divided the 5G standard into two releases. Releases 15 and 16 of the 5G standard, corresponds to New Radio (NR) Phases 1 and 2, respectively. There are similarities between LTE and NR Phase 1 such as the use of orthogonal frequency division multiplexing (OFDM). Details of differences are summarized in Table 2.8 [163].

Deploying a significant quantity of new hardware is necessary to fully implement NR. A staged strategy has been suggested to keep using current hardware. There are two versions: a standalone (SA)Âăversion that uses an NR core and is totally independent of the LTE core network, and a non-standalone version (NSA) that uses the LTE core [163].

Table 2.8:: Details of differences between LTE and NR.

Parameter	Long Term Evaluation	New Radio
Frequency of Operation	Up to 6 GHz	Up to 6 GHz, 28 GHz, 39 GHz, others mmWave bands (Up to 52 GHz)
Carrier Bandwidth	Max: 20 MHz	Max: 100 MHz (at <6 GHz) Max: 1 GHz (at >6 GHz)
Carrier Aggregation	Up to 32	Up to 16
Analog Beamforming (dynamic)	Not Supported	Supported
Digital Beamforming	Up to 8 Layers	Up to 12 Layers
Channel Coding	Data: Turbo Coding and Control: Convolution Coding	Data: LDPC Coding and Control: Polar Coding
Subcarrier Spacing	15 KHz	15 KHz, 30 KHz, 60 KHz, 120 KHz, 240 KHz,
Self-Contained Subframe	Not Supported	Can Be Implemented
Spectrum Occupancy	90% of Chanel Bandwidth	UP to 98% of Chanel Bandwidth

2.4 Summary

Initially, the chapter presented some basic knowledge and comparison of popular categories of OMA scheme, MIMO systems, and multiuser beamforming techniques. Later on, a comprehensive review and comparison of NOMA scheme and its popular categories are presented. Moreover, the performance of popular categories of NOMA such as PD-NOMA, SCMA, MUSA, and PDMA along with their state-of-the-art review is presented in terms of working principle, design feature, user-rate, system capacity, and BER. Observation of the first part revealed that orthogonal access to resources is restricted by the number of available resources while non-orthogonality allows multiple users on a single resource. OMA-based schemes may not meet the emerging requirements of NGN including massive device connectivity and very high spectral efficiency. Thus, there is a dire need for improvement in access schemes.

Furthermore, challenges in the implementation of emerging NGN such as IoT, VANET, SG, and mobile networks are discussed. Moreover, challenges in implementation and requirements of SG are explained in detail along with the discussion of how PD-NOMA can full fill these requirements? Moreover, a state-of-the-art review of SG-assisted wireless communication technology is presented to find the appropriate communication infrastructure for SG. To sum up, existing wired and wireless communication technologies are quite sufficient to counter the challenges of the NGN network such as the SG communication network, however, the exponential growth of the SG needs exceptional communication technology. This section expounded that the latest 5G technology i.e. PD-NOMA can fulfill these requirements.

In the last section, the fundamental concept and causes of IN are presented. A comprehensive literature review on IN mitigation techniques along with their state-of-the-art comparison is presented. According to the studies, DNN has the ability to detect IN through its ability to check the uncertainty and learn from affected samples. In last, the performance comparison between different IN mitigation techniques, and the performance of popular NOMA schemes are presented in presence of IN. As per the results, PD-NOMA can perform better than other NOMA schemes in presence of IN.

Taking into account the background material discussed in this chapter, the subsequent chapters discuss the proposed scheme, optimum allocation of resources, and proposed IN mitigation technique for multiuser SG communication.

CHAPTER 3

SYSTEM MODEL

The understanding of the potential of NOMA applications - those devised for improving spectral efficiency and error-free transmission - motivated the researcher to propose a composite multiuser access scheme. Moreover, research in SG communication continues to progress especially with the current focus on both theoretical and field experiments. In this respect, the proposed scheme is based on the combination of orthogonal and non-orthogonal user access and is evaluated in practical scenarios.

3.1 Primordial System Model

SMs are located outside of houses, building, offices, shops, etc. The channel condition of SMs is often different because they are placed at an appropriate distance. In this scenario, PD-NOMA is a suitable multiple access scheme because it utilizes power division between users according to channel conditions or distance from BS. However, if two or more SMs are at the same distance from BS having the same channel condition, OMA would be an ideal scheme.

Considering four SMs are located outside the house in the system model SM_{1a}, SM_{1b}, SM_{2a}, and SM_{2b}. SM_{1a}, SM_{1b} and SM_{2a}, SM_{2b} are at the same distance from BS as shown in Fig. 3.1. Power division access is not possible between SMs in each pair. Therefore, to implement OFDMA, the entire bandwidth is equally divided between SMs in each pair. SM_{1a}, SM_{2a} and SM_{1b}, SM_{2b} are at different

distances from BS ultimately the distance between SMs in a pair is enough to apply power division access. Therefore, to implement PD-NOMA, the entire power is divided between SMs in each pair and each pair of these SMs uses half bandwidth. The resource allocation of these SMs is presented in Table 3.1.

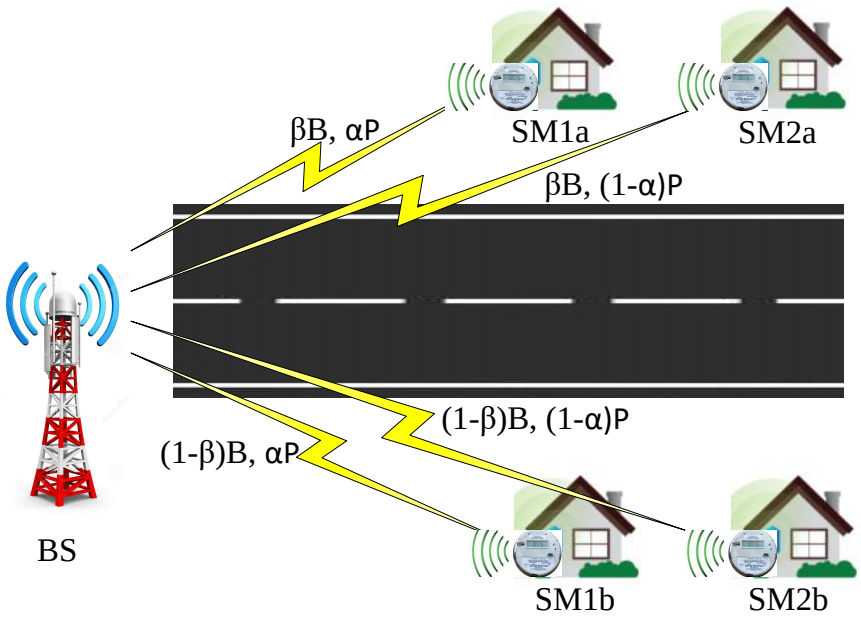

Figure 3.1:: Primordial SG communication system model.

Table 3.1:: Resource allocation to SMs.

Smart Meter (SM)	**Dist. from BS (d)**	**Bandwidth (B)**	**Power (P)**
SM_{1a}	R_1	βB	αP
SM_{1b}	R_1	$(1-\beta)B$	αP
SM_{2a}	R_2	βB	$(1-\alpha)P$
SM_{2b}	R_2	$(1-\beta)B$	$(1-\alpha)P$

Where α is the fraction of the total power P, known as power allocation coefficient and β is the fraction of the total bandwidth B, known as bandwidth allocation coefficient. h is the channel gain coefficient and n is the AWGN samples.

For the OFDMA scheme, the received vector for the l_{th} SMs can be written as:

$$y_l = h_l s_l \sqrt{\alpha_l P} + n \tag{3.1}$$

For the PD-NOMA scheme, the received vector for the l_{th} SMs can be written as:

$$y_l = h_l s_l \sqrt{\alpha_l P} + h_l s_t \sqrt{\alpha_t P} + n \tag{3.2}$$

For the OFDMA scheme, the SNR for the l_{th} SMs is given by:

$$SNR_l = \frac{P|h_l|^2}{\beta_l B N_0} \tag{3.3}$$

For the PD-NOMA scheme, the SNR for the l_{th} SMs is given by:

$$SNR_l = \frac{\alpha_l P_l |h_l|^2}{\sum_{t \neq l} \alpha_t P + B N_0} \tag{3.4}$$

The sum-rate R_{OFDMA} for the OFDMA systems can be written as:

$$R_{OFDMA} = \sum_{l=1}^{L} \beta_l B \log_2 \left(1 + \frac{P|h_l|^2}{\beta_l B N_0}\right) \tag{3.5}$$

The sum-rate $R_{PD-NOMA}$ for the PD-NOMA systems can be written as:

$$R_{PD-NOMA} = B \sum_{l=1}^{L} \log_2 \left(1 + \frac{\alpha_l P_l |h_l|^2}{\sum_{t \neq l} \alpha_t P + B N_0}\right) \tag{3.6}$$

where $\sum_{l=1}^{L} \beta_l B = B$ and $\sum_{l=1}^{L} \alpha_l P = P$. N_O is the noise spectral density watt/sec/Hz, $N = W N_O$.

Therefore, the SNRs for SM_{1a}, SM_{1b}, SM_{2a} and SM_{2b} can be written as:

$$SNR_{1a} = \frac{\alpha P |h_{1a}|^2}{\beta B N_0} \tag{3.7a}$$

$$SNR_{1b} = \frac{\alpha P |h_{1b}|^2}{(1-\beta) B N_0} \tag{3.7b}$$

$$SNR_{2a} = \frac{(1-\alpha) P |h_{2a}|^2}{\alpha P |h_{2a}|^2 + \beta B N_0} \tag{3.7c}$$

$$SNR_{2b} = \frac{(1-\alpha) P |h_{2b}|^2}{\alpha P |h_{2a}|^2 + (1-\beta) B N_0} \tag{3.7d}$$

The data rates for SM_{1a}, SM_{1b}, SM_{2a} and SM_{2b} can be written as:

$$R_{1a} = \beta B \log_2 \left(1 + \frac{\alpha P |h_{1a}|^2}{\beta B N_0}\right) \tag{3.8}$$

$$R_{1b} = (1-\beta)B\log_2\left(1+\frac{\alpha P|h_{1b}|^2}{(1-\beta)BN_0}\right) \tag{3.9}$$

$$R_{2a} = \beta B\log_2\left(1+\frac{(1-\alpha)P|h_{2a}|^2}{\alpha P|h_{2a}|^2+\beta BN_0}\right) \tag{3.10}$$

$$R_{2b} = (1-\beta)B\log_2\left(1+\frac{(1-\alpha)P|h_{2b}|^2}{\alpha P|h_{2a}|^2+(1-\beta)BN_0}\right) \tag{3.11}$$

The total system capacity can be written as:

$$C_{Composite} = B\Bigg[\beta\Bigg\{\log_2\left(1+\frac{\alpha P|h_{1a}|^2}{\beta BN_0}\right)\Bigg)+\log_2\left(1+\frac{(1-\alpha)P|h_{2a}|^2}{\alpha P|h_{2a}|^2+\beta BN_0}\right)\Bigg)\Bigg\}+ (1-\beta)\Bigg\{\log_2\left(1+\frac{\alpha P|h_{1b}|^2}{(1-\beta)BN_0}\right)+\log_2\left(1+\frac{(1-\alpha)P|h_{2b}|^2}{\alpha P|h_{2a}|^2+(1-\beta)BN_0}\right)\Bigg\}\Bigg] \tag{3.12}$$

The above equation (3.12) represents the system capacity of the primordial system model. SMs that are close to BS have high channel gain than farther SMs because channel gain often depends on the path. BS has to offer more power to those SMs have low channel condition to maintain fairness among SMs [16].

3.2 Extended System Model

SMs/users are randomly distributed within the coverage area or in a cell. Due to the spatial division of the OBF, PD-NOMA with OBF can be considered as an appropriate combination for the SM communication network. The Random distributed SMs can access the network by employing OBF. To implement communication infrastructure for randomly distributed SMs, there is a need to deploy a BS with multiple antenna system among SMs and other communication units. Moreover, a grid station or substations can work as a BS.

In this section, the mathematical expression of the average achievable system capacity for the proposed system model is derived. OBF with PD-NOMA is Implemented by considering the combined effect of background noise and IN. For IN, Gaussian and Laplacian models are considered with Bernoulli arrival rate of impulse. Furthermore, the performance in practical scenarios of IN is analyzed to find the actual loss.

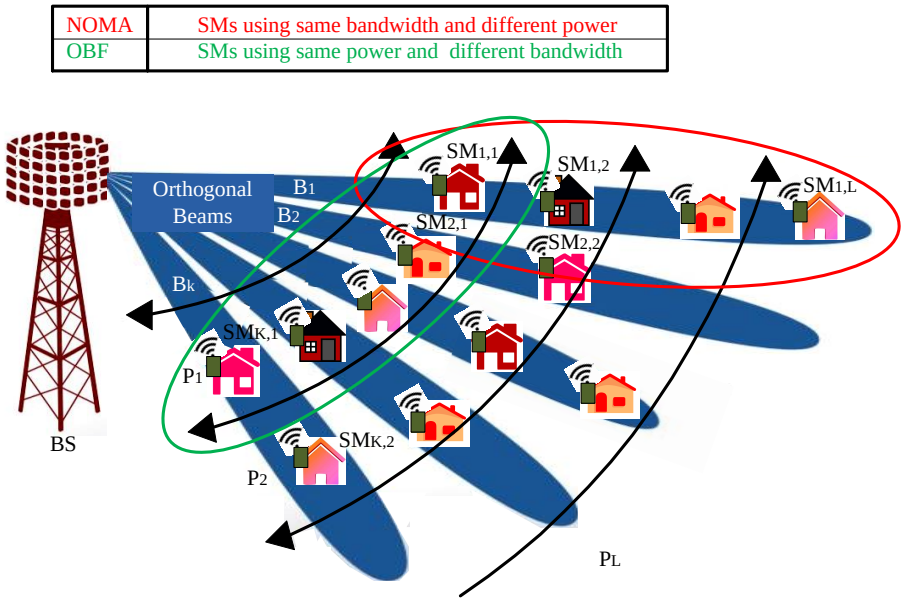

Figure 3.2:: Extended SG communication system model.

Let us assume an SG communication system where the GS, acts as a BS, and transmits data to SMs, as shown in Fig. 3.2. The system model consists of K numbers of orthogonal beams/clusters, and BS allocates a fraction of bandwidth βB to each beam, where β is the bandwidth allocation coefficient. In addition, the model system consists of L number of power levels, and BS allocates a fraction of power αP to each SM, where α is the power allocation coefficient. While B is the total system bandwidth and P is the total available power for a single beam. BS allocates power $P_1 = \alpha_1 P$ to the closest SM and $P_l = \alpha_l P$ to the farthest SM. Furthermore, BS allocates bandwidth $B_1 = \beta_1 B$ to first beam and $B_k = \beta_k B$ to k_{th} beam.

where:

$$h_1 > h_2 > h_3 > \cdots > h_l$$

$$\alpha_1 < \alpha_2 < \alpha_3 < \cdots < \alpha_l$$

$$\alpha_1 + \alpha_2 + \alpha_3 + \cdots + \alpha_l = 1$$

$$\alpha_1 P + \alpha_2 P + \alpha_3 P + \cdots + \alpha_l P = P$$

$$\beta_1 + \beta_2 + \beta_3 + \cdots + \beta_k = 1$$

$$\beta_1 B + \beta_2 B + \beta_3 B + \cdots + \beta_k B = B$$

Where α is the fraction of the total power P, known as power allocation coefficient and β is the fraction of the total bandwidth B, known as bandwidth allocation coefficient. h is the channel gain coefficient and n is the AWGN samples.

BS receives information about the position of SMs (R as distance from BS, angle of arrival θ and channel condition h) through CSI. SMs which are located within the same beam utilize PD-NOMA in which the bandwidth is same but power is different. The SMs which are located under different beams utilize different orthogonal bandwidths by employing OBF. In PD-NOMA, BS allocates different power to different SMs according to their channel condition or link distance. At the receiver end, SM utilizes SIC to extract its own signal from the superimposed signal by subtracting the other SMs signals.

The BS is served by N_t antenna array and is divided into K sub-transmission units by employing OBF. Each sub-transmission unit consists of L number of SMs. Each SM has a single receiving antenna, therefore the total number of SMs that a BS can serve is $K \times L$ and the total M number of SMs are present under one BS. The BS can split data streams for each beam using beamforming by assigning a weight vector to each of K beams. The weight vectors $\{w_n\}_{n=1}^{N_t}$ are unitary orthogonal vectors, where $w_n \in C^{N_t \times 1}$ is a beamforming vector with $\|w_n\| = 1$. In order to reduce interference among beams, a set of OBF vectors is used among all groups of SMs. The orthogonality of beams considered is to be maintained during transmission [15].

3.3 Noise Analysis in Smart Grid/Smart Meter

The channel of SG communication is contaminated by power system noises and interferences caused by external electromagnetic disturbances. The performance of the SM is affected by the IN present in the power system. Therefore, it is important to analyze and develop an appropriate model for IN which helps in recovering the loss caused by IN [10].

The input BPSK information signal (s) is transmitted through the channel. The received symbol y_l at the output of the l_{th} receiver after matched filtering is

given below:

$$y_l = h_l s_l + \xi \tag{3.13}$$

where h is the channel gain coefficient and s is the transmitted BPSK information-bearing signal with average energy E_b ($s_1 = \sqrt{E_b}$ or $s_0 = -\sqrt{E_b}$ along with the same apriori probabilities) and ξ is the combined noise level (AWGN and IN). However, IN changes more quickly with time in comparison with background noise. Hence, a combined statistical noise model is required which includes the impact of IN and background noise [8]. The Bernoulli-Gaussian model and the Laplacian-Gaussian model are the best model for IN as the probability distribution curve is close to the actual IN scenario.

3.3.1 Bernoulli-Gaussian Model

It is difficult to model the exact representation of the arrival of IN, however, the Bernoulli random process and the IN have two common properties; (i) the amplitude of the impulse has occurred for a short duration and it is considerably higher than the background noise, (ii) the time of arrival of an impulse is random, but it arrives with probability. Therefore, Bernoulli random process can be used in the modeling of the arrival of impulses. According to the Bernoulli-Gaussian noise model, the total noise can be expressed as:

$$\xi = n_G + bn_I \tag{3.14}$$

where n_G and n_I are AWGN with variances σ_G^2 and σ_I^2, and mean $\mu = 0$. Also, b is known as Bernoulli random sequence, unconstrained of n_G and n_I, along with parameter p (probability). The arrival of IN follows the Bernoulli probability distribution. The values of the noise n_G and n_I follow the Gaussian probability distribution and using [135, 136] the PDF is given as:

$$P_{N_{G,I}}(n_{G,I}) = \frac{1}{\sqrt{2\pi\sigma_{G,I}^2}} \exp\left(\frac{-(n_{G,I}-\mu)^2}{2\sigma_{G,I}^2}\right)$$

According to the central limit theorem, the noise is independent and identically distributed random variables, and its PDF is given as:

$$P_n(x) = (1-p)\mathbf{G}(x, 0, \sigma_G^2) + p\mathbf{G}(x, 0, \sigma_G^2 + \sigma_I^2) \tag{3.15}$$

where $G(x, 0, \sigma_G^2)$ is a Gaussian PDF with variance σ_G^2 and mean $\mu_x = 0$. ξ_0 is the average combined noise power (AWGN and IN) can be written as:

$$\xi_o = E[n^2] \tag{3.16}$$

$$\xi_o = E[n_G^2] + E[b^2]E[n_I^2] \tag{3.17}$$

$$\xi_o = \sigma_G^2 + p\,\sigma_I^2 \tag{3.18}$$

Equation (3.18) shows that the average combined noise power depends on both the average Gaussian noise power and the average IN power (Gaussian distributed) with probability (p).

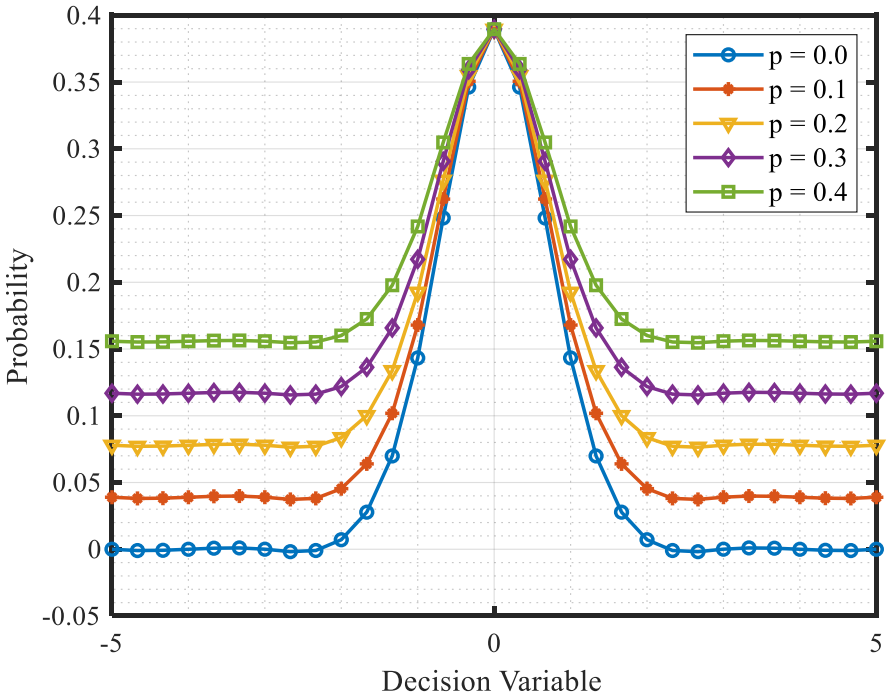

Figure 3.3:: PDF of Bernoulli-Gaussian model with parameter p, where $p \in \{0.0 - 0.5\}$.

3.3.2 Laplacian-Gaussian Model

The second model is non-Gaussian which is considered to model the impulses. The PDF of the Laplacian model has a heavier tail that indicates its PDF comes up to zero more slowly as in comparison with Gaussian noise PDF. The PDF of Laplace

distributions is more closely related to impulses distribution. The PDF of Laplacian distributed noise with variance $2c^2$ and zero mean is given by:

$$P_{N_I}(n_I) = \frac{1}{2c} \exp\left(-\frac{|n_I|}{c}\right)$$

The noise is independent and identically distributed random variables and its PDF is given as:

$$P_n(x) = (1-p)\mathbf{G}(x, 0, \sigma_G^2) + p\mathbf{L}(x, 0, 2c_I^2) \tag{3.19}$$

The noise n_G follows the Gaussian probability distribution and the noise n_I follows the Laplace probability distribution. The arrival rate of impulses is described by Bernoulli random variable r with the parameter p (probability) [137]. According to the Laplacian-Gaussian noise model, the average combined noise power can be written as:

$$\xi_o = E[n_G^2] + E[r^2]E[n_I^2] \tag{3.20}$$

$$\xi_o = \sigma_G^2 + p\ 2c^2 \tag{3.21}$$

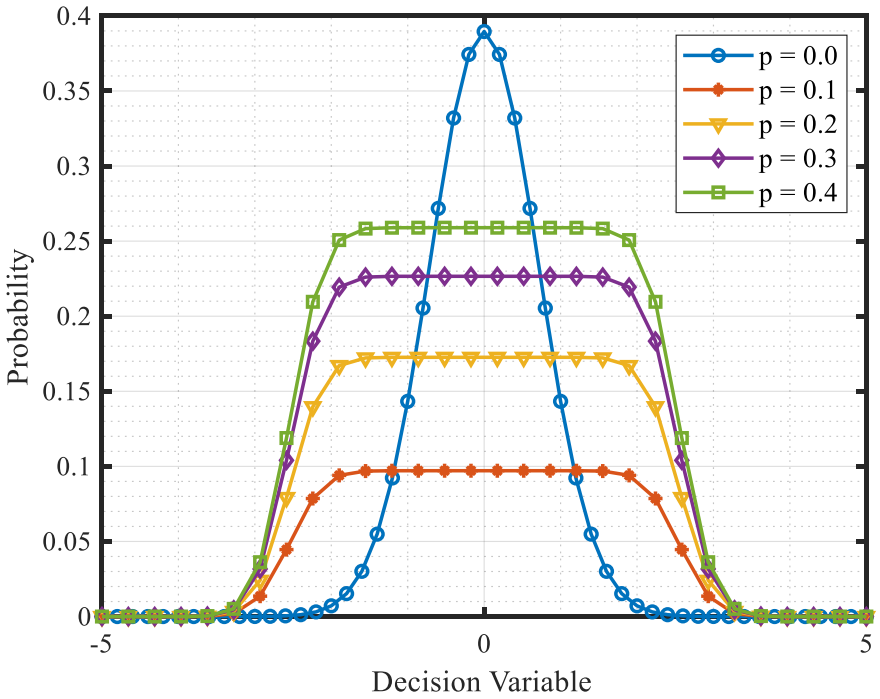

Figure 3.4:: PDF of Laplacian-Gaussian model with parameter p, where $p \in \{0.0 - 0.5\}$.

Equation (3.21) shows that the average combined noise power depends on both the average Gaussian noise power and the average IN power (Laplacian distributed) with probability (p).

The combined probability distribution of Gaussian noise and IN (Gaussian distributed with the probability of arrival of impulses p,) is expressed in equation (3.15) and plotted in Fig. 3.3 for different values of p. On the other hand, the combined probability distribution of Gaussian noise and IN (Laplacian distributed with the probability of arrival of impulses p,) is expressed in equation (3.19) and plotted in Fig. 3.4 for different values of p. It is clearly seen from Fig. 3.3 and Fig. 3.4 that the Laplacian-Gaussian distribution is not exactly similar to the Bernoulli-Gaussian distribution because IN is considered Laplace distributed in Laplacian-Gaussian model as while in Gaussian distributed in Bernoulli-Gaussian. From Fig. 3.3 and Fig. 3.4, it is observed that the PDF of the Laplacian-Gaussian model has heavy tail than the PDF of the Bernoulli-Gaussian model. It indicates the PDF of Laplacian-Gaussian model move towards zero more slowly as compared to the Bernoulli-Gaussian model. Therefore a large number of impulses with short amplitude can be considered in this model. It is noticed from Fig. 3.3 and Fig. 3.4, that the joint PDF of both models is very similar to the derived expression.

3.4 Conventional and Orthogonal Beamforming

In conventional multiuser beamforming, several SMs are employed at the same frequency and time, thus SMs produce interference among themselves, which results in low SNR, small throughput, and high interference [26]. The BS with multiple antenna array serves every SM of each beam. When all beams utilize CBF, for the k_{th} beam, the received signal at $SM_{k,1}, SM_{k,2}$, and $SM_{k,l}$ can be written as:

$$y_{k,1} = h_{k,1}\sqrt{\alpha_{k,1}P}x_{k,1} + h_{k,1}\sum_{t=1,t\neq l}^{L-1}\sqrt{\alpha_{k,t}P}x_{k,t} + h_{k,1}\sum_{i=1,i\neq k}^{K-1}\{w_i\sum_{t=1}^{L}\sqrt{\alpha_{i,t}P}x_{i,t}\} + \xi \tag{3.22}$$

$$y_{k,2} = h_{k,2}\sqrt{\alpha_{k,2}P}x_{k,2} + h_{k,2}\sum_{t=1,t\neq l}^{L-1}\sqrt{\alpha_{k,t}P}x_{k,t} + h_{k,2}\sum_{i=1,i\neq k}^{K-1}\{w_i\sum_{t=1}^{L}\sqrt{\alpha_{i,t}P}x_{i,t}\} + \xi \tag{3.23}$$

similarly

$$y_{k,l} = h_{k,l}\sqrt{\alpha_{k,l}P}x_{k,l} + h_{k,l}\sum_{t=1,t\neq l}^{L-1}\sqrt{\alpha_{k,t}P}x_{k,t} + h_{k,l}\sum_{i=1,i\neq k}^{K-1}\{w_i\sum_{t=1}^{L}\sqrt{\alpha_{i,t}P}x_{i,t}\} + \xi \tag{3.24}$$

where the first term is the received signals for $SM_{k,l}$, the second term is the intra-beam interference, the third term is the inter-beam interference and the last term is the combined noise level (AWGN and IN). $W_k = [w_1, w_2, ..., w_i, ..., w_{N_t}, K]$ is denoted as a set of beamforming weight vectors. $|h_{k,1}|, |h_{k,2}|$ and $|h_{k,l}|$ are the corresponding channel attenuation factor for the link between the BS and the SM. $x_{k,1}, x_{k,2}$ and $x_{k,l}$ are transmitted data from the BS to $SM_{k,1}, SM_{k,2}$ and $SM_{k,l}$. α is known as the power allocation coefficient for the SMs, P is the total available power for a single beam. Therefore, the SNRs for $SM_{k,1}, SM_{k,2}$, and $SM_{k,l}$ in the presence of inter-beam interference can be written as:

$$SNR_{k,1} = \frac{\alpha_{k,1}P|h_{k,1}|^2}{\xi_o + \sum_{i=1,i\neq k}^{K-1}\{w_i\sum_{t=1}^{L}\alpha_{i,t}P\}\}|h_{k,2}|^2} \tag{3.25}$$

$$SNR_{k,2} = \frac{\alpha_{k,2}P|h_{k,2}|^2}{\xi_o + \{\alpha_{k,1}P + \sum_{i=1,i\neq k}^{K-1}\{w_i\sum_{t=1}^{L}\alpha_{i,t}P\}\}|h_{k,2}|^2} \tag{3.26}$$

similarly

$$SNR_{k,l} = \frac{\alpha_{k,l}P|h_{k,l}|^2}{\xi_o + \{\sum_{t=1,t\neq l}^{L-1}\alpha_{k,t}P + \sum_{i=1,i\neq k}^{K-1}\{w_i\sum_{t=1}^{L}\alpha_{i,t}P\}\}|h_{k,l}|^2} \tag{3.27}$$

For the OFDMA system, the SNR for the l_{th} user can be written as:

$$SNR_{k,l} = \frac{\alpha P|h_{k,l}|^2}{\xi_o + \{\sum_{i=1,i\neq k}^{K-1}w_i\}L\alpha P|h_{k,l}|^2} \tag{3.28}$$

Spectral efficiency increases by CBF however, due to inter-beam interference overall system capacity does not improve. Therefore, the proposed OBF can be evaluated to improve spectral efficiency by minimizing inter-beam interference.

This research presents an OBF scheme for proposed model that can ensure zero interference between beams/sectors even if the number of SMs are large. To produce the orthogonal beams among the sectors, Gram-Schmidt orthogonalization is used [164, 165]. The i_th sub-transmission unit of BS i.e. BS_i with N_t antennas generates a beam for the i_th sector. Remaining $k-1$ sub-transmission units of BS

generate $k-1$ orthogonal beams for $k-1$ sectors with BS_i. The BS_i transmit data to l number of SMs without any interference with other $l \times (k-1)$ SMs present in $k-1$ sectors by using the OBF vectors. To generate $k-1$ orthogonal beams for $(k-1)_{th}$ BS, let weight vector w_i for the i_{th} sector be obtained by an arbitrary vector v_i as:

$$w_i = \frac{u_i}{|u_i|} = \frac{v_i}{|v_i|} \tag{3.29}$$

Remaining orthogonal vectors w_{k-1} can be calculated as:

$$u_{k-1} = v_{k-1} - \sum_{j=1}^{k-2} \frac{u_{k-1}^H v_{k-1}}{u_j^H u_j} v_j \tag{3.30}$$

The normalized orthogonal vector can be calculated as:

$$w_{k-1} = \frac{u_{k-1}}{|u_{k-1}|} \tag{3.31}$$

To calculate orthogonal weighting vectors, iterate the method till $(k-1)_{th}$. The calculated OBF w_{k-1} vectors are orthogonal to BS_i's vector w_i, because w_{k-1} vectors are created using Gram-Schmidt orthogonalization process on the basis of w_i. Thus, the created w_{k-1} and the w_i meet the following property.

$$w_i^* w_k = \begin{cases} 1, & i = k \\ 0, & i \neq k \end{cases} \tag{3.32}$$

where $(\cdot)^*$ symbolizes the conjugate transpose of a matrix or vector. As a result, transmitted signals don't interfere each other because the weighting vectors for BS_k are orthogonal, for $k = 1, 2, 3, \cdots$. Therefore, space division access is achievable. Due to OBF vectors, after the cancellation of inter-beam interference equations (3.22), (3.23) and (3.24) can be simplified as:

$$y_{k,1} = h_{k,1}\sqrt{\alpha_{k,1}P}x_{k,1} + h_{k,1}\sum_{t=1}^{L-1}\sqrt{\alpha_{k,t}P}x_{k,t} + \xi \tag{3.33}$$

$$y_{k,2} = h_{k,2}\sqrt{\alpha_{k,2}P}x_{k,2} + h_{k,2}\sum_{t=1}^{L-1}\sqrt{\alpha_{k,t}P}x_{k,t} + \xi \tag{3.34}$$

similarly

$$y_{k,l} = h_{k,l}\sqrt{\alpha_{k,l}P}x_{k,l} + h_{k,l}\sum_{t=1}^{L-1}\sqrt{\alpha_{k,t}P}x_{k,t} + \xi \tag{3.35}$$

Therefore the SNRs for$SM_{k,1}, SM_{k,2}$ and $SM_{k,l}$ become as:

$$SNR_{k,1} = \frac{\alpha_{k,1} P |h_{k,1}|^2}{\xi_o} \tag{3.36}$$

$$SNR_{k,2} = \frac{\alpha_{k,2} P |h_{k,2}|^2}{\xi_o + \alpha_{k,1} P |h_{k,2}|^2} \tag{3.37}$$

similarly

$$SNR_{k,l} = \frac{\alpha_{k,l} P |h_{k,l}|^2}{\xi_o + \sum_{t=1,t\neq l}^{L=1} \alpha_{k,t} P |h_{k,l}|^2} \tag{3.38}$$

For OFDMA system, the SNR for l_{th} user can be written as:

$$SNR_{k,l} = \frac{\alpha P |h_{k,l}|^2}{\xi_o} \tag{3.39}$$

3.4.1 For PD-NOMA

The SNR for the l_{th} SM can be written as:

$$SNR_l = \frac{\alpha_{k,l} P |h_{k,l}|^2}{\xi_o + \sum_{t=1,t\neq l}^{L=1} \alpha_{k,t} P |h_{k,l}|^2} \tag{3.40}$$

The SNR of the l_{th} SM for the k_{th} conventional beam can be written as:

$$SNR_{k,l} = \frac{\alpha_{k,l} P |h_{k,l}|^2}{\xi_o + \{\sum_{t=1,t\neq l}^{L-1} \alpha_{k,t} P + \sum_{i=1,i\neq k}^{K-1} \{w_i \sum_{t=1}^{L} \alpha_{i,t} P\}\} |h_{k,l}|^2} \tag{3.41}$$

The SNR of the l_{th} SM for k_{th} orthogonal beam can be written as:

$$SNR_{k,l} = \frac{\alpha_{k,l} P |h_{k,l}|^2}{\xi_o + \sum_{t=1,t\neq l}^{L=1} \alpha_{k,t} P |h_{k,l}|^2} \tag{3.42}$$

User-rate of the l_{th} SM can be written as:

$$R_l = \beta_k B \log_2 \left(1 + \frac{\alpha_{k,l} P |h_{k,l}|^2}{\xi_o + \sum_{t=1,t\neq l}^{L=1} \alpha_{k,t} P |h_{k,l}|^2}\right) \tag{3.43}$$

User-rate of the l_{th} SM for k_{th} conventional beam can be written as:

$$R_{k,l} = \beta_k B \log_2 \left(1 + \frac{\alpha_{k,l} P |h_{k,l}|^2}{\xi_o + \{\sum_{t=1,t\neq l}^{L-1} \alpha_{k,t} P + \sum_{i=1,i\neq k}^{K-1} \{w_i \sum_{t=1}^{L} \alpha_{i,t} P\}\} |h_{k,l}|^2}\right) \tag{3.44}$$

User-rate of the l_{th} SM for k_{th} orthogonal beam can be written as:

$$R_{l,k} = \beta_k B \log_2 \left(1 + \frac{\alpha_{k,l} P |h_{k,l}|^2}{\xi_o + \sum_{t=1,t\neq l}^{L=1} \alpha_{k,t} P |h_{k,l}|^2}\right) \tag{3.45}$$

System capacity for the l_{th} number of user in a single beam can be written as:

$$C_{PD-NOMA(i=1)} = \sum_{t=1}^{L} R_l \tag{3.46}$$

System capacity for the l_{th} number of users utilize single conventional beam can be written as:

$$C_{PD-NOMA(k=1)} = \sum_{t=1}^{L} \beta_k B_k \log_2 \left(1 + \frac{\alpha_{k,l} P |h_{k,l}|^2}{\xi_o + \{\sum_{t=1,t\neq l}^{L-1} \alpha_{k,t} P + \sum_{i=1,i\neq k}^{K-1} \{w_i \sum_{t=1}^{L} \alpha_{i,t} P\}\} |h_{k,l}|^2}\right) \tag{3.47}$$

System capacity for the l_{th} number of users utilize single orthogonal beam can be written as:

$$C_{PD-NOMA(k=1)} = \sum_{t=1}^{L} \beta_k B_k \log_2 \left(1 + \frac{\alpha_{k,l} P |h_{k,l}|^2}{\xi_o + \sum_{t=1,t\neq l}^{L=1} \alpha_{k,t} P |h_{k,l}|^2}\right) \tag{3.48}$$

Total system capacity for the $l \times k$ number of users can be written as:

$$C_{PD-NOMA(BF)} = \beta_k B \sum_{i=1}^{K} C_{PD-NOMA(k)} = \beta_k B \sum_{i=1}^{K} \sum_{t=1}^{L} R_l \tag{3.49}$$

Total system capacity for the $l \times k$ number of users utilizing PD-NOMA and conventional beams can be written as:

$$C_{PD-NOMA(CBF)} = \beta_k B \sum_{i=1}^{K} \left\{ \sum_{t=1}^{L} \log_2 \left(1 + \frac{\alpha_{k,l} P |h_{k,l}|^2}{\xi_o + \{\sum_{t=1,t\neq l}^{L-1} \alpha_{k,t} P + \sum_{i=1,i\neq k}^{K-1} \{w_i \sum_{t=1}^{L} \alpha_{i,t} P\}\} |h_{k,l}|^2}\right)\right\} \tag{3.50}$$

Total system capacity for the $l \times k$ number of users utilizing PD-NOMA and orthogonal beams can be written as:

$$C_{PD-NOMA(OBF)} = \beta_k B \sum_{i=1}^{K} \left\{ \sum_{t=1}^{L} \log_2 \left(1 + \frac{\alpha_{k,l} P |h_{k,l}|^2}{\xi_o + \sum_{t=1,t\neq l}^{L=1} \alpha_{k,t} P |h_{k,l}|^2}\right)\right\} \tag{3.51}$$

3.4.2 For OFDMA

The SNR for the l_{th} SM can be written as:

$$SNR_l = \frac{\alpha P |h_{k,l}|^2}{\xi_0} \tag{3.52}$$

The SNR of the l_{th} SM for the k_{th} conventional beam can be written as:

$$SNR_{k,l} = \frac{\alpha P|h_{k,l}|^2}{\xi_o + \{\sum_{i=1,i\neq k}^{K-1} w_i\} L\alpha P|h_{k,l}|^2} \tag{3.53}$$

The SNR of the l_{th} SM for the k_{th} orthogonal beam can be written as:

$$SNR_{k,l} = \frac{\alpha P|h_{k,l}|^2}{\xi_o +} \tag{3.54}$$

User-rate of the l_{th} SM can be written as:

$$R_l = \beta_l B \log_2 \left(1 + \frac{\alpha P|h_{k,l}|^2}{\xi_0}\right) \tag{3.55}$$

User-rate of the l_{th} SM for the k_{th} conventional beam can be written as:

$$R_{k,l} = \beta_{l,k} B \log_2 \left(1 + \frac{\alpha P|h_{k,l}|^2}{\xi_o + \{\sum_{i=1,i\neq k}^{K-1} w_i\} L\alpha P|h_{k,l}|^2}\right) \tag{3.56}$$

User-rate of the l_{th} SM for the k_{th} orthogonal beam can be written as:

$$R_{k,l} = \beta_{l,k} B \log_2 \left(1 + \frac{\alpha P|h_{k,l}|^2}{\xi_o}\right) \tag{3.57}$$

System capacity for the l_{th} number of users for a single beam can be written as:

$$C_{OFDMA(i=1)} = \sum_{t=1}^{L} R_l \tag{3.58}$$

System capacity for the l_{th} number of users utilizing a single conventional beam can be written as:

$$C_{OFDMA(k=1)} = \sum_{t=1}^{L} \beta_l B \log_2 \left(1 + \frac{\alpha P|h_{k,l}|^2}{\xi_0 + \{\sum_{i=1,i\neq k}^{K-1} w_i\} L\alpha P|h_{k,l}|^2}\right) \tag{3.59}$$

System capacity for the l_{th} number of users utilizing a single orthogonal beam can be written as:

$$C_{OFDMA(k=1)} = \sum_{t=1}^{L} \beta_l B \log_2 \left(1 + \frac{\alpha P|h_{k,l}|^2}{\xi_0}\right) \tag{3.60}$$

Total system capacity for the $l \times k$ number of users can be written as:

$$C_{OFDMA(BF)} = \beta_k B \sum_{i=1}^{K} C_{OFDMA(k)} = \beta_k B \sum_{i=1}^{K} \sum_{t=1}^{L} R_l \tag{3.61}$$

Total system capacity for the $l \times k$ number of users utilizing OFDMA and conventional beams can be written as:

$$C_{OFDMA(CBF)} = \sum_{i=1}^{K} \left\{ \sum_{t=1}^{L} \beta_{i,t} B \log_2 \left(1 + \frac{\alpha P |h_{k,l}|^2}{\xi_0 + \{\sum_{i=1, i \neq k}^{K-1} w_i\} L \alpha P |h_{k,l}|^2} \right) \right\} \quad (3.62)$$

Total system capacity for the $l \times k$ number of users utilizing OFDMA and orthogonal beams can be written as:

$$C_{OFDMA(OBF)} = \sum_{i=1}^{K} \left\{ \sum_{t=1}^{L} \beta_{i,t} B \log_2 \left(1 + \frac{\alpha P |h_{k,l}|^2}{\xi_0} \right) \right\} \quad (3.63)$$

Implementation of OBF can effectively reduce inter-beam interference therefore, without degradation of the spectral efficiency of PD-NOMA with OBF can be implemented.

$$C_{PD-NOMA(OBF)} = \sum_{i=1}^{K} \beta_k B \left\{ \sum_{t=1}^{L} \log_2 \left(1 + \frac{\alpha_{k,l} P |h_{k,l}|^2}{\xi_o + \sum_{t=1, t \neq l}^{L-1} \alpha_{k,t} P |h_{k,l}|^2} \right) \right\} \quad (3.64)$$

$$C_{OFDMA(OBF)} = \sum_{i=1}^{K} \left\{ \sum_{t=1}^{L} \beta_{i,t} B \log_2 \left(1 + \frac{\alpha P |h_{k,l}|^2}{\xi_o} \right) \right\} \quad (3.65)$$

The results of the comparison between equation (3.64) and equation (3.65) show that the SMs/user's throughput in PD-NOMA is much higher than OFDMA when it comes to large numbers of SMs. In PD-NOMA each SM utilizes the entire bandwidth of the system, while in OFDMA each new SM divides the bandwidth and utilizes its own share. In OFDMA simple receiver is required to decode the desired signal. In PD-NOMA at the receiver end, a signal cancellation scheme is required because signals of all SMs are superimposed by BS before transmission. The BS allocates unique power to each SM according to its position from BS. Each SM cancels all undesired stronger signals by using the SIC scheme and considers undesired weaker signals as noise. Therefore, the receiver complexity of PD-NOMA is much higher than OFDMA because the PD-NOMA system is receiver-centric rather than transmitter-centric as in the OFDMA system.

3.5 Spectral Efficiency and Energy Efficiency Trade-off

For SE-EE tradeoff, two user model for PD-NOMA and OFDMA are considered. Their achievable data rate can be expressed as:

$$R_1 = B\log_2\left(1+\frac{\alpha_1 P|h_1|^2}{\xi_0}\right) \tag{3.66}$$

$$R_2 = B\log_2\left(1+\frac{\alpha_2 P|h_2|^2}{\alpha_1 P|h_2|^2+\xi_0}\right) \tag{3.67}$$

Therefor, the sum-rate can be expressed as:

$$R = B\left\{\log_2\left(1+\frac{\alpha_1 P|h_1|^2}{\xi_0}\right)+\log_2\left(1+\frac{\alpha_2 P|h_2|^2}{\alpha_1 P|h_2|^2+\xi_0}\right)\right\} \tag{3.68}$$

where $\alpha_1 P$ and $\alpha_2 P$ are the power allocated to SM_1 and SM_2, h_1 and h_2 are the channel gains, respectively and ξ_0 is the average combined noise power. Total power consume at the receiver is P, can be written as:

$$P = P_t + P_c + P_{SIC} \tag{3.69}$$

Where $P_t = \sum_{l=1}^{L}\alpha_l P$ is the actual transmitting power, P_c is the constant power consumption of circuit, P_{sic} is the SIC power consumption for one iteration and $P_{SIC} = \sum_{i=1}^{K-1} P_{i(sic)}$ is the SIC power consumption for k-1 iteration. Energy efficiency (bit/joule) can be written as:

$$EE = \frac{R}{BP} \tag{3.70}$$

$$EE = \frac{\left\{\log_2\left(1+\frac{\alpha_1 P|h_1|^2}{\xi_0}\right)+\log_2\left(1+\frac{\alpha_2 P|h_2|^2}{\alpha_1 P|h_2|^2+\xi_0}\right)\right\}}{\sum_{l=1}^{L}\alpha_l P + P_c + \sum_{i=1}^{K-1} P_{i(sic)}} \tag{3.71}$$

Spectral efficiency (bit/sec/Hertz) can be written as:

$$SE = \frac{R}{B} \tag{3.72}$$

$$SE = \left\{\log_2\left(1+\frac{\alpha_1 P|h_1|^2}{\xi_0}\right)+\log_2\left(1+\frac{\alpha_2 P|h_2|^2}{\alpha_1 P|h_2|^2+\xi_0}\right)\right\} \tag{3.73}$$

For the L number of users:

$$EE = \frac{\sum_{i=1}^{L} \log_2 \left(1 + \frac{\alpha_{k,l} P |h_{k,l}|^2}{\xi_o + \sum_{t=1,t\neq l}^{L-1} \alpha_{k,t} P |h_{k,l}|^2}\right)}{\sum_{l=1}^{L} \alpha_l P + P_c + \sum_{i=1}^{K-1} P_{i(sic)}} \tag{3.74}$$

$$SE = \sum_{i=1}^{L} \log_2 \left(1 + \frac{\alpha_{k,l} P |h_{k,l}|^2}{\xi_o + \sum_{t=1,t\neq l}^{L-1} \alpha_{k,t} P |h_{k,l}|^2}\right) \tag{3.75}$$

For the $L \times K$ number of users:

$$EE = \frac{\sum_{i=1}^{K} \left\{ \sum_{i=1}^{L} \log_2 \left(1 + \frac{\alpha_{k,l} P |h_{k,l}|^2}{\xi_o + \sum_{t=1,t\neq l}^{L-1} \alpha_{k,t} P |h_{k,l}|^2}\right)\right\}}{\sum_{l=1}^{L} \alpha_l P + P_c + \sum_{i=1}^{K-1} P_{i(sic)}} \tag{3.76}$$

$$SE = \sum_{i=1}^{K} \left\{ \sum_{i=1}^{L} \log_2 \left(1 + \frac{\alpha_{k,l} P |h_{k,l}|^2}{\xi_o + \sum_{t=1,t\neq l}^{L-1} \alpha_{k,t} P |h_{k,l}|^2}\right)\right\} \tag{3.77}$$

NGN mainly focuses on the optimum SE-EE tradeoff. In this respect, circuit power, SIC power consumption, and transmission power are included to design the practicable energy model when analyzing the SE-EE tradeff. The above analytical results help in the finding of optimal green point on the SE-EE curve.

3.6 IN Practical Scenarios

To analyze the practical performance of the proposed scheme for SG in the presence of IN, three IN scenarios are considered based on impulsive environment. In the German city of Karlsruhe, a series of measurements were made at seven different sites over the period of 320 000 s or 89 hours in the year 2000 to collect the data for impulsive scenarios [166]. These scenarios are categorized as weakly disturbed, heavily disturbed, and medium disturbed. The total number of impulses that appear in a second is known as the average impulse rate λ_{Avg} and dr specifies the real disturbed time (in ratio) is given by:

$$dr = \frac{\sum_{i=1}^{J} t_{w,i}}{T_{Tot}} \tag{3.78}$$

where $t_{w,i}$ is the width of the i_{th} impulse in sec and j is the total number of impulses occurring in time T_{Tot} (sec). The characteristics for all the above scenarios are taken

from practical circumstances and itemized in Table 3.2 [142].

Table 3.2:: Characteristics of IN scenarios.

S.No.	**Scenario**	$d_{r(Avg)}(\%)$	λ_{Avg}
1	Weakly disturbed	0.00135	0.122
2	Medium disturbed	0.00632	1.04
3	Heavily disturbed	0.0327	5.11

The amplitude and width of IN follow the Gaussian distribution. This means that with a probability of (p) and random IN power (N_I), each data symbol can be independently affected by IN.

$$\xi_0 = N_G + drN_I \tag{3.79}$$

where N_G is AWGN power. To calculate the average IN duration per unit time, the dr expressed in equation (3.78) is utilized. The arrival of IN is characterized by the Poisson process with impulse rate λ/sec. Average dr and SNR with the average dr are given below [142].

$$dr(Avg) = \lambda T_{Noise} \tag{3.80}$$

$$SNR_{dr} = \frac{\alpha_l P|h_l|^2}{\sum_{t=1,t\neq l}^{L-1} \alpha_t P|h_l|^2 + N_G + drN_I} \tag{3.81}$$

The above equation (3.81) is achievable SNR for different noise scenarios, where T_{Noise} is the average impulse duration and dr can be average or instantaneous. Impulses occur for very a short time and increase the noise level up to 50 dB, therefore the only noise amplitude cannot explain the actual disturbance/loss of bits. Therefore, the actual loss of bits/information can be expressed as:

$$\text{Loss of bits} = R_{WithImp} - R_{WithoutImp} \tag{3.82}$$

The above equation shows the actual information loss in terms of the number

of bits [15]. However, a detection technique is needed that detects the corrupted and uncorrupted bits. For example, the DNN approach can be effective in this respect.

3.7 Results and Discussions

PD-NOMA scheme is extremely successful in terms of system-level throughput when the channels are dissimilar for users. The reason behind this is users' access to the PD-NOMA system on the basis of power division. Different power allocation is possible if the channel condition of users is different. Users who are close to BS often have high channel gain than farther users as channel gain depends on the distance from BS. PD-NOMA can offer more power to users who have low channel condition to maintain fairness among users.

3.7.1 Simulation Setup

Through the simulation setup, the proposed scheme has been evaluated in terms of user data rate, sum-rate capacity, and spectral and energy efficiency over IN-contaminated Rayleigh fading channels by mathematical and simulation analyses. The theoretical analyses have been verified by performing Monte Carlo simulations via Matlab. The main simulation parameters and assumptions [163] are itemized in Table 3.3.

The carrier frequency of 2 GHz in the range of FR1, 30 GHz in the range of FR2, and the total bandwidth is 10 MHz is considered in the simulation. The bandwidth of 10 MHz is assumed for all NOMA users, while for OMA the total bandwidth 10 MHz is divided equally among all users within the single sector. The total transmits power is set to 46 dBm. To reduce inter-beam interference, the Gram-Schmidt process takes a set of linearly independent vectors and constructs orthonormal basis vectors. The power of IN having an approximately flat frequency response over the spectrum within the range of {0 - 50} dB is considered. Moreover,

the probability of IN is taken within the range of {0.1 - 0.4}. Weak, medium, and heavy IN scenarios are considered for practical impulsive noise environments.

The simulation of the sum-rate capacity is done by first generating random inputs i.e. distances of the users from BS and sorting the distances of the users in descending order. Moreover, the distances between users are compared with each other to find a sufficient difference between users. Then Rayleigh fading coefficients with zero mean and unit variance are generated for all users. By Multiplying each user's fading coefficient with the square root of the variance, the channel gain for each user is finally estimated. Average IN noise is considered in the initial simulation, then randomly generated IN is convolved with AWGN. After all the runs, the average achievable sum-rate is obtained.

Table 3.3:: Simulation parameters for proposed system model.

S.No.	**Parameter**	**Value**
1	Inter-site distance	500 m
2	Minimum distance between UE and cell site	35 m
3	BS total transmission power	46 dBm
4	Receiver noise density	−174 dBm/Hz
5	Carrier frequency	2 GHz
6	System bandwidth	10 MHz
7	Number of subbands	1 & 12
8	Number of antennas at each user	1
9	Number of antennas at BS, N_t	12 (Number of sector/beam)
10	Antenna gain at BS/User	0 dBm
11	Channel estimation	Ideal
12	IN power	0 dB to 50 dB

13	Disturbance Ratio, dr	0.00135%, 0.00632% & 0.0327%

Power allocation scheme for multiuser single carrier PD-NOMA starts by setting the power allocation parameter for the weakest user $\alpha_l = 3/4$. Since, $h_1 > h_2 > h_3 > \cdots > h_l$ and $\alpha_1 < \alpha_2 < \alpha_3 < \cdots < \alpha_l$. Therefore, $\alpha_{l-1} = 3/4(1 - \alpha_l)$, $\alpha_{l-2} = 3/4(1 - (\alpha_l + \alpha_{l-2}))$ and $\alpha_1 = 3/4(1 - (\alpha_l + \alpha_{l-2} + \cdots + \alpha_2))$.

3.7.2 Primordial System Model

Theoretically, in PD-NOMA each user utilizes the entire bandwidth therefore, as the number of users increases sum-rate capacity also increases. Nevertheless, whenever the number of users increases, the SIC error, the inter-user interference, and the residual interference (due to the SIC error) also increase. The sum-rate capacity of PD-NOMA system with an increasing number of users/SMs is shown in Fig. 3.5 as described in equation (3.6). The sum-rate capacity in PD-NOMA depends on the power allocation and noise power of each user. The total noise power is the sum of two factors: one is the product of PSD of AWGN and the subcarrier bandwidth, and the other is the user's residual interference after SIC. In PD-NOMA, on the basis of the large power difference between the users, PD-NOMA differentiates signals at the receiver by using the SIC scheme. All users utilize the same time-frequency. In the PD-NOMA system, the strong user cancels weak users' signals by implementing SIC and the weak user considers strong users' signals as noise. With the increase of every new user, inter-user interference increases. Therefore, the curve becomes straight if the number of SMs increases greatly as shown in Fig. 3.5.

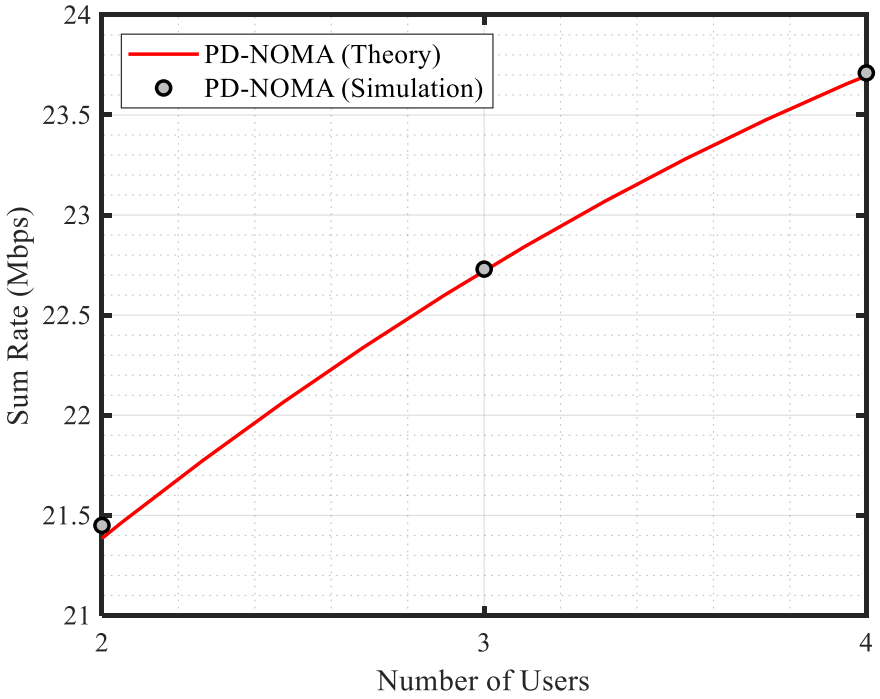

Figure 3.5:: PD-NOMA users/SMs sum-rate capacity.

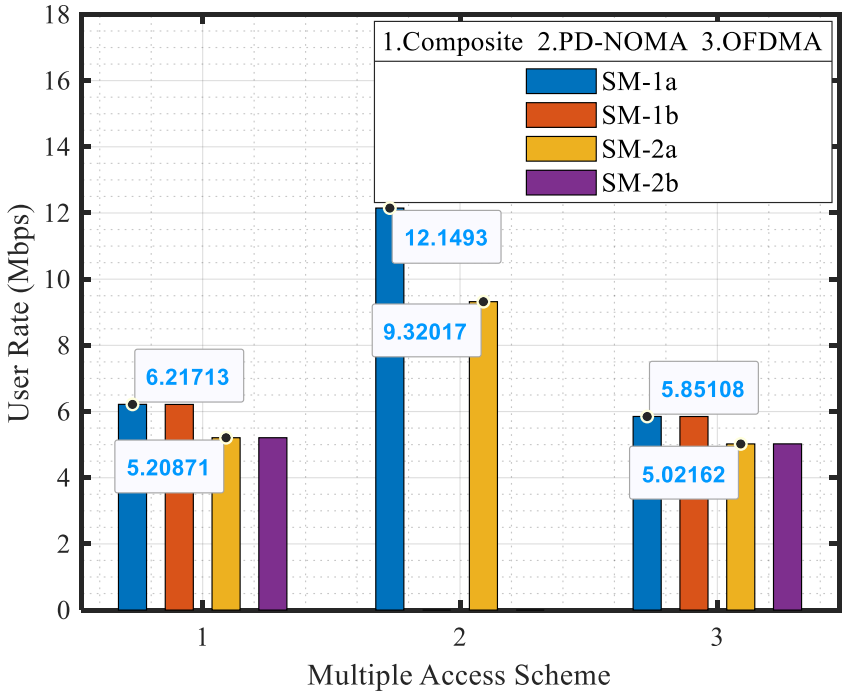

Figure 3.6:: Individual user data rate with different multiple access schemes.

More power is allocated for farther SMs than nearer SMs as per the defined

power allocation scheme. Individual SMs data rates are illustrated in Fig. 3.6 with OFDMA, PD-NOMA, and Composite schemes. SMs utilizing PD-NOMA, provide more data rates than OFDMA. In OFDMA, bandwidth is divided among all SMs while in PD-NOMA, the entire bandwidth is utilized by each SM at the marginal cost of inter-user interference. PD-NOMA is not applicable for SMs that are at the same distance from BS due to the same channel condition. Since SM_{1a}, SM_{1b} and SM_{2a}, SM_{2b} are at the same distance from BS, therefore, only two SMs can employ on PD-NOMA scheme in four user system model as shown in Fig. 3.6. On the other hand, the proposed composite scheme offers an improved data rate as compared to OFDMA and allows all users to employ the composite scheme. In the proposed composite scheme, total bandwidth is divided into only two subcarriers for each pair of SMs (SM_{1a}, SM_{2a} and SM_{1b}, SM_{2b}) and power division is applied between SMs in each pair. While in the OFDMA system, the total bandwidth is divided into four subcarriers for each OFDMA SMs.

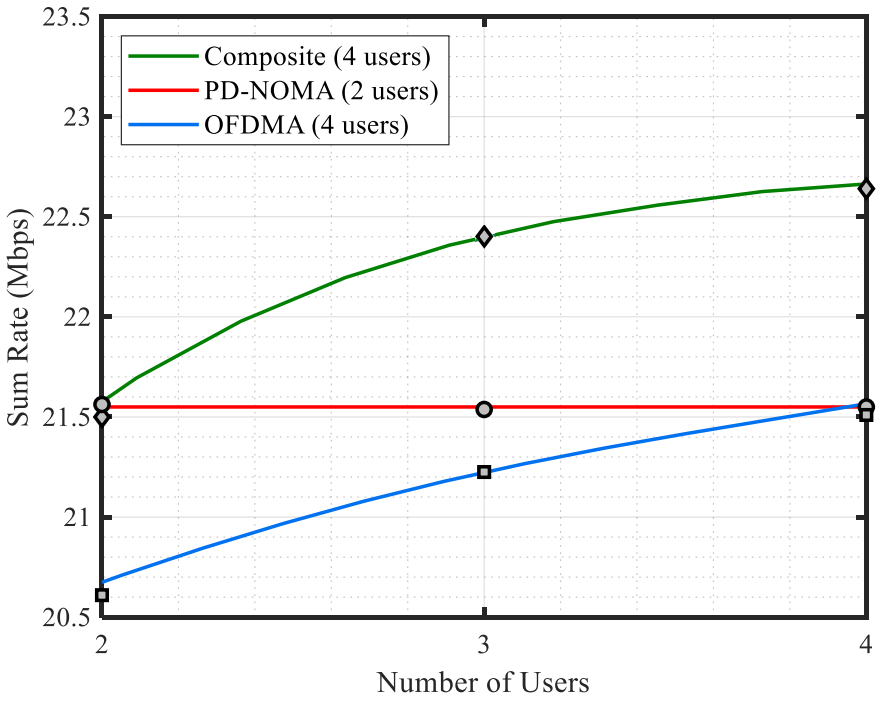

Figure 3.7:: System capacity with number of users.

The sum-rate capacity of OFDMA, PD-NOMA, and Composite scheme are

shown in Fig. 3.7 as described in equations (3.5), (3.6), and (3.12). Theoretically, in OFDMA, the sum-rate capacity is not affected if the number of users increases. PD-NOMA provides no great impact in this model because it accommodates only two SMs. The composite scheme provides better sum-rate capacity than OFDMA and PD-NOMA because every SM in the composite scheme utilizes complete bandwidth at the marginal cost of SIC. Bandwidth can be divided into SMs whenever two or more SMs are at the same distance from BS. Moreover, the Composite scheme provides a fair data rate for each SM by selecting appropriate power according to the channel condition of SMs.

3.7.3 Extended System Model

The extended proposed scheme is based on PD-NOMA and OBF and the result of this scheme is compared with the existing OFDMA in presence of IN for $L = 10$ users within a single beam/cluster. Moreover, OBF is compared with CBF. The proposed scheme is analyzed in the practical IN scenario to evaluate the effect of IN on the data rate of individual SMs.

The BS is considered at the center of the cell and SMs are randomly distributed within the cell. 10 SMs within a single beam ($k = 1$) are considered for initial simulation. It is assumed that perfect CSI is available at BS and during a single round trip, channel characteristics remain the same. Fig. 3.8 illustrates the effect of IN on the system capacity of the proposed scheme and existing OFDMA scheme as described in equations (3.48) and (3.60). Due to OBF, inter-beam interference does not degrade the SNR, however, IN reduces the system capacity. Both curves (with and without IN) of PD-NOMA increase because each new SM in PD-NOMA utilizes the entire bandwidth at the marginal cost of inter-user interference. Contrarily in OFDMA, each new SM shares the bandwidth, therefore, theoretically, the capacity remains the same. It is observed from Fig. 3.8 that if the number of serving SMs is 7-8, the proposed scheme can still perform better than OFDMA even

in presence of IN. The proposed scheme offers a 3 Mbit/sec higher data rate than the traditional OFDMA scheme, leading to better system performance in the case of 10 SMs/users in a sector of a cell.

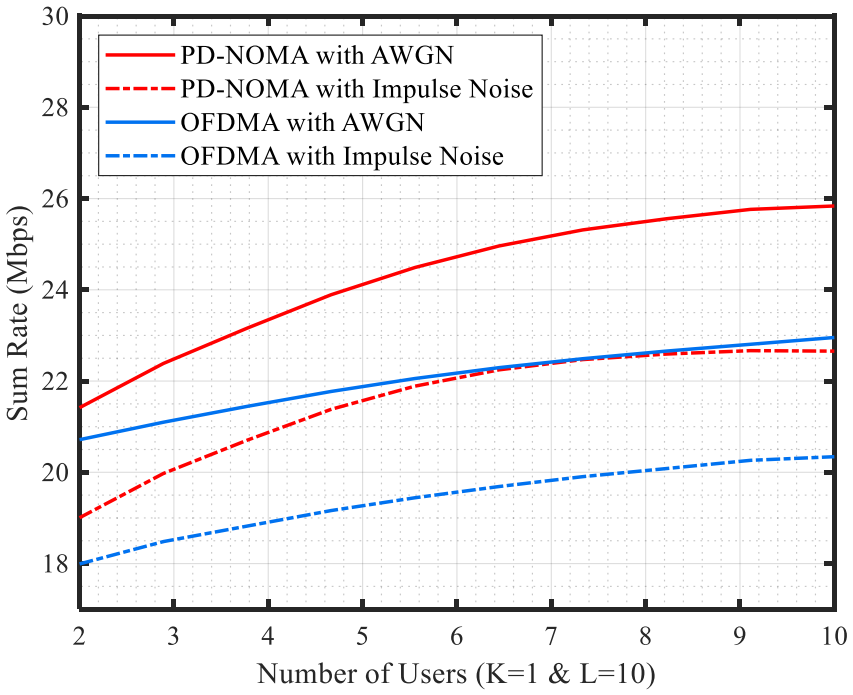

Figure 3.8:: System capacity with AWGN and IN.

Minimizing the null coverage area causes the main lobes to interfere with each other which ultimately, causes high inter-beam interference in CBF. Moreover, further increase in inter-beam interference is caused by the interference of side lobes with the main lobe. Furthermore, the CBF scheme requires feedback information or a feedback channel. The method to achieve correct feedback information is quite difficult as it utilizes a substantial amount of power, and increases latency. Orthogonal beams are produced by using Gram-Schmidt process and all beams are orthogonal to each other, therefore, the inter-beam interference becomes negligible, even if two lobes slightly overlap. Finally, SIC is used to reduce intra-beam interference, i.e., interference among the users having the same orthogonal weights employing the same beam.

Fig. 3.9 illustrates that the proposed scheme i.e. PD-NOMA with OBF ac-

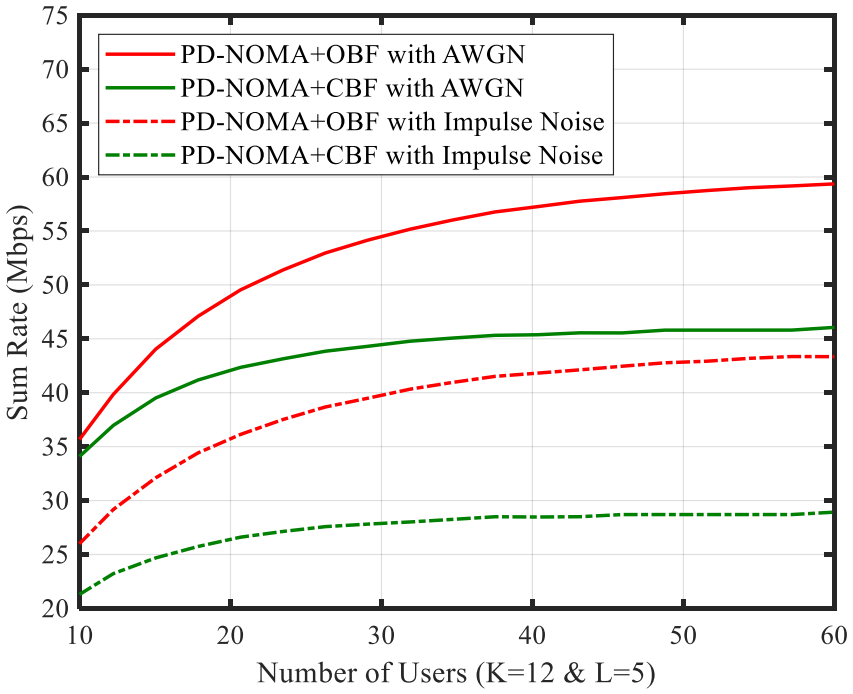

Figure 3.9:: Data rate with conventional and OBF.

commodates a comparatively large number of users before the throughput gain is saturated. 60 SMs within 12 beams ($K = 1$ & $L = 5$), 5 SMs/beam are considered as per equations (3.50) and (3.51) for simulation. After minimizing inter-beam interference by using orthogonal weight vectors, the proposed scheme (PD-NOMA with OBF) offers 17 Mbit/sec more data rate than PD-NOMA with CBF without increasing the feedback bits and latency. The performance increases with the increase in the number of users per cell, till the throughput gain is saturated.

Fig. 3.10 shows the effect of IN on system capacity in practical IN scenarios which are described by weakly, heavily, and medium disturbance ratios. Practical measurement of these scenarios is published in [142]. The characteristic parameters of these scenarios are listed in Table 3.3, which helps in the practical implementation of the proposed scheme. By considering 10 users (K=1 & L=10), as per equation (3.48), the performance of the proposed scheme has been evaluated in weak and medium disturbance scenarios. Results show that the achievable capacity of the proposed scheme in weak and medium scenarios decreases by 1 Mbit/sec but it

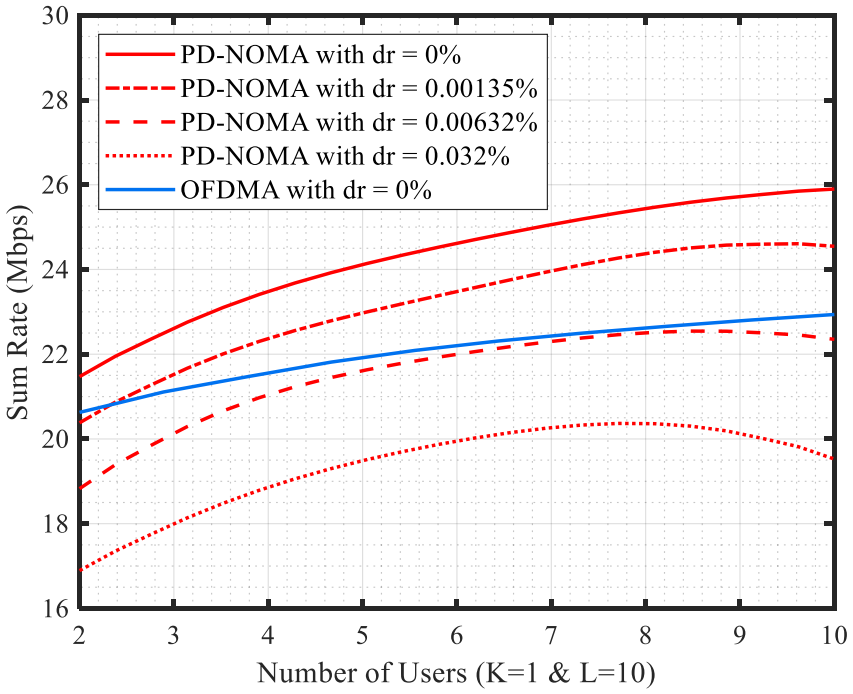

Figure 3.10:: Effect of dr on capacity, dr = 0.00135%, dr = 0.00632% & dr = 0.0327%.

is still better than conventional OFDMA. In a heavily disturbed scenario e.g. an industrial area, the achievable capacity of the system is highly degraded. Therefore, in such scenarios, noise mitigation techniques are required as discussed in chapter 5.

Impulse can increase the noise level up to 50 dB but for a very short period of time, typically 50 μsec with average arrival rate 5 sec^{-1} and average inter-arrival time of 200 msec . As a result, several bit errors or even burst of errors occurs for an instant. But this statistic does not show the actual loss in terms of individual user data rate. In PD-NOMA, the data rate of near and farther SM are not the same, it depends on interference plus noise. The slight change in noise can greatly affect the data rate of a farther/weak user but not necessarily a SIC performing user (nearer/strong). In the PD-NOMA, power division access allows affected users to reduce the effect of IN by increasing the power of the affected user, however, it increases the inter-user interference. In this context, the loss of data in bit/sec

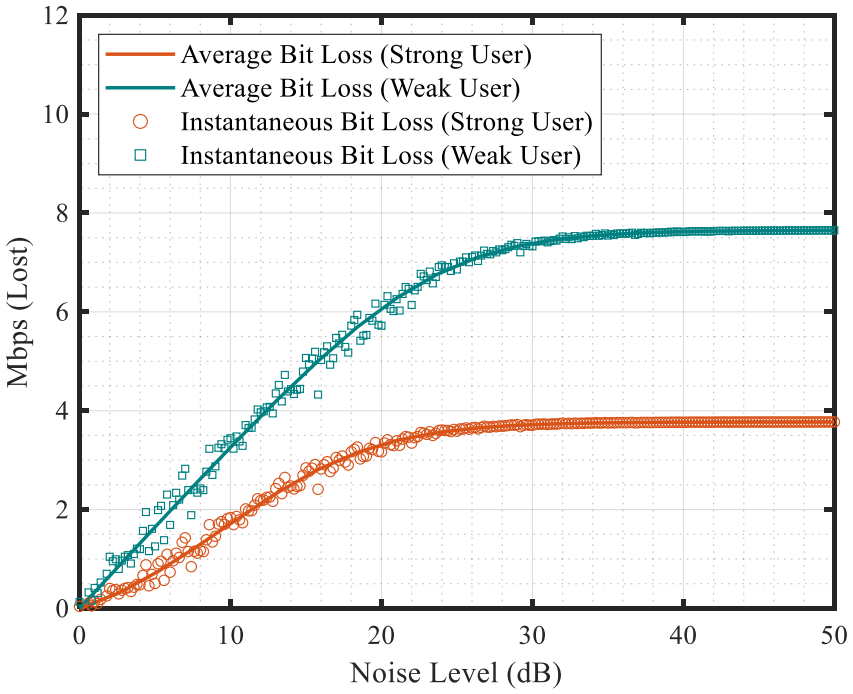

Figure 3.11:: Bits lost/sec due IN with parameter N_I, where $N_I \in \{0 - 50\ dB\}$.

due to the different levels of impulse amplitude is shown in Fig. 3.11 as described in equations (3.81) and (3.82). If the communication link receives average noise $\sigma_I = 30$ dB then the data rate of farther SM decreases by 7.5 Mbit/sec which is 4 Mbit/sec more than the nearer SM. However, nearer SM loses only approximately 50% of its data rate while farther SM loses approximately 80% of its data rate. Nearer SM performs SIC and cancels all the interferences generated by other users' signals, therefore nearer SM can handle IN much better than the farther SM. On the other hand, farther SM does not perform SIC and treats with IN and other users' signals as noise.

One of the key constraints in the implementation of IoT is to supply continuous and sufficient power to IoT devices. Because most IoT devices operating in the field suffer from energy deficiency due to limited power supply by battery. To extend the operating life of IoT devices, authors recently proposed radio frequency energy harvesting as an alternate for battery replacement [97]. RF source is more reliable and controllable to assure a specified amount of indispensable energy trans-

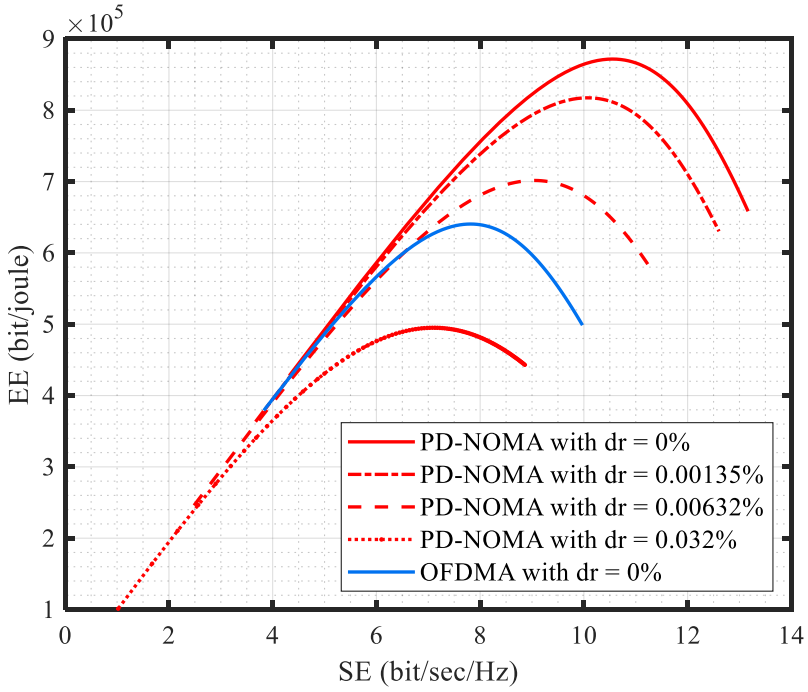

Figure 3.12:: SE-EE tradeoff in presence of IN.

fer. Additionally, RF with beamforming can transfer power to IoT devices that are far-off from the transmitting side in any direction. Furthermore, SG applications such as the meters and sensors need costly maintenance and regular replacement of batteries. Using energy harvesting can dramatically reduce the ongoing costs of running the SG.

RF energy harvesting requires an energy-efficient communication system and in this respect, PD-NOMA can respond better than other schemes. The effect of IN on SE-EE tradeoff is shown in Fig. 3.12 and described in equations (3.71) and (3.73). It is observed from Fig. 3.12, that the green point - which is the best SE-EE tradeoff- is inversely related to the dr. Nevertheless, PD-NOMA with average IN ($dr = 0.00632$) performs better than OFDMA without IN because all PD-NOMA users utilize the same spectrum, therefore, the green point of PD-NOMA with IN is much higher than OFDMA without IN. Hence, PD-NOMA offers the best SE-EE tradeoff. The proposed scheme can serve the use of several different energy harvesting applications.

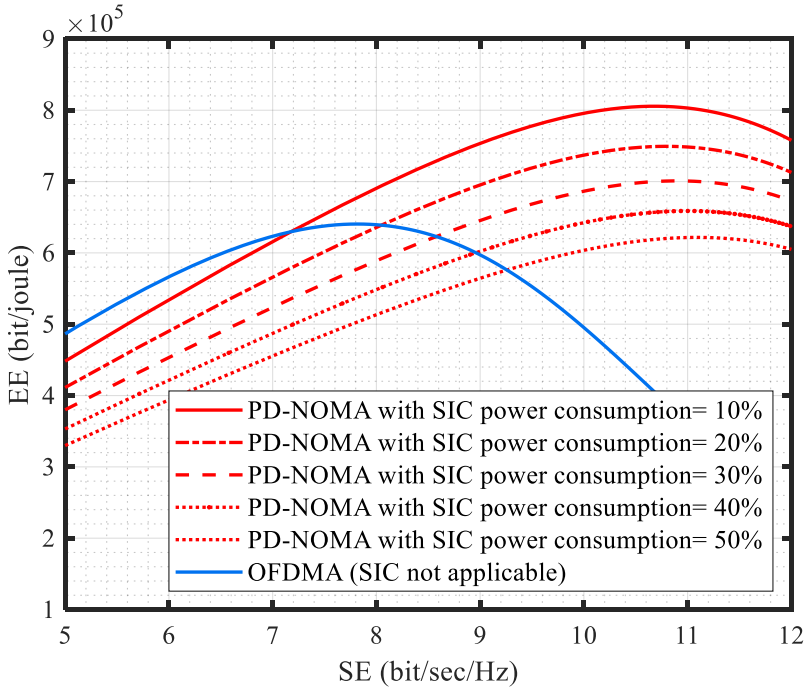

Figure 3.13:: SE-EE tradeoff with SIC power consumption

The dynamic nature of the VANET and the mobility of vehicles imposes a serious challenge that is to minimize transmission delay. Most of the existing schemes for VANETs do not support the low latency during transmission over a wireless link for information sharing from one vehicle to another vehicle and vehicle to roadside unit [100]. On the other hand, PD-NOMA offers low latency by utilizing minimal resources. For the case of four users orthogonal scheme requires 4 times slots to complete the whole transmission such as TDMA. TDMA utilizes 4 ms (1-time slot is 1 ms) while PD-NOMA utilizes a single time slot (i.e. 1 ms) to complete the transmission. This greatly decreases the latency. This shows the effectiveness of the PD-NOMA scheme in future communication technologies.

The effect of SIC computation on SE-EE tradeoff is shown in Fig. 3.13. The total SIC computational power is divided into unit power for each SIC iteration then the total power consumption is calculated with circuit power consumption for each user. It is observed from the simulation result that the closest user requires more computation power than the farther user because it performs more SIC com-

putation. The peak point of SE-EE curve degrades by SIC computation because more computation needs more energy. A user performing less or no SIC iteration faces more inter-user interference. The peak point of SE-EE curve degrades by inter-user interference. Therefore, it is a tradeoff among peak point, SIC computation, and interference. However, power consumption in SIC computation does not affect the performance of vehicle networks because vehicles have their own multiple energy sources. Nevertheless, SIC computation can affect the performance of energy harvesting networks, therefore authors have proposed a parallel and group SIC computation rather than sequential SIC computation [167]. On other hand, the proposed scheme offers very low latency as compared to existing orthogonal schemes which makes it suitable for VANETs.

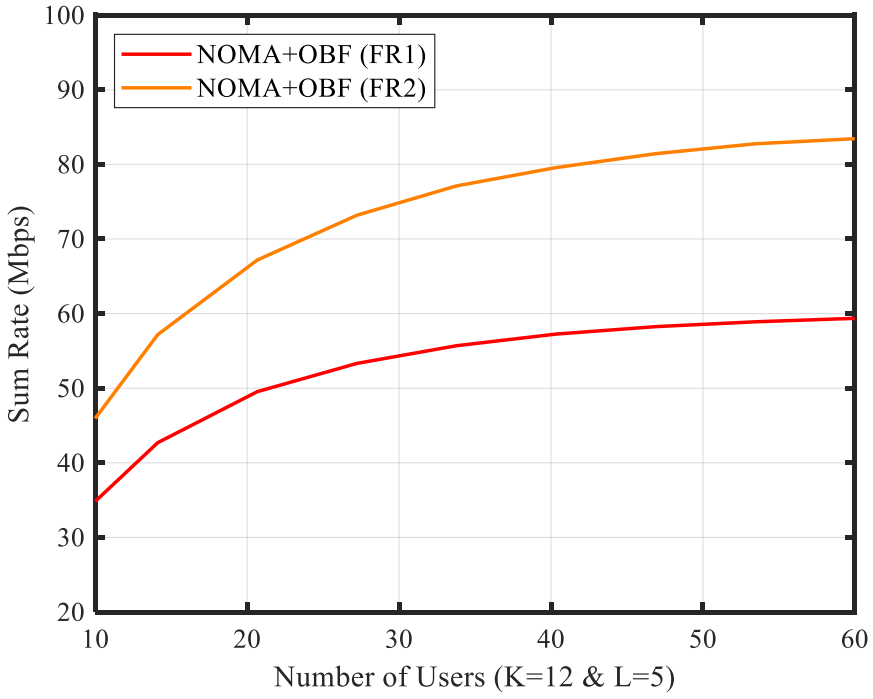

Figure 3.14:: Performance of proposed scheme in mmwave frequency range.

Motivated by the aforementioned results of research in respect to PD-NOMA, a new technology consisting of PD-NOMA with mmWave has been presented. Fig. 3.14 illustrates the combination of the proposed scheme in mmWave. According to ITU, the system configuration standard for 5G systems for mobile networks,

recommends frequency ranges as Frequency Range 1 (FR1 < 6GHz) and Frequency Range 2 (FR2 = from 6 - 100 GHz). The sum-rate comparison of the proposed scheme in FR1 (2GHz) and FR2 (30 GHz) is shown in Fig. 3.14 [163]. The mmWave-PD-NOMA in FR 2 offers 40.4% higher sum-rate capacity than PD-NOMA in FR 1 for 60 users (K=12 & L=5). While mmWave faces more path loss as compared to FR 1. The higher bandwidth of FR 2 allows a higher data rate. Therefore, the fall of cell radius is more suitable for mmWave networks otherwise the greater path loss is experienced. It is clarified from the result that the proposed PD-NOMA scheme in the mmWave frequency range is capable of outperforming in short-range applications such as VANET, e.t.c.

3.8 Summary

In this chapter, a four-user composite multiple access scheme based on a combination of OMA and NOMA is proposed. Encouraged by the results, an extended version of the system model is presented i.e. a composite multiple access scheme based on OBF and NOMA. The purpose of the proposed scheme is to exchange information between SG, SMs, and other communication units in the presence of IN. In this scheme, the intra-beam interference is reduced using SIC, and the inter-beam interference is reduced by employing orthogonal beams. Gram-Schmidt orthogonalization is used to produce the orthogonal beams among the sectors. According to the simulation and numerical findings, the proposed scheme offers a 3 Mbit/sec higher data rate and 0.24 Mbit/joule greater energy efficiency than the traditional OFDMA scheme, leading to better system performance in the case of 10 SMs/users in a sector of a cell. Another significant achievement of the proposed scheme is that it does not cause inter beam interference and provides 17 Mbit/sec higher data rate by using OBF compared to CBF in the case of 60 SMs/users in 12 sectors of a cell.

Furthermore, the effects of IN on the proposed scheme are investigated by modeling two different noise distributions, Bernoulli-Gaussian model and Laplacian-

Gaussian model. Different impulsive noise practical scenarios are used to simulate the practical performance of the proposed scheme. Lastly, the overall performance of the proposed scheme is compared with traditional OFDMA in terms of the number of users, system capacity, nearer and farther user data rate, the effect of OBF on data rate, spectral and energy efficiency, the actual loss of bits and different frequency range.

The research identified a limitation in the user access process while employing a user for a particular beam. Furthermore, the observed data rate revealed that an individual user can greatly affect the system capacity which leads to performance loss. Therefore the algorithm-1, algorithm-2, and an optimal power allocation scheme are proposed in the next chapter.

CHAPTER 4

OPTIMAL RESOURCE ALLOCATION

The selection of a user to a particular resource block depends on two criteria, one is a selection of beam and the second is the selection of user order within the beam. Afterward, power is allocated to the user which differs from OFDMA because PD-NOMA is a combination of superposition and interference cancellation techniques.

The system model consists of K numbers of orthogonal beams/clusters, and BS allocates a fraction of bandwidth βB to each beam, where β is the bandwidth allocation coefficient. In addition, the system model consists of L number of power levels, and BS allocates a fraction of power αP to each SM, where α is the power allocation coefficient. While B is the total system bandwidth and P is the total available power for a single beam. BS allocates power $P_1 = \alpha_1 P$ to the closest SM and $P_l = \alpha_l P$ to the farthest SM. Furthermore, BS allocates bandwidth $B_1 = \beta_1 B$ to first beam and $B_k = \beta_k B$ to k_{th} beam.

where:

$$h_1 > h_2 > h_3 > \cdots > h_l$$

$$\alpha_1 < \alpha_2 < \alpha_3 < \cdots < \alpha_l$$

$$\alpha_1 + \alpha_2 + \alpha_3 + \cdots + \alpha_l = 1$$

$$\alpha_1 P + \alpha_2 P + \alpha_3 P + \cdots + \alpha_l P = P$$

$$\beta_1 + \beta_2 + \beta_3 + \cdots + \beta_k = 1$$

$$\beta_1 B + \beta_2 B + \beta_3 B + \cdots + \beta_k B = B$$

BS receives information of SMs about their position (R as distance from BS, angle of arrival θ and channel condition h) through CSI. SMs which are located within the same beam utilize PD-NOMA in which the bandwidth is same but power is different. SMs which are located under different beams utilize different orthogonal bandwidths by employing OBF. In PD-NOMA, BS allocates different power to different SMs according to their channel condition or link distance. At the receiver end, SM utilizes SIC to extract its own signal from the superimposed signal by subtracting the other SMs signals.

Several single users can be scheduled at the same time for the same subband by implementing the proportional fair scheduling scheme at BS in the PD-NOMA system. The scheduling procedures for users are described in Fig. 4.1 [70]. First, the BS selects sets of users known as the NOMA candidate user set, in which total users cannot exceed N_{max}. The selected user set is prepared by using the total number of possible combinations of users within one single cell. Secondly, for every user set, BS allocates the transmission power by using a power allocation scheme. The scheduling matrix for the corresponding user set is estimated on behalf of power assignment ratios. Thirdly, with the help of the maximum scheduling matrix, the scheduler decides the candidate user sets on each subband for data transmission. Finally, for every allocated subband, the scheduler estimates equivalent SNRs for every single scheduled user.

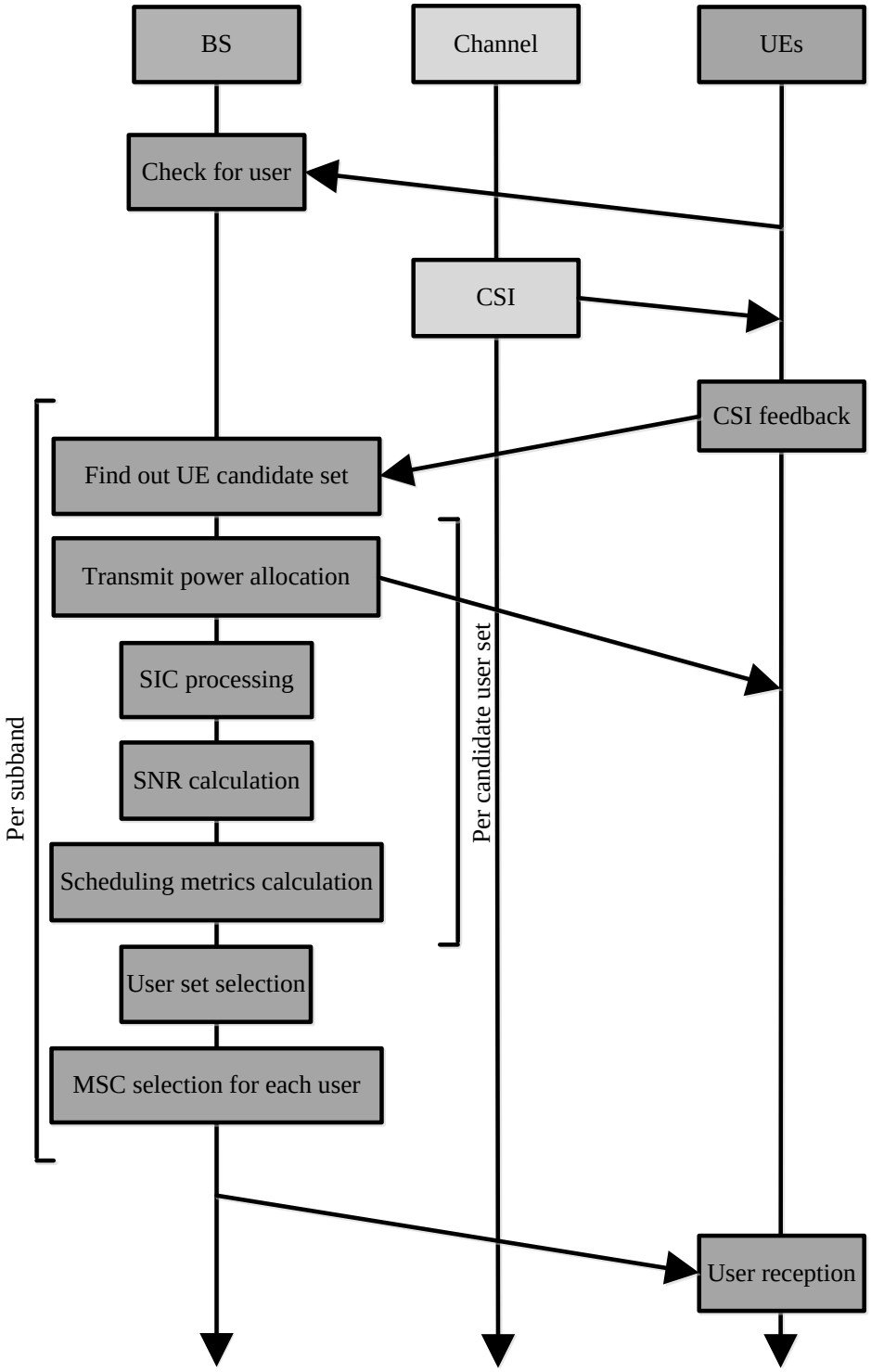

Figure 4.1:: Scheduling algorithm for PD-NOMA.

The BS is served by N_t antenna array and is divided into K sub-transmission units by employing OBF. Each sub-transmission unit consists of L number of SMs.

Each SM has a single receive antenna, therefore the total number of SMs that a BS can serve is $K \times L$ and the total M number of SMs are present under one BS. The BS can split data streams for each beam using beamforming by assigning a weight vector to each of K beams. The weight vectors $\{w_n\}_{n=1}^{N_t}$ are unitary orthogonal vectors, where $w_n \in C^{N_t \times 1}$ is a beamforming vector with $\|w_n\| = 1$. In order to reduce interference among beams, a set of OBF vectors is used among all groups of SMs. The orthogonality of beams considered is to be maintained during transmission.

4.1 Algorithm 1: For Allocating Accessing Scheme to SMs

SMs are randomly distributed within the cell area. Some SMs are located at the same distance from BS and some are at different distances. BS collects the information about the location of SMs through CSI and selects an access scheme. The selection process is done in two steps as depicted in algorithm 1. In the first step, the selection of beam or bandwidth is done. BS receives the angular position and distance of each SM. The angular position of each SM is compared with the beam-width of each beam. The group of SMs having the same angle of arrival (located within the same beam), BS allocates the same bandwidth (line 1-9). In the second step, power is allocated to each SM based on their distance from BS in ascending order. To allocate the power, the BS allocates power P_1 to nearer SMs, then checks the distance between two consecutive SMs. If distance between consecutive SMs is greater than d_{min}, BS allocates power P_2 to second SM. If the distance is less than d_{min}, the scheme allows to change of the consecutive SMs pair by replacing the farther SM. Each true condition increases the power allocation sequence (line 10-19). This process is repeated till the L number of SMs are selected (line 12) [15].

Algorithm 1: For allocating access scheme to SMs

Selection of beam for SMs:

1. inputs: $m, k, A_{k,l}$ where k is the number of orthogonal beams,
. m is the number of user in single beam and
. $A_{k,l}$ is a matrix to save user access details.
2. $l = 0$
3. for $j = 1 : m$
4. for $i = 1 : k$
5. if $\theta_j > \theta_i$ AND $\theta_j < \theta_{i+1}$
6. include j_{th} SMs into l_{th} position of i_{th} beam
7. update $A_{i,l+1} \leftarrow \{R_j, \theta_j\}$
8. end
9. end

Selection of power level for SMs:

10. initiate SMs set: $A_{k,l}$

$$A_{k,l} = \{(R_{1,1}, \theta_{1,1}), (R_{1,2}, \theta_{1,2}), (R_{1,3}, \theta_{1,3}), \cdots, (R_{1,l}, \theta_{1,l})$$
$$(R_{2,1}, \theta_{2,1}), (R_{2,2}, \theta_{2,2}), (R_{2,3}, \theta_{2,3}), \cdots, (R_{2,l}, \theta_{2,l})$$
$$\vdots$$
$$(R_{k,1}, \theta_{k,1}), (R_{k,2}, \theta_{k,2}), (R_{k,3}, \theta_{k,3}), \cdots, (R_{k,l}, \theta_{k,l})\}$$

11. for $i = 1 : k$
12. for $t = 1 : l$
13. sort $A_{i,t} \ni R_{i,1} < R_{i,2} < R_{i,3} < \cdots < R_{i,l}$
14. if $t = 1$ assign $SM\{R_{i,1}, \theta_{i,1}\} \rightarrow \{\alpha_1 P\}$
15. then if $R_{i,t} - R_{i,t-1} \geq R_{min}$
16. then assign $SM\{R_{i,t}, \theta_{i,t}\} \rightarrow \{\alpha_2 P\}$
17. else $\alpha_{i,t-1} P = \{\alpha_{i,t} P\}$
18. end
19. end

4.2 Power Optimization

The power allocation in PD-NOMA differs from OFDMA since PD-NOMA is a combination of superposition and interference cancellation techniques. To allocate power to each SM/user, firstly, the effect of power on the system capacity is investigated. Then, an algorithm is presented to allocate the power and maximize the sum-rate capacity.

Problem Formation:

$$C_{(PD-NOMA)} = \sum_{k=1}^{K} B_k \left\{ \sum_{l=1}^{L} \log_2 \left(1 + \frac{\alpha_{k,l} P |h_{k,l}|^2}{\xi_o + \sum_{t=1, t\neq l}^{L-1} \alpha_{k,t} P |h_{k,l}|^2} \right) \right\} \tag{4.1}$$

Let's consider a single beam scenario ($k = 1$) which will be applicable for all the beams which are orthogonal to each other. Using the Shannon capacity formula, the utility function is given as:

$$\text{maximize } B \sum_{l=1}^{L} \log_2 \left(1 + \frac{\alpha_{k,l} P |h_{k,l}|^2}{\xi_o + \sum_{t=1, t\neq l}^{L-1} \alpha_{k,t} P |h_{k,l}|^2} \right) \qquad \forall t, l \in L$$

subject to

$$C_1 \colon \sum_{l=1}^{L} \alpha_l P \leq P$$

$$C_2 \colon \alpha_l P > 0$$

$$C_3 \colon B \log_2 \left(1 + \frac{\alpha_{k,l} P |h_{k,l}|^2}{\xi_o + \sum_{t=1, t\neq l}^{L-1} \alpha_{k,t} P |h_{k,l}|^2} \right) \geq R_{min}$$

where C_1: the sum of all users' allocated power must be less than or equal to the total power, C_2: every user must get some allocated power, and C_3 : every user must get greater than or equal to the minimum data rate.

Let $h_1, h_2, h_3, \cdots, h_l$ are the channel condition for user $1, 2, 3, \cdots l$. Suppose the channel condition of consecutive users is in descending order and mathematically expressed as:

$$h_1 > h_2 > h_3 > \cdots > h_l \tag{4.2}$$

The power allocation is carried out sequentially such that every following user is assigned the power only if the preceding user has already been assigned the power. Mathematically, this condition is expressed as follows:

$$\alpha_{l+1}P > 0 \text{ only if } \alpha_l P > 0 \tag{4.3}$$

where α is the power allocation coefficient. Therefore, according to the problem formulation, the utility function with dependent variables αP can be denoted by $f(\alpha_1 P, \alpha_2 P, \alpha_3 P, \cdots \alpha_l P)$ and can be rewritten as:

$$\begin{aligned}
&= \log_2\left(1 + \frac{\alpha_1 P|h_1|^2}{\xi_0}\right) + \log_2\left(1 + \frac{\alpha_2 P|h_2|^2}{\xi_0 + \alpha_1 P|h_2|^2}\right) \\
&\quad + \log_2\left(1 + \frac{\alpha_3 P|h_3|^2}{\xi_0 + (\alpha_1+\alpha_2)P|h_2|^2}\right) + \cdots \\
&\quad + \log_2\left(1 + \frac{\alpha_{l-1} P|h_{l-1}|^2}{\xi_o + \sum_{t=1,t\neq l}^{L-2} \alpha_t P|h_{l-1}^2|}\right) \\
&\quad + \log_2\left(1 + \frac{\alpha_l P|h_l|^2}{\xi_o + \sum_{t=1,t\neq l}^{L-1} \alpha_t P|h_l^2|}\right)
\end{aligned} \tag{4.4}$$

$$\begin{aligned}
&= \log_2(\xi_0 + \alpha_1 P|h_1|^2) - \log_2(\xi_0) + \log_2(\xi_0 + (\alpha_1+\alpha_2)P|h_2|^2) \\
&\quad - \log_2(\xi_0 + \alpha_1 P|h_2|^2) + \cdots + \log_2 \sum_{t=1}^{L}(\xi_0 + \alpha_t P|h_L|^2) \\
&\quad - \log_2 \sum_{t=1}^{L-1}(\xi_0 + \alpha_t P|h_L|^2)
\end{aligned} \tag{4.5}$$

In the next step, the first-order partial derivative of f is taken with respect to each dependent variable to find the effect of dependent variables on the utility function.

$$\begin{aligned}
\frac{\partial f}{\partial(\alpha_1 p)} =& \frac{h_1}{\xi_0 + \alpha_1 P|h_1|^2} - \frac{h_2}{\xi_0 + \alpha_1 P|h_2|^2} \\
&+ \frac{h_2}{\xi_0 + (\alpha_1+\alpha_2)P|h_2|^2} - \cdots
\end{aligned}$$

$$\begin{aligned}
\frac{\partial f}{\partial(\alpha_2 p)} =& \frac{h_2}{\xi_0 + \sum_{t=1}^{2} \alpha_t P|h_2|^2} - \frac{h_3}{\xi_0 + \sum_{t=1}^{2} \alpha_t P|h_3|^2} \\
&+ \frac{h_3}{\xi_0 + \sum_{t=1}^{3} \alpha_t P|h_3|^2} - \cdots
\end{aligned}$$

$$\vdots$$

$$\frac{\partial f}{\partial(\alpha_{L-1}p)} = \frac{h_{L-1}}{\xi_0 + \sum_{t=1}^{L-1}\alpha_t P|h_{L-1}|^2} - \frac{h_L}{\xi_0 + \sum_{t=1}^{L-1}\alpha_t P|h_L|^2} + \frac{h_l}{\xi_0 + \sum_{t=1}^{L}\alpha_t P|h_L|^2} - \cdots$$

$$\frac{\partial f}{\partial(\alpha_L p)} = \frac{h_l}{\xi_0 + \sum_{t=1}^{L}\alpha_t P|h_L|^2}$$

Considering the channel condition according to the supposition: $h_1 > h_2 > h_3 > \cdots > h_l$, in above equations, each pair of consecutive terms yield positive result, i.e.

$$\begin{aligned} &\frac{h_1}{\xi_0 + \alpha_1 P|h_1|^2} - \frac{h_2}{\xi_0 + \alpha_1 P|h_2|^2} \geq 0 \\ &\frac{h_2}{\xi_0 + \sum_{t=1}^{2}\alpha_t P|h_2|^2} - \frac{h_3}{\xi_0 + \sum_{t=1}^{2}\alpha_t P|h_3|^2} \geq 0 \\ &\frac{h_{L-1}}{\xi_0 + \sum_{t=1}^{L-1}\alpha_t P|h_{L-1}|^2} - \frac{h_L}{\xi_0 + \sum_{t=1}^{L-1}\alpha_t P|h_L|^2} \geq 0 \end{aligned} \tag{4.6}$$

Furthermore, every preceding equation consists of more terms than the following equations. Based on these analyses, the power allocation problem can be summarized as follows:

$$\frac{\partial f}{\partial(\alpha_1 P)} > \frac{\partial f}{\partial(\alpha_2 P)} > \frac{\partial f}{\partial(\alpha_3 P)} > \cdots > \frac{\partial f}{\partial(\alpha_L P)} \tag{4.7}$$

The above expression shows that the improved sum-rate is obtained by increasing the power of every preceding user in comparison to the following users. Therefore, by shifting power from the farther user to nearer user can improve $f(\alpha_1 P, \alpha_2 P, \alpha_3 P \cdots, \alpha_l P)$. The shifting of power should continue till the farther user power reaches its minimum threshold. Furthermore, the nearer user should not obtain power beyond its maximum threshold. The power shifting process is repeated from farther user to the nearer user [168], which is mathematically given as:

$$SM\{\alpha_1 P\} \leftarrow SM\{\alpha_2 P\} \leftarrow SM\{\alpha_3 P\} \leftarrow \cdots \leftarrow SM\{\alpha_L P\} \tag{4.8}$$

4.2.1 Optimum Power Allocation Scheme

For the problem of maximization of the sum-rate of the proposed scheme, R_{min} is considered as the minimum rate to avoid user outage. The minimum/target rate R^* of the user can be written as:

$$R^* = \log_2(1 + \gamma^*)$$

where γ^* is the optimal SNR.

$$\gamma^* = 2^{R^*} - 1$$

$$\gamma_l^* = \frac{\alpha_l^* P|h_l|^2}{\xi_0 + \sum_{t=1,t\neq l}^{L-1} \alpha_t P|h_l|^2}$$

where

$$\alpha_l^* + \sum_{t=1,t\neq l}^{L-1} \alpha_t = 1$$

$$\sum_{t=1,t\neq l}^{L-1} \alpha_t = 1 - \alpha_l^*$$

$$\gamma_l^* = \frac{\alpha_l^* P|h_l|^2}{\xi_0 + (1 - \alpha_l^*)P|h_l|^2}$$

$$\alpha_l^* = \gamma_l^* \frac{\xi_0 + P|h_l|^2}{P|h_l|^2(1 + \gamma_l^*)}$$

$$\alpha_{l-1}^* = \gamma_{l-1}^* \frac{\xi_0 + (P|h_{l-1}|^2 - \alpha_l^* P|h_{l-1}|)}{P|h_{l-1}|^2(1 + \gamma_{l-1}^*)}$$

$$\alpha_{l-2}^* = \gamma_{l-2}^* \frac{\xi_0 + (P|h_{l-2}|^2 - \alpha_l^* P|h_{l-2}| - \alpha_{l-1}^* P|h_{l-2}|)}{P|h_{l-2}|^2(1 + \gamma_{l-2}^*)}$$

$$\vdots$$

$$\alpha_{l-r}^* = \gamma_{l-r}^* \frac{\xi_0 + (P|h_{l-r}|^2 - \sum_{t=l-r,t\neq r}^{l} \alpha_t^* P|h_{l-r}|)}{P|h_{l-r}|^2(1 + \gamma_{l-r}^*)}$$

finally

$$\alpha_1^* = 1 - \sum_{t=l-1,t\neq l}^{1} \alpha_t$$

α_1^*, $\alpha_2^* \cdots \alpha_l^*$ are the optimal power allocations (OPA) coefficient for the problem of maximization of the sum-rate.

4.2.2 Fractional Power Allocation Scheme

Fractional Power Allocation (FPA) scheme for multiuser single carrier PD-NOMA starts by setting the power allocation parameter for the weakest user $\alpha_l = 3/4$. Since, $h_1 > h_2 > h_3 > \cdots > h_l$ and $\alpha_1 < \alpha_2 < \alpha_3 < \cdots < \alpha_l$. Therefore, $\alpha_{l-1} = 3/4(1-\alpha_l)$, $\alpha_{l-2} = 3/4(1-(\alpha_l+\alpha_{l-2}))$ and $\alpha_1 = 3/4(1-(\alpha_l+\alpha_{l-2}+\cdots+\alpha_2))$. Each PD-NOMA user utilizes the entire available bandwidth while bandwidth is equally divided among orthogonal beams. Since,

$$h_1 > h_2 > h_3 > \cdots > h_l$$

$$\alpha_1 < \alpha_2 < \alpha_3 < \cdots < \alpha_l$$

$$\alpha_{l-1} = F(1-\alpha_l)$$

$$\alpha_{l-2} = F(1-(\alpha_l+\alpha_{l-2}))$$

$$\vdots$$

$$\alpha_1 = F(1-(\alpha_l+\alpha_{l-2}+\cdots+\alpha_2))$$

4.3 Bandwidth Optimization

To allocate optimum bandwidth to each beam/cluster, firstly the effect of individually allocated bandwidth on the system capacity is investigated. Using the Shannon capacity formula, the utility function is given as:

$$\text{maximize} \sum_{k=1}^{K} \beta_k B \sum_{l=1}^{L} \log_2 \left(1 + \frac{\alpha_{k,l} P |h_{k,l}|^2}{\xi_o + \sum_{t=1, t\neq l}^{L-1} \alpha_{k,t} P |h_{k,l}|^2}\right)$$

$$\forall l \in L \quad k \in K$$

subject to

$$C_1\colon \sum_{k=1}^{K} \beta_k B \leq B$$

$$C_2\colon \beta_k B \geq 0$$

$$C_3\colon \beta_k B \log_2\left(1 + \frac{\alpha_{k,l} P|h_{k,l}|^2}{\xi_o + \sum_{t=1,t\neq l}^{L-1} \alpha_{k,t} P|h_{k,l}|^2}\right) \geq R_{min}$$

where C_1: the sum of all users' allocated bandwidth must be less than or equal to the total bandwidth, C_2: every user must get some allocated bandwidth, and C_3 : every user must get greater than or equal to the minimum data rate.

Let's assume that the bandwidth for orthogonal beams satisfies the condition as given below:

$$B_1 + B_2 + B_3 + \cdots + B_k = B \tag{4.9}$$

where B is the total bandwidth and B_1, B_2, B_3 and B_k are the fraction of bandwidth allocated to $1_{st}, 2_{nd}, 3_{rd}$ and k_{th} beams also, $B_k = \beta_k B$. Therefore, according to the problem formulation, the utility function with dependent variables βB can be denoted by $f(\beta_1 B, \beta_2 B, \beta_3 B, \cdots \beta_k B)$ and is rewritten as follows:

$$\begin{aligned}
=& B_k \log_2\left(1 + \frac{\alpha_1 P|h_1|^2}{\xi_0}\right) + B_k \log_2\left(1 + \frac{\alpha_2 P|h_2|^2}{\xi_0 + \alpha_1 P|h_2|^2}\right) \\
&+ B_k \log_2\left(1 + \frac{\alpha_3 P|h_3|^2}{\xi_0 + (\alpha_1 + \alpha_2) P|h_2|^2}\right) + \cdots \\
&+ B_k \log_2\left(1 + \frac{\alpha_{l-1} P|h_{l-1}|^2}{\xi_o + \sum_{t=1,t\neq l}^{L-2} \alpha_t P|h_{l-1}^2|}\right) \\
&+ B_k \log_2\left(1 + \frac{\alpha_l P|h_l|^2}{\xi_o + \sum_{t=1,t\neq l}^{L-1} \alpha_t P|h_l^2|}\right)
\end{aligned} \tag{4.10}$$

In the next step, the first-order partial derivative of f is taken with respect to each dependent variable to find the effect of dependent variables on the utility function.

$$\begin{aligned}\frac{\partial f}{\partial(\beta_1 B)} =& \log_2\left(1+\frac{\alpha_1 P|h_1|^2}{\xi_0}\right)+\log_2\left(1+\frac{\alpha_2 P|h_2|^2}{\xi_0+\alpha_1 P|h_2|^2}\right)\\ &+\log_2\left(1+\frac{\alpha_3 P|h_3|^2}{\xi_0+(\alpha_1+\alpha_2)P|h_2|^2}\right)+\cdots\\ &+\log_2\left(1+\frac{\alpha_{l-1}P|h_{l-1}|^2}{\xi_o+\sum_{t=1,t\neq l}^{L-2}\alpha_t P|h_{l-1}^2|}\right)\\ &+\log_2\left(1+\frac{\alpha_l P|h_l|^2}{\xi_o+\sum_{t=1,t\neq l}^{L-1}\alpha_t P|h_l^2|}\right)\end{aligned}$$

$$\begin{aligned}\frac{\partial f}{\partial(\beta_2 B)} =& \log_2\left(1+\frac{\alpha_1 P|h_1|^2}{\xi_0}\right)+\log_2\left(1+\frac{\alpha_2 P|h_2|^2}{\xi_0+\alpha_1 P|h_2|^2}\right)\\ &+\log_2\left(1+\frac{\alpha_3 P|h_3|^2}{\xi_0+(\alpha_1+\alpha_2)P|h_2|^2}\right)+\cdots\\ &+\log_2\left(1+\frac{\alpha_{l-1}P|h_{l-1}|^2}{\xi_o+\sum_{t=1,t\neq l}^{L-2}\alpha_t P|h_{l-1}^2|}\right)\\ &+\log_2\left(1+\frac{\alpha_l P|h_l|^2}{\xi_o+\sum_{t=1,t\neq l}^{L-1}\alpha_t P|h_l^2|}\right)\end{aligned}$$

$$\vdots$$

$$\begin{aligned}\frac{\partial f}{\partial(\beta_{k-1} B)} =& \log_2\left(1+\frac{\alpha_1 P|h_1|^2}{\xi_0}\right)+\log_2\left(1+\frac{\alpha_2 P|h_2|^2}{\xi_0+\alpha_1 P|h_2|^2}\right)\\ &+\log_2\left(1+\frac{\alpha_3 P|h_3|^2}{\xi_0+(\alpha_1+\alpha_2)P|h_2|^2}\right)+\cdots\\ &+\log_2\left(1+\frac{\alpha_{l-1}P|h_{l-1}|^2}{\xi_o+\sum_{t=1,t\neq l}^{L-2}\alpha_t P|h_{l-1}^2|}\right)\\ &+\log_2\left(1+\frac{\alpha_l P|h_l|^2}{\xi_o+\sum_{t=1,t\neq l}^{L-1}\alpha_t P|h_l^2|}\right)\end{aligned}$$

$$\begin{aligned}\frac{\partial f}{\partial(\beta_k B)} =& \log_2\left(1+\frac{\alpha_1 P|h_1|^2}{\xi_0}\right)+\log_2\left(1+\frac{\alpha_2 P|h_2|^2}{\xi_0+\alpha_1 P|h_2|^2}\right)\\ &+\log_2\left(1+\frac{\alpha_3 P|h_3|^2}{\xi_0+(\alpha_1+\alpha_2)P|h_2|^2}\right)+\cdots\\ &+\log_2\left(1+\frac{\alpha_{l-1}P|h_{l-1}|^2}{\xi_o+\sum_{t=1,t\neq l}^{L-2}\alpha_t P|h_{l-1}^2|}\right)\\ &+\log_2\left(1+\frac{\alpha_l P|h_l|^2}{\xi_o+\sum_{t=1,t\neq l}^{L-1}\alpha_t P|h_l^2|}\right)\end{aligned}$$

The above equations can be summarized as follows:

$$\frac{\partial f}{\partial(\beta_1 B)} = \frac{\partial f}{\partial(\beta_2 B)} = \frac{\partial f}{\partial(\beta_3 B)} = \cdots = \frac{\partial f}{\partial(\beta_k B)} \tag{4.11}$$

The above expression shows that the improved sum-rate is independent of the allo-

cation of bandwidth to beams. Therefore, to keep the fairness index close to unity, equal bandwidth is allocated to each orthogonal beam.

4.4 Algorithm 2: Allocation of Optimum Power

On the basis of the optimization results, equal bandwidth is allocated to each beam while an algorithm is proposed for the allocation of optimum power to the users.

Algorithm 2: For allocating optimal power to SMs

---

1. inputs: from algorithm 1: input $A_{k,l}, \alpha_{k,t}\ P \geq P_{min}$
2. initialize optimal power matrix: $P^*_{k,l}$
3. for $i = 1 : k$
4. for $t = l : 1$
5. if $\alpha_{k,t}P > P_{min}$
6. than $\alpha_{k,t}P - P_{min} = P'_{k,t}$
7. $P^*_{k,t} \leftarrow \alpha_{k,t}P - P'_{k,t}$
8. for $t = l : 1$
9. $\alpha_{k,t-1}P \leftarrow \alpha_{k,t-1}P + P'_{k,t}$
10. till $\alpha_{k,t-1}P = P_{max}$
11. $\alpha_{k,t-2}P \leftarrow \alpha_{k,t-2}P + P'_{k,t}$
12. end
13. else $\alpha_{k,t}P = P_{min}$
14. $t = t - 1$
15. end
16. end

Let's consider the inputs from algorithm 1: k is the number of orthogonal

beams, m is the number of users in a single beam, and $A_{k,l}$ is a matrix from algorithm 1 which consists of each user access information. Algorithm 2 step by step optimizes the power of each user. First, matrix $A_{k,l}$ is the input from algorithm 1 and output matrix of optimal power $P^*_{k,l}$ is initialized (line 1 & 2). The rows of input matrix A represent the beams and the row elements represent the power of users within the beam in ascending order i.e. from nearest to the farthest user. Consider each row of $A_{k,l}$ one by one, (line 4):

(i) If the power of the last user of the first row is greater than P_{min}, then its power is reduced to the level of P_{min} (lines 5-7). Later on, the remaining power is shifted to the next user in descending order (lines 9-11). The power shifting process continues till the receiving user gets power equivalent to P_{max} (line 10). If the power of any user is already equal to P_{max} then the process shifts directly to the next user in descending order (line 13 & 14). The power shifting process is repeated until it reaches the first user of the first row/beam, (line 8).

(ii) If the first user does not get its P_{max} during the process mentioned in (i), the process in (i) is repeated by decreasing the order by 1 from the last (line 4).

(iii) (i) and (ii) are repeated for all beams (line 3) [15].

4.5 Results and Discussions

The effect of the optimal power and bandwidth allocation on the proposed scheme has been analyzed through Matlab-based simulations. For this purpose, the standard 3GPP LTE parameters have been considered. The main simulation parameters and assumptions [163] are itemized in Table 4.1.

4.5.1 Simulation Setup

The carrier frequency of 2 GHz in the range of FR1, 30 GHz in the range of FR2, and the total bandwidth of 10 MHz is considered in the simulation. The bandwidth of 10 MHz is assumed for all NOMA users, while for OMA the total bandwidth 10 MHz is divided equally among all users within the single sector. A hexagonal cell layout is considered. 500 meters are taken as Inter-site distance and 35 meters are considered as the minimum distance between UE and cell site. The total transmitted power is set to 46 dBm. Distance-dependent path loss with the decay factor of 3.76 is considered for simulation. Moreover, instantaneous multipath fading is taken into account in the propagation model. Each user is equipped with a single antenna while K number of antennas are available at BS. The power of random IN - having an approximately flat frequency response over the spectrum - within the range of {0-5} dB is considered. Weak, medium, and heavy IN scenarios are considered for practical impulsive noise environments. The proposed scheme takes user location as input which is based on the geographical distance between each user and the BS. Later on, this input is used in algorithm 1 and algorithm 2 to allocate particular beam and power among users.

Table 4.1:: Simulation parameters for optimal resource allocation.

S.No.	Parameter	Value
1	Inter-site distance	500 m
2	Minimum distance between UE and cell site	35 m
3	BS total transmission power	46 dBm
4	Receiver noise density	-174 dBm/Hz
5	Carrier frequency	2 GHz
6	System bandwidth	10 MHz
7	IN power	0 dB to 50 dB

8	Disturbance Ratio, dr	0.00135%, 0.00632% & 0.0327%

The user ordering strategy is considered in algorithm 1 and power allocation is considered in algorithm 2. On the basis of these algorithms, the results are shown in Fig. 4.2 and 4.3. Using algorithm 1,10 users are selected out of 100 users for the first beam and power is allocated to these users by using algorithm 2. Similarly, algorithms 1 & 2 are used to select users of other beams. It is evident from the results that the proposed algorithm can efficiently allocate resources to improve the sum-rate of the proposed scheme.

The effect of dr on user ordering strategy based power allocation is shown in Fig. 4.4, Fig. 4.5, Fig. 4.6 and Fig. 4.7. The noise environment is not always the same. In different noise environments, IN behavior is different which causes the change in power allocation to get the desired result. The results illustrate the change in power allocation in different real-life noise scenarios. Approximately 40 dB more power is required in high noise scenario compared to a low noise scenario. Moreover, 52 dB more power is required in comparison to the absence of IN.

Fig. 4.8 and Fig. 4.9 illustrate the comparison of the OPA with FPA in terms of individual user data rate in which 4 Mbps is the minimum acceptable rate. Furthermore, Fig. 4.8 and Fig. 4.9 show individual user data rate and corresponding allocated power.

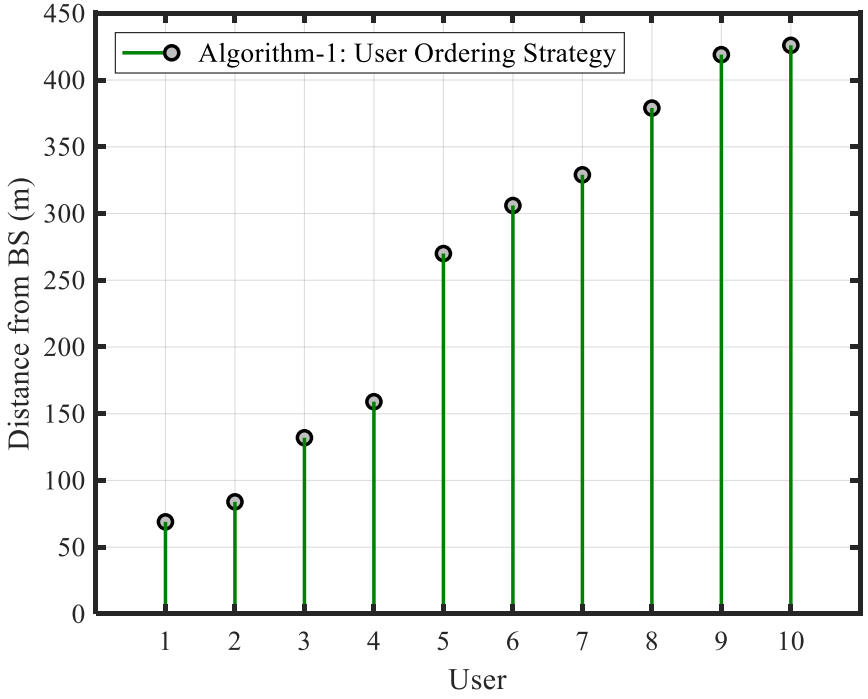

Figure 4.2:: Algorithm 1: user ordering strategy.

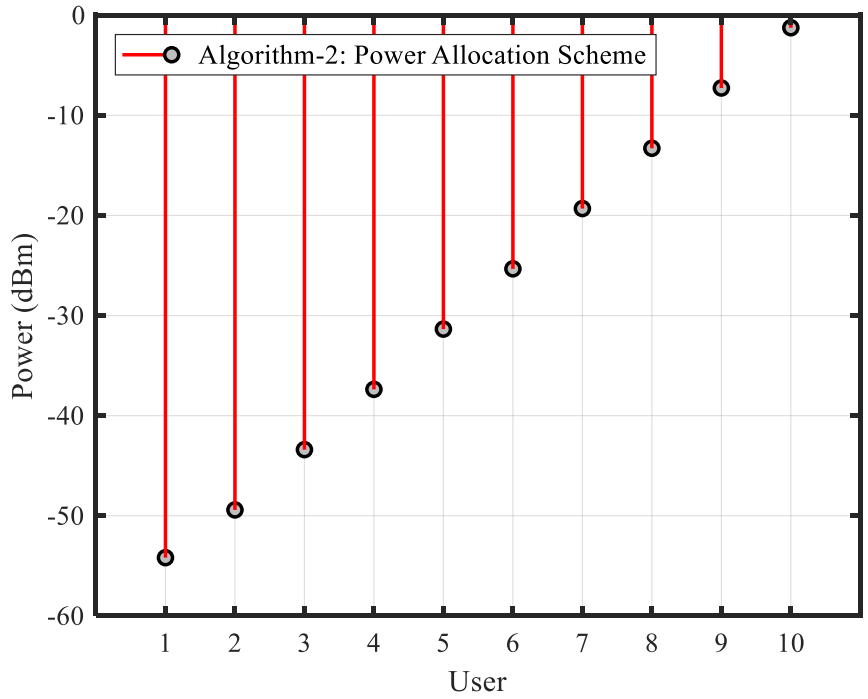

Figure 4.3:: Algorithm 2: power allocation scheme.

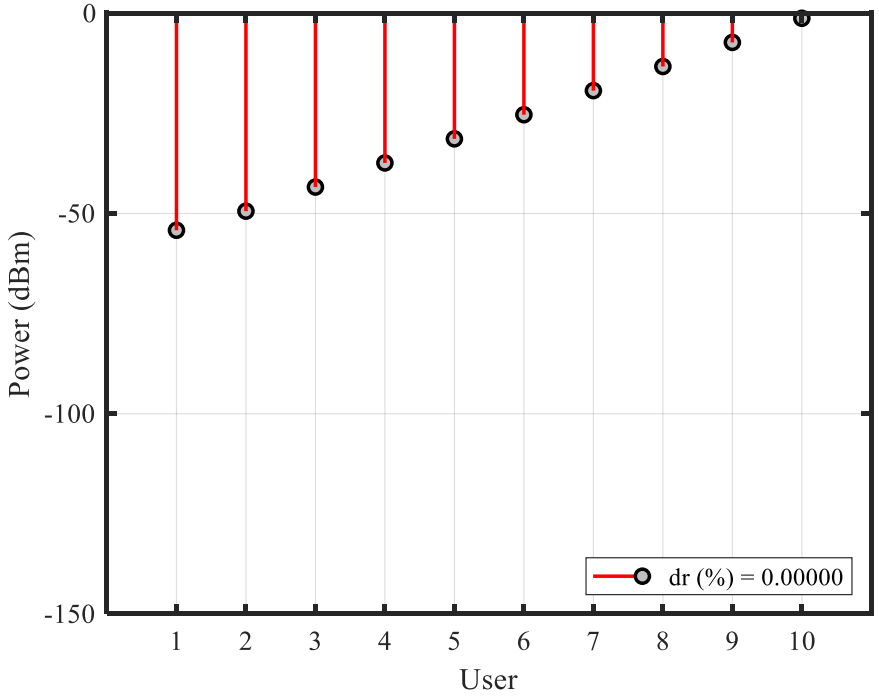

Figure 4.4:: Effect of dr (0) on algorithm 2: power allocation scheme.

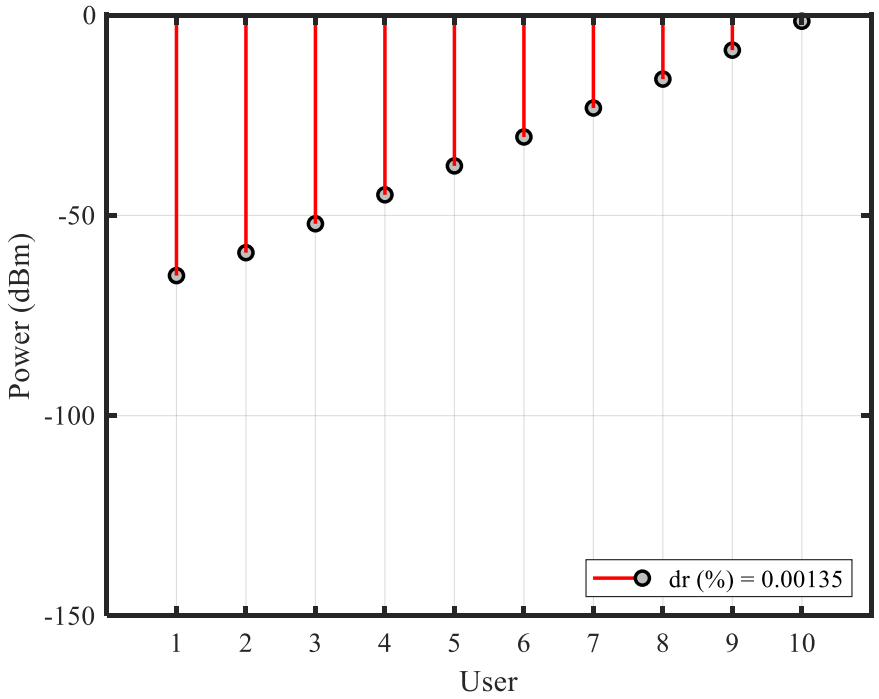

Figure 4.5:: Effect of dr (0.00135) on algorithm 2: power allocation scheme.

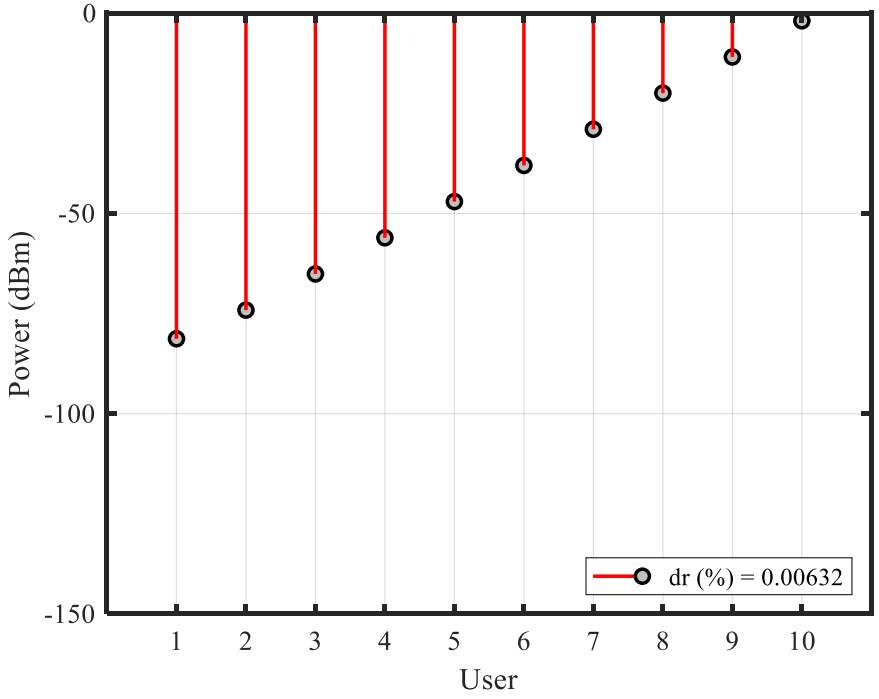

Figure 4.6:: Effect of dr (0.00632) on algorithm 2: power allocation scheme.

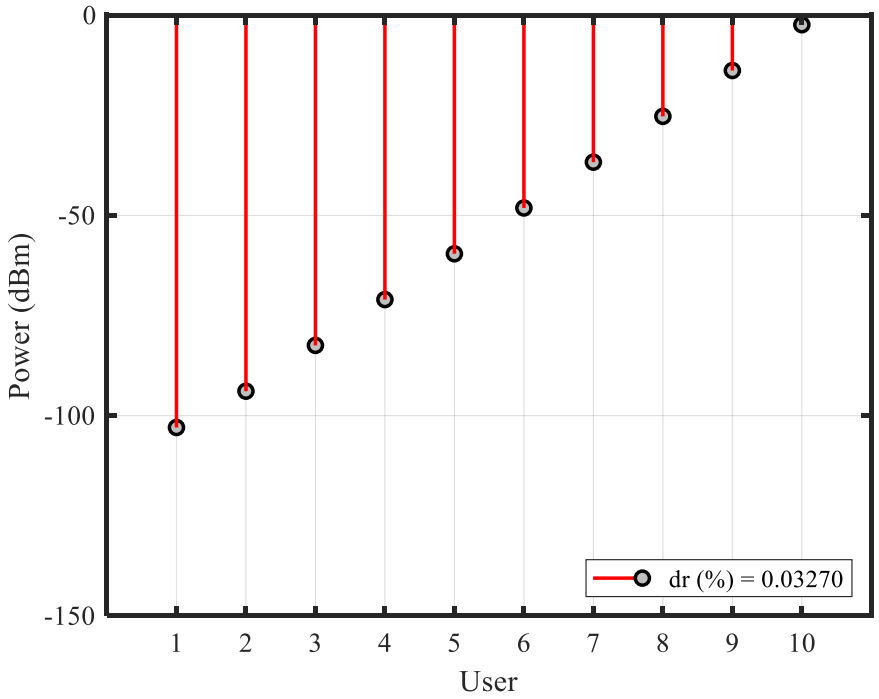

Figure 4.7:: Effect of dr (0.03270) on algorithm 2: power allocation scheme.

It is evident from Fig. 4.9 that FPA performs very poor and the data rate of

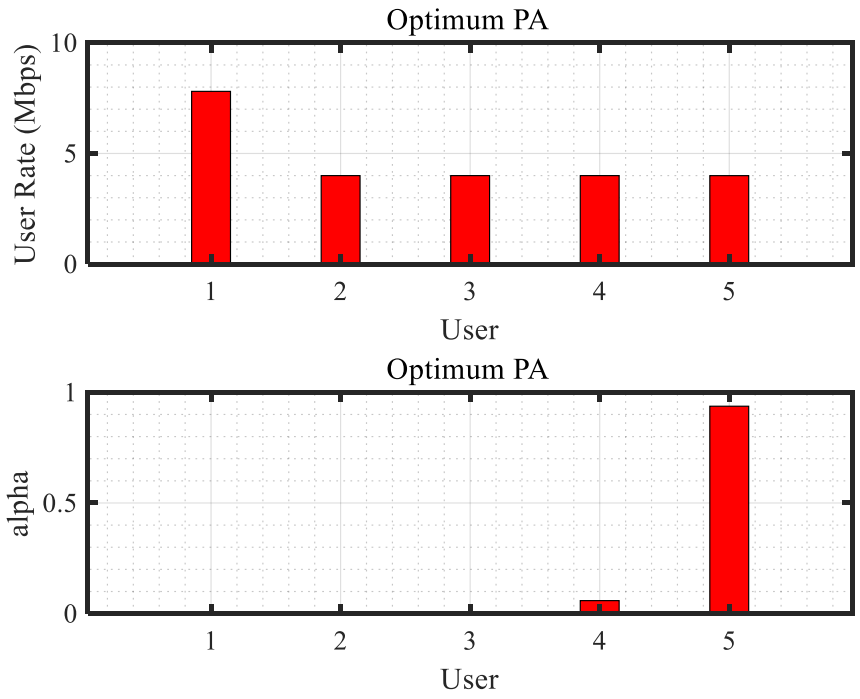

Figure 4.8:: Sum-rate of proposed scheme using OPA.

two users out of four is less than 1 Mbps. The reason behind it, FPA neither uses the instantaneous CSI nor considers the targeted data rate into account. Simply, FPA allocates a fixed fraction of power to each user which leads to encouraging user outages. While in OPA, the selection of power coefficient is dynamic so that each user gets the required threshold data rate i.e. R_{min} as shown in Fig. 4.8. Furthermore, to increase the sum-rate according to algorithm 2, if a user receives more data rate than R_{min} then the data rate is reduced to R_{min} by reducing the level of P_{min}. The residual power is transferred to lower order users. The result of this process is shown in Fig.4.8.

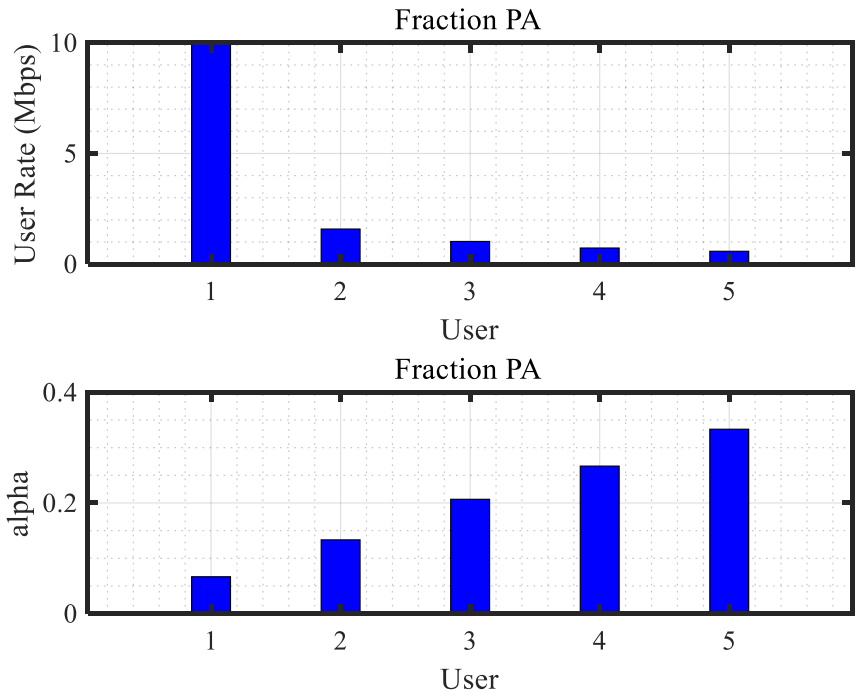

Figure 4.9:: Sum-rate of proposed scheme using FPA.

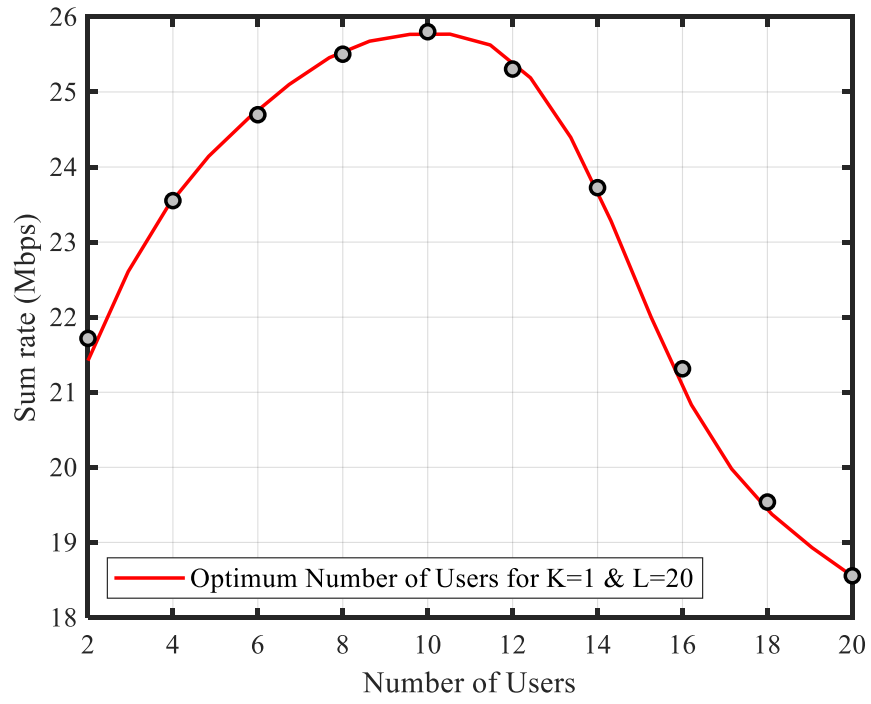

Figure 4.10:: Optimum number of users for PD-NOMA downlink system.

In the single carrier PD-NOMA scheme, the maximum possible number of

users who employ simultaneously without degrading the sum-rate is considered as the peak point of the curve, as shown in Fig. 4.10. For the optimum sum-rate, the bound is related to the capability of interference tolerance, noise power, target rate, and required SNR for demodulation (power allocation). Rayleigh fading channel which is contaminated by IN is considered, and stochastic analysis is used to find the optimum number of users for PD-NOMA-based systems. It is clearly seen from Fig. 4.10 that maximum 10 users in a sector can employ simultaneously on the proposed scheme without degrading the sum-rate in presence of IN.

The problem of maximization of the sum-rate of the proposed scheme from equation (4.1) is illustrated in Fig. 4.10. The system capacity initially increases and then saturates. This initial increase is due to the reason that the interference levels are manageable. It is a tradeoff between the number of users and inter-user interference. Optimum power allocation can overcome the inter-user interference but allows only an optimum number of users. If the number of users increases the inter-user interference also increases. Therefore, users consisting of low channel condition with high interference degrade the overall capacity.

4.6 Summary

In this chapter, for the PD-NOMA downlink system, algorithm 1 has been presented which is based on the user ordering strategy for the selection of an access scheme. The selection process is done in two steps. In the first step, the selection of beam or bandwidth is done. In the second step, power is allocated to each user based on their distance from BS in ascending order. The performance of the ordering strategy is observed in terms of the maximum number of permissible users in a single beam and the capability of employing farther users from the BS. Secondly, the power and bandwidth optimization is achieved, under the constraints of ergodic user-rate and total transmission power. The results of the optimization revealed that the optimum power allocation scheme achieves the higher sum-rate, by identifying the users who

influence more on system capacity. On the basis of the optimization results, algorithm 2 has been presented for the optimum power allocation. The purpose of the optimum power allocation scheme is to ensure that each user gets a minimum data rate. Finally, the maximum possible number of users has been estimated who can employ simultaneously on the PD-NOMA scheme without degrading the sum-rate over the IN-contaminated Rayleigh fading channel.

The unique traits of the PD-NOMA scheme i.e. non-orthogonal resource allocation and subsequent interference make PD-NOMA users more sensitive to IN. The aforesaid issues are catered to in the next chapter to mitigate the impact of IN on PD-NOMA-based systems.

CHAPTER 5

NOISE ANALYSIS AND MITIGATION TECHNIQUE

This chapter is divided into two sections. The first section deals with IN analysis and the end result of IN analysis provides us with a closed-form expression of BER. In the second section, DNN based IN mitigation and IN classification approaches have been presented which proved to be effective for BER performance.

5.1 Bit Error Rate Performance

The channel used for communication is affected by different types of noises which are present in the environment. In this noisy channel condition, different kinds of noise degrade the data transmission. These noises include asynchronous impulsive, synchronous impulsive to the mains frequency, periodic impulsive asynchronous to the mains frequency, narrow-band, and colored background noise. These five different types of noises can be summed up into two main noises, IN and AWGN.

The input BPSK information signal s, with average energy E_b ($s_1 = \sqrt{E_b}$ or $s_0 = -\sqrt{E_b}$ with equal apriori probabilities), is transmitted over the channel with combined noise amplitude ξ of IN and AWGN. The decoder detects the signals of the user by SIC while the other users' signals are treated as noises. For two user PD-NOMA model the received symbol for user 1 (lower-order user) in the presence

of IN can be written as:

$$y_1 = s_1\sqrt{\alpha_1 P}h_1 + s_2\sqrt{\alpha_2 P}h_1 + \xi \tag{5.1}$$

And received symbol for user 2 (higher-order user) in the presence of IN can be written as:

$$y_2 = s_2\sqrt{\alpha_2 P}h_2 + s_1\sqrt{\alpha_1 P}h_2 + \xi \tag{5.2}$$

where s_1 and s_2 are the transmitted symbols, α_1 and α_2 are the power allocation coefficients and h_1 and h_2 are the channel coefficients for user 1 and user 2 respectively.

For the l_{th} user, the received symbol in presence of IN can be written as:

$$y_l = s_l\sqrt{\alpha_l P}h_l + \sum_{t=1,t\neq l}^{L-1} s_t\sqrt{\alpha_t P}h_l + \xi \tag{5.3}$$

where s_l and s_t are the transmitted symbols for l_{th} and t_{th} users respectively and h_l is the channel coefficient for the l_{th} user.

5.1.1 PDF and CDF of Instantaneous SNR

In PD-NOMA scheme, users' signals which are closer to BS are assumed to be interference and farther ones to BS are treated as noise. The second term in equation (5.3) $\sum_{t=1,t\neq l}^{L-1} s_t\sqrt{\alpha_t P}h_l + \xi = \chi$ represents the level of the inter-cell interference for the l_{th} user. Also, $\chi_0 = \sum_{t=1,t\neq l}^{L-1} \alpha_t P|h_l|^2$ is the average power of inter-cell interference which is considered as noise. P is the total power for all users. α is power allocation coefficient, $\alpha_1 + \alpha_2 + \alpha_3 + \cdots + \alpha_l = 1$ and h is the fading coefficients of wireless channel. Now the above equation becomes:

$$y_l = s_l\sqrt{\alpha_l P}h_l + \chi + \xi \tag{5.4}$$

SNR for SM_l/UE_l can be written as:

$$SNR_l = \frac{\alpha_l E_b|h_l|^2}{\chi_0 + \xi_0} \tag{5.5}$$

The channel is represented as a Rayleigh fading channel. The PDF of Rayleigh fading channel with random variable $v = h$ is given by:

$$f_h(v) = \frac{v}{\sigma_h^2} \exp\left(\frac{-v^2}{2\sigma_h^2}\right) \tag{5.6}$$

and its scatter path defined by m_{th} moment is given by:

$$\mathrm{E}[h^m] = (2\sigma_h^2)^{m/2}\Gamma\left(\frac{m}{2}+1\right) \tag{5.7}$$

Average received SNR, $\bar{\gamma}$ can be defined as:

$$\bar{\gamma} = \mathrm{E}[\gamma] = \frac{\alpha_l E_b \mathrm{E}[h^2]}{\chi_0 + \xi_0} \tag{5.8}$$

where E_b is the bit energy and $E[h^2]$ is 2_{nd} moment. Let γ denote the instantaneous output SNR, defined as follows:

$$\gamma = \frac{\alpha_l E_b h_l^2}{\chi_0 + \xi_0} \tag{5.9}$$

Through two degrees of freedom, $|h|^2$ is chi-square distributed with the condition that random variable $|h|$ is Rayleigh distributed. Also, γ is chi square distributed if $|h|^2$ is chi square distributed. Hence, the PDF of γ can be expressed as:

$$f(\gamma) = \frac{1}{\bar{\gamma}} \exp^{\frac{\gamma}{\bar{\gamma}}} \ , \ \bar{\gamma} > 0 \tag{5.10}$$

The PDF of instantaneous SNR for the proposed scheme over Rayleigh fading channel with random variable $u = h^2$ can be written as:

$$f_\gamma(u) = \frac{1}{\left(\frac{\alpha_i E_b}{\chi_0+\xi_0}\right)} \exp^{\frac{\left(\frac{\alpha_i E_b u\gamma}{\chi_0+\xi_0}\right)}{\left(\frac{\alpha_i E_b}{\chi_0+\xi_0}\right)}} \tag{5.11}$$

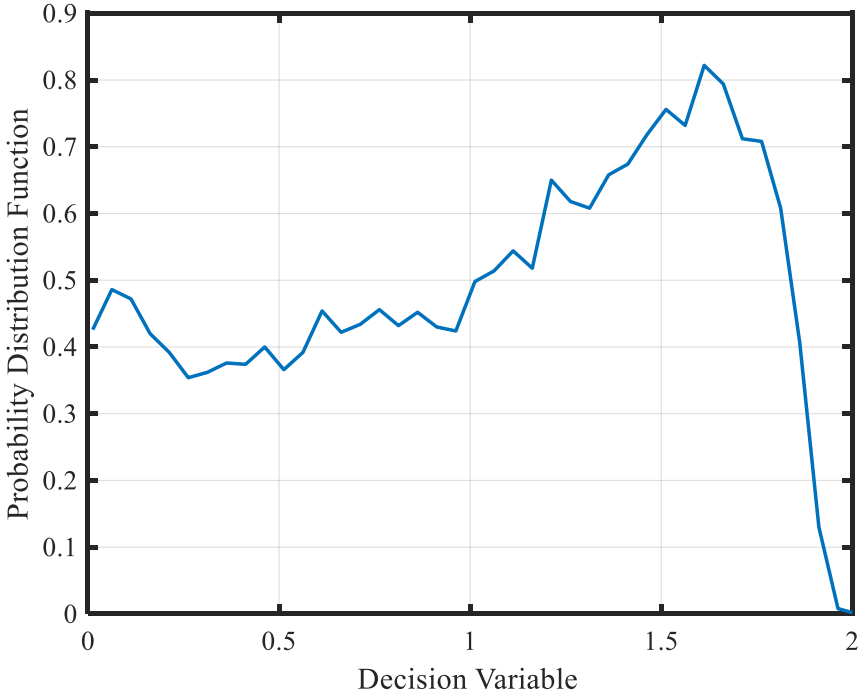

Figure 5.1:: PDF of instantaneous SNR.

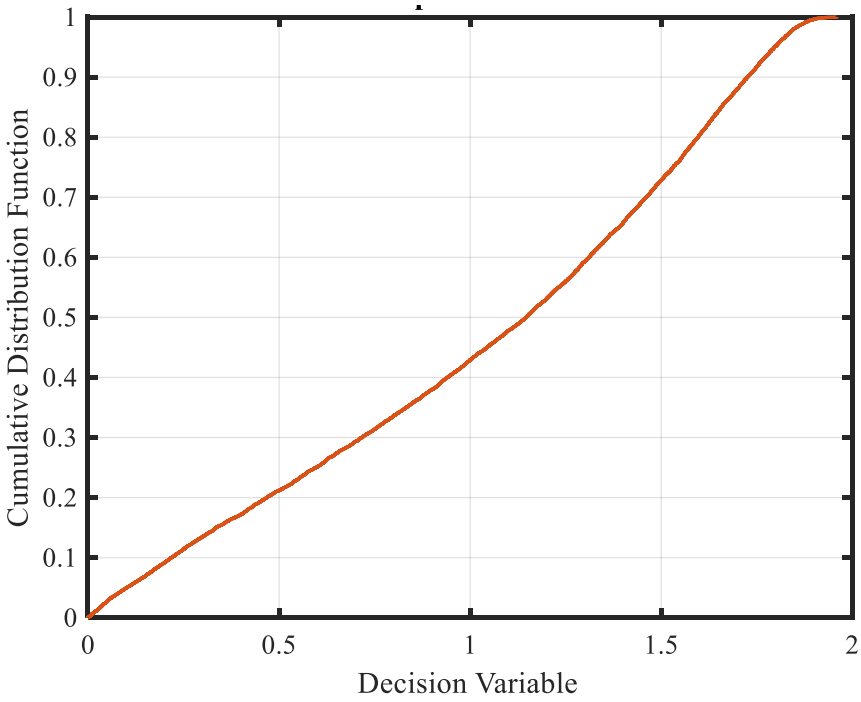

Figure 5.2:: CDF of instantaneous SNR.

Fig. 5.1 and Fig. 5.2 are the results of an analytical framework for estimating

significant statistical tools i.e. PDF and CDF of instantaneous SNR. The analysis is based on equation (5.11) that has been extracted for the PD-NOMA downlink system. In which the SIC receiver operates over Rayleigh fading channels and in the interference of other user signals, and IN. The achieved consequences specify the combination of interference and fading which can highly affect the performance of the system. Furthermore, the obtained equations are used to investigate the performance of the PD-NOMA system in terms of the average bit error probability.

5.1.2 Closed Form of BER Expression

The BER is given by:

$$P_e = \int_0^\infty P_e(e/u) f_\gamma(u) du \tag{5.12}$$

where the BER, $P(e|\cdot)$ which depends on γ. Considering the instantaneous SNR, the PDF of y depends on h^2 and s, from equations (3.15) and (5.3) can be written as:

$$\begin{aligned} p(y|h^2, s_0) = & \frac{1-p}{\sqrt{\pi(\chi_0 + 2\sigma_G^2)}} \exp\left(\frac{-(l + \sqrt{h^2 \alpha E_b})}{\chi_0 + 2\sigma_G^2}\right) \\ & + \frac{p}{\sqrt{\pi(\chi_0 + 2\sigma_G^2 + 2\sigma_I^2)}} \exp\left(\frac{-(l + \sqrt{h^2 \alpha E_b})}{\chi_0 + 2\sigma_G^2 + 2\sigma_I^2}\right) \end{aligned} \tag{5.13}$$

$$\begin{aligned} p(y|h^2, s_1) = & \frac{1-p}{\sqrt{\pi(\chi_0 + 2\sigma_G^2)}} \exp\left(\frac{-(l - \sqrt{h^2 \alpha E_b})}{\chi_0 + 2\sigma_G^2}\right) \\ & + \frac{p}{\sqrt{\pi(\chi_0 + 2\sigma_G^2 + 2\sigma_I^2)}} \exp\left(\frac{-(l - \sqrt{h^2 \alpha E_b})}{\chi_0 + 2\sigma_G^2 + 2\sigma_I^2}\right) \end{aligned} \tag{5.14}$$

The conditional BER which depends on h^2, when the transmitted symbol S_j ($j = 0, 1, $) is received as:

$$P(e|h^2, s_j) = \frac{1}{2}(1-p) Q\left(\sqrt{\frac{h^2 \alpha E_b}{\chi_0 + 2\sigma_G^2}}\right) + \frac{1}{2} p\, Q\left(\sqrt{\frac{h^2 \alpha E_b}{\chi_0 + 2\sigma_G^2 + 2\sigma_I^2}}\right) \tag{5.15}$$

The conditional BER which depends on γ can be written as:

$$P(e|\gamma) = P(e|h^2, s_0) = P(e|h^2, s_1) \tag{5.16}$$

$$P(e|\gamma) = \frac{1}{2}(1-p)Q\left(\sqrt{\frac{h^2\alpha E_b}{\chi_0 + 2\sigma_G^2}}\right) + \frac{1}{2}p\,Q\left(\sqrt{\frac{h^2\alpha E_b}{\chi_0 + 2\sigma_G^2 + 2\sigma_I^2}}\right) \tag{5.17}$$

The integral form of the BER by substituting equations (5.11) and (5.17) in equation (5.12) can be expressed as:

$$\begin{aligned} P_e = \int_0^\infty \Bigg\{ & (1-p)\ \frac{\chi_0 + 2\sigma_G^2}{\alpha_i E_b}\ Q\left(\sqrt{\frac{h^2\alpha E_b}{\chi_0 + 2\sigma_G^2}}\right)\exp^{u_\gamma} \\ & +\ p\ \frac{\chi_0 + 2\sigma_G^2 + 2\sigma_I^2}{\alpha_i E_b} Q\left(\sqrt{\frac{h^2\alpha E_b}{\chi_0 + 2\sigma_G^2 + 2\sigma_I^2}}\right)\exp^{u_\gamma}\Bigg\} d\gamma \end{aligned} \tag{5.18}$$

The first part of the equation (5.18):

$$P_e = \frac{1}{\left(\frac{\alpha E_b}{\chi_0 + 2\sigma_G^2}\right)} \int_0^\infty Q\left(\sqrt{\frac{h^2\alpha E_b}{\chi_0 + 2\sigma_G^2}}\right)\exp\left(\frac{\left(\frac{\alpha_i E_b h^2}{\chi_0 + 2\sigma_G^2}\right)}{\left(\frac{\alpha_i E_b}{\chi_0 + 2\sigma_G^2}\right)}\right) d\gamma \tag{5.19}$$

$$P_e = \frac{1}{2\bar{\gamma}} \int_0^\infty Q\left(\sqrt{\gamma}\right)\exp\left(-\frac{\gamma}{\bar{\gamma}}\right) d\gamma \tag{5.20}$$

$$P_e = \frac{1}{2\bar{\gamma}}\left[Q(\sqrt{\gamma})(-\bar{\gamma})\exp\left(-\frac{\gamma}{\bar{\gamma}}\right)\Big|_0^\infty - \int_0^\infty (-\bar{\gamma})\exp\left(-\frac{\gamma}{\bar{\gamma}}\right)\frac{-1}{\sqrt{\pi}}\exp\left(-\gamma\right)\gamma^{-1/2} d\gamma\right] \tag{5.21}$$

Since;

$$Q(\sqrt{x}) = \frac{1}{\sqrt{\pi}}\int_x^\infty e^{-t}t^{-1/2}dt$$

$$\frac{dQ(\sqrt{x})}{dx} = \frac{-1}{\sqrt{\pi}}e^{-x}x^{-1/2}$$

Therefore,

$$P_e = \frac{1}{2\bar{\gamma}}\left[-\bar{\gamma}Q(\sqrt{\gamma})\exp\left(-\frac{\gamma}{\bar{\gamma}}\right)\Big|_0^\infty - \frac{\bar{\gamma}}{\sqrt{\pi}}\int_0^\infty \exp\left[-\gamma\left(\frac{\bar{\gamma}+1}{\bar{\gamma}}\right)\right]\gamma^{-1/2}d\gamma\right] \tag{5.22}$$

$$\begin{aligned} &= \int_0^\infty \exp\left[-\gamma\left(\frac{\bar{\gamma}+1}{\bar{\gamma}}\right)\right]\gamma^{-1/2}d\gamma \\ &= \int_0^\infty \exp(-u)\left(\frac{\bar{\gamma}}{\bar{\gamma}+1}\right)u^{-1/2}\left(\frac{\bar{\gamma}}{\bar{\gamma}+1}\right)du \\ &= \left(\frac{\bar{\gamma}}{\bar{\gamma}+1}\right)^{1/2}\int_0^\infty \exp(-u)u^{-1/2} = \sqrt{\pi}\sqrt{\frac{\bar{\gamma}}{\bar{\gamma}+1}}Q(\sqrt{u}) \\ &= \sqrt{\pi}\sqrt{\frac{\bar{\gamma}}{\bar{\gamma}+1}}Q\left(\sqrt{\frac{\bar{\gamma}+1}{\bar{\gamma}}}\sqrt{\gamma}\right) \end{aligned} \tag{5.23}$$

Now, equation (5.20) becomes:

$$P_e = \frac{1}{2\bar{\gamma}}\left[-\bar{\gamma}Q(\sqrt{\gamma})\exp\left(\frac{\gamma}{\bar{\gamma}}\right) - \bar{\gamma}\sqrt{\frac{\bar{\gamma}}{\bar{\gamma}+1}}Q\left(\sqrt{\frac{\bar{\gamma}+1}{\bar{\gamma}}}\sqrt{\gamma}\right)\right]_0^{\infty} \tag{5.24}$$

$$P_e = \frac{1}{2}\left(1 - \sqrt{\frac{\bar{\gamma}}{\bar{\gamma}+1}}\right) \tag{5.25}$$

$$P_e = \frac{1}{2}\left(1 - \sqrt{\frac{\alpha E_b}{\alpha E_b + \chi_0 + 2\sigma_G^2}}\right) \tag{5.26}$$

Similarly, the second part of the equation (5.18):

$$P_e = \frac{1}{\left(\frac{\alpha E_b}{\chi_0+2\sigma_G^2+2\sigma_I^2}\right)} \int_0^{\infty} Q\left(\sqrt{\frac{h^2\alpha E_b}{\chi_0 + 2\sigma_G^2 + 2\sigma_I^2}}\right) \exp\left(\frac{\left(\frac{\alpha_i E_b h^2}{\chi_0+2\sigma_G^2+2\sigma_I^2}\right)}{\left(\frac{\alpha_i E_b}{\chi_0+2\sigma_G^2+2\sigma_I^2}\right)}\right) d\gamma \tag{5.27}$$

$$P_e = \frac{1}{2}\left(1 - \sqrt{\frac{\alpha E_b}{\alpha E_b + \chi_0 + 2\sigma_G^2 + 2\sigma_I^2}}\right) \tag{5.28}$$

$$P_e = \frac{1}{2}(1-p)\left(1 - \sqrt{\frac{\alpha E_b}{\alpha E_b + \chi_0 + 2\sigma_G^2}}\right) + \frac{1}{2}p\left(1 - \sqrt{\frac{\alpha E_b}{\alpha E_b + \chi_0 + 2\sigma_G^2 + 2\sigma_I^2}}\right) \tag{5.29}$$

The above equation (5.29) can measure the number of error bits that occur during the transmission over Rayleigh fading channel contaminated by IN. To achieve the required performance, the variables of the expression can be tuned according to the characteristics of the impulsive channel which helps in designing the receiver [18].

5.2 Deep Learning Approaches for IN Mitigation and Classification

The system model for IN detection and classification in NOMA symbols using a DNN is shown in Fig. 5.3. The communication channel is contaminated by Rayleigh fading and IN. In the pre-processing step, conversion of NOMA noisy/noiseless symbols into sample bits is carried out which is followed by DNN training. The trained DNN then performs either the detection or the classification of IN in test NOMA symbols.

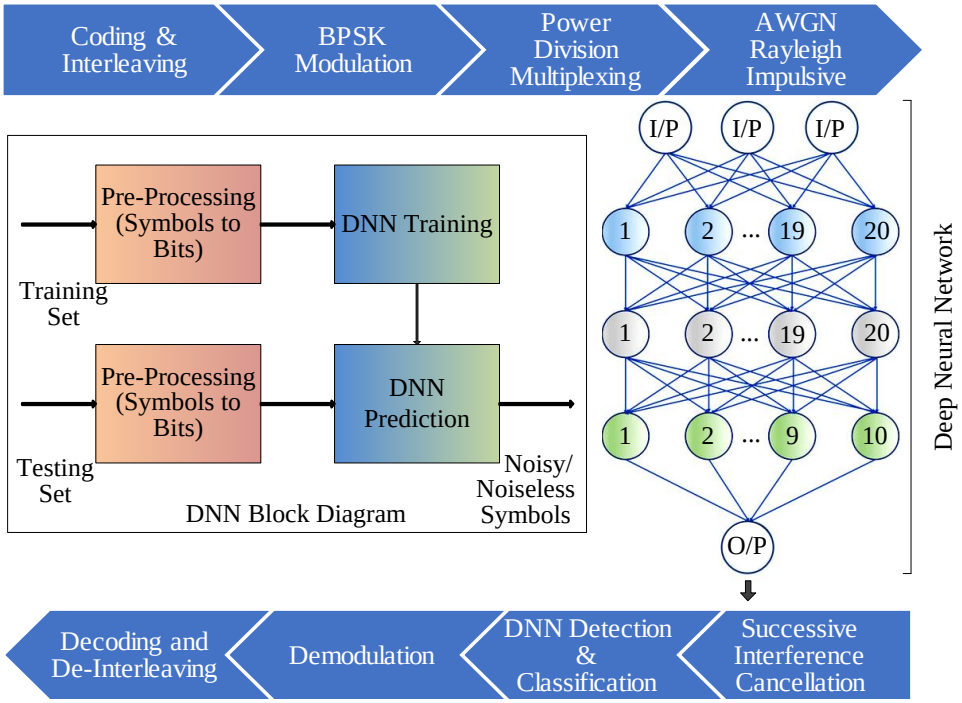

Figure 5.3:: Deep learning approaches for IN mitigation and classification in PD-NOMA-based systems.

5.2.1 Existing IN Suppressing Strategies

The classical IN detection approaches perform blanking and clipping by setting an optimum threshold. The threshold-based IN mitigation scheme is described as a memoryless nonlinear mitigation approach like blanking, clipping, and blanking/clipping.

5.2.1.1 Blanking

In the blanking method, the received signal is substituted by null if the signal is above the blanking threshold T_B for IN cancellation at the receiver. No change is

accrued in the phase and other parameters and only amplitude is changed [153].

$$r_i = \begin{cases} r_i & |r_i| < T_b \\ 0 & |r_i| > T_b \end{cases} \tag{5.30}$$

where T_B is known as the blanking threshold and r_i is the received vector.

5.2.1.2 Clipping

The clipping method performs IN cancellation by clipping the received signal at T_C level if the signal is above the threshold T_C. A clipping algorithm is used for the cancellation of IN at the receiver where IN include by the channel during communication. In clipping, no change is accrued in the phase and other parameters except the amplitude [153].

$$r_i = \begin{cases} r_i & |r_i| < T_c \\ T_c e^{jarg(r_i)} & |r_i| > T_c \end{cases} \tag{5.31}$$

where T_C is known as the clipping threshold.

5.2.1.3 Blanking/Clipping

The blanking/clipping hybrid method clips the received signal at T_1 level if signal amplitude lies between the threshold T_1 & T_2. The received signal is substituted by null if the signal is above the threshold T_2 and remains unchanged if it is lower than the threshold T_1. In this method, only the amplitude changes, and the rest of the parameters remain unchanged [153].

$$r_i = \begin{cases} r_i & |r_i| < T_1 \\ T_1 e^{jarg(r_i)} & T_1 < |r_i| \leq T_2 \\ 0 & |r_i| > T_2 \end{cases} \tag{5.32}$$

where the blanking threshold (T_2) is greater than the clipping threshold (T_1).

5.3 Proposed DNN for IN Detection

In order to detect IN, a deep learning strategy is devised as a DNN which search out the instances of IN corrupted samples. Theoretically, deep learning is a subset of machine learning which learns and improves its own performance using machine learning algorithms. In this section, the layout of the proposed DNN, its input features, output, and signal detection approach are presented.

5.3.1 DNN Layout

The proposed DNN is designed with three fully connected hidden layers $U^{[1]}$, $U^{[2]}$ and $U^{[3]}$, each of which consists of n_1, n_2 and n_3 neurons respectively. Increasing the number of layers and neurons does not affect the performance of the DNN, however, it increases the complexity of the network. Therefore, the number of layers and neurons are chosen by performing repeated experiments so that minimum training loss is achieved. The input to the DNN is a set of three features denoted by $z = [z^1, z^2, z^3]^T$ which are discussed in the next subsection and the output is represented by $o/p^{'}$. An activation function af at each layer enables connection from the preceding layer to the following layer using parameter matrix and bias vector. The parameter matrix W and bias vector q connect the hidden layers with each other and to the output layer using the number of neurons (n_r) chosen for the R_{th} layer. The output has one layer which generates a binary sequence of 0 or 1. The relationship between the hidden layers and the output layer $o^{'}$ is given by:

$$U^{[1]} = p^{[1]}(W^{[1]}z + q^{[1]}) \tag{5.33}$$

$$U^{[2]} = p^{[2]}(W^{[2]}U^{[1]} + q^{[2]}) \tag{5.34}$$

$$U^{[3]} = p^{[3]}(W^{[3]}U^{[2]} + q^{[3]}) \tag{5.35}$$

$$o/p^{'} = p^{[4]}(W^{[4]}U^{[3]} + q^{[4]}) \tag{5.36}$$

$$ReLU(z) = max(z, 0) \tag{5.37}$$

$$Sgmd(z) = \frac{1}{1 + e^{-z}} \tag{5.38}$$

Here $ReLU(z)$ represents Rectified Linear Unit as an activation function which is used by the hidden layers to give 0 when the input z is less than 0 and gives a value equal to z otherwise. The activation function applied by the output is the Sigmoid function denoted by $Sgmd(z)$ and is rounded off to give either 0 or 1 as the output. The training performance of DNN is measured using a cost function which calculates the average error associated with a predicted value of output for a training dataset. The error cost function is directly proportional to the difference of true output and predicted output as described below: [169].

$$\begin{aligned} Error(W, q) = -\frac{1}{k}[\sum_{p=1}^{k} o/p_j \log(\hat{o/p_j}) + (1 - o/p_j) \\ + \log(1 - \hat{o/p_j})] + \frac{\lambda}{2k} \sum_{r=1}^{R-1} \sum_{p=1}^{n_r} \sum_{q=1}^{n_r+1} W_{pq}^2 \end{aligned} \tag{5.39}$$

Here k are training samples, λ is the regularization parameter and n_r is the number of neurons in R_{th} layer. The DNN uses Backpropagation, short for "backward propagation of errors," and is trained with Adam's Optimizer [170] to optimize the network performance. While training, the DNN computes the values of parameter matrices W and the bias vectors q to reduce the error function $Error(W, q)$.

5.3.2 I/P Features Used in DNN for IN Detection

Correct I/P feature extraction and feature relationship with the output can help to eliminate the problem of over-fitting which is often faced while training the DNN. The input features should be chosen so that redundancy is removed from the learning patterns of DNN, enabling better classification of samples as corrupted or uncorrupted. The noise patterns in the data samples can be identified if the test sample bit is analyzed along with its neighboring samples. The input layer comprises of the input sample value and the following two features:

1. ROAD Statistic Value: The ROAD statistic is widely used to detect noise

in 2-D images. It gives a high value for noisy samples and produces a low value otherwise [160]. In this research, the ROAD score is calculated using the following steps for 1-D sample data bits stored in a vector with dimensions of×:

(a) The deviation magnitude between the current sample s_i and the remaining samples in the neighborhood (both right and left neighbors of data samples) is denoted by Absd(i) and is calculated as:

$$Absd(i) = |s_i - [s_{i-n}, ..., s_{i-1}, s_{i+1}, ..., s_{i+n}]| \tag{5.40}$$

(b) Sort Absd(i) values in increasing order:

$$arr(i) = sort(Absd(i)) \tag{5.41}$$

(c) The ROAD feature is computed by adding up the first n_0 values of arr(i):

$$ROAD = \sum_{i=1}^{n} arr(i) \tag{5.42}$$

2. Difference Median Output: The Difference median output is represented by err_i as follows:

$$err_i = s_i - median([s_{i-n}, ..., s_i, ..., s_{i+n}]) \tag{5.43}$$

where the variable median represents a standard moving average filter taking median as the central tendency of any 2n + 1 samples at a time.

5.3.3 IN Signal Detection

DNN is a conceptual approach that has been widely used to represent complex non-linear systems with the help of proper training. To learn about IN instances in the incoming sample values, the chosen DNN inputs include incoming sample value, difference median output feature, and ROAD statistic feature which are discussed above. The value of both input features is found to be high for an input IN sample and low for an input noiseless sample. Based on the learning of statistical traits of

noisy samples, the DNN output is a binary sequence of 0's and 1's where 1 represents a noisy sample detection and 0 represents an un-corrupted sample.

5.3.4 Proposed DNN for IN Classification

Due to randomly varying amplitudes of the impulse, it becomes a difficult task to classify a noisy sample as high or low impulse. To tackle this problem, a DNN is proposed to classify the IN into high and low impulse categories. Similar to the IN detection DNN in Section V, IN classification DNN comprises of 3 hidden layers with n_1, n_2 and n_3 neurons, one input layer, and one output layer. ReLU function and Sigmoid Layer are chosen as activation functions in the hidden layers and output layer respectively. The feed-forward neural network uses the Backpropagation algorithm for training and Adam's Optimizer for optimizing the network performance. The input consists of an input sample and two computed features helpful in IN classification. The output consists of one layer which generates a binary sequence of 0 and 1. '0' at location k as an output shows that the received sample k is corrupted with low IN whereas '1' as an output indicates that the received sample contains high IN. The relationships among input, hidden, and output layers have already been explained in the previous section.

5.3.5 I/P Features Used in DNN for IN classification

Although the arrival of IN is random and so is its amplitude but in theory, it follows binomial distribution. According to the PDF, the occurrence of high amplitude samples is less than the low amplitude samples in PD-NOMA symbols. The high and low noise patterns in the corrupted samples can be identified if the current sample is analyzed along with its neighboring samples. For this purpose, following two significant features which are helpful in IN classification are chosen as input features along with the input sample value:

1. Difference Median Output: The Difference median output is represented in equation (5.43) is denoted by *erri*. The value of *erri* feature is proven to be high for a high IN sample and low for low IN data.

2. Average Occurrence Probability Output: The average value of occurrence probability of 64 samples (current sample and the next 63 samples) [143] is chosen as the second input feature for proposed DNN because it's a strong indicator of high or low impulsivity. Since a high impulse arrival is less frequent than a low impulse, the chances of its occurrence are low. This phenomenon is reflected in small values of the average probability output for high IN occurrence and vice versa [18].

5.4 Results and Discussions

A typical PD-NOMA downlink system is considered in which a single BS allocates power to different users. All users are equipped with a single antenna and a flat fading Rayleigh channel (contaminated by IN) is considered for the link between each user and BS. Moreover, BPSK modulation technique is considered for computational convenience. The Bernoulli-Gaussian model is used for the representation of IN. Assume the channel as a quasi-static channel, therefore during transmission channel characteristics remain the same.

5.4.1 BER Performance of PD-NOMA System in Presence of IN

The BER performance of the proposed scheme has been evaluated over IN-contaminated Rayleigh fading channels by mathematical and simulation analyses. The theoretical analyses have been verified by performing Monte Carlo simulations via Matlab. The major simulation parameters and assumptions are taken from 3GPP LTE [163] and listed in Table 5.1.

5.4.1.1 Simulation Setup

The total transmits power is set to 46 dBm. Distance-dependent path loss with the decay factor of 3.76 is considered for simulation. Instantaneous multipath fading is taken into account in the propagation model. Each user is equipped with a single antenna while K number of antennas are available at BS. The power of IN - having an approximately flat frequency response over the spectrum - within the range of {0 - 50} dB and the probability of IN within the range of {0.1 - 0.4} are considered. Weak, medium, and heavy IN scenarios are considered for practical impulsive noise environments.

Further verification of theoretical BER over IN-contaminated Rayleigh fading channel is done by simulation. 1 Mbits are considered as input for BPSK transmission and reception. By initializing the random function, 10^6 bits are generated with an equal probability of 0 and 1. BPSK modulation technique for input bits is selected for computational convenience. Coefficients of AWGN (with zero mean and variance) and Rayleigh channel are generated. The coefficient of AWGN is multiplied by the range of Eb/No and the coefficient of Rayleigh fading is multiplied by BPSK symbols. Finally, randomly generated IN is added to the input vector before the reception. At receiving end, equalization is achieved for receive symbols by Rayleigh fading equalizer. Afterward, hard decoding is done by taking the real value of the output of the equalizer. All output values greater than 0.5 are considered 1 rest are 0. Lastly, the errors are counted by comparing the output of the hard decoder with input symbols.

Table 5.1:: Simulation parameters for BER.

S.No.	**Parameter**	**Value**
1	Number of bits for simulation	1 Mbits
2	Range of SNR	-3 to 35

3	BS total transmission power	46 dBm
4	Receiver noise density	−174 dBm/Hz
5	Carrier frequency	2 GHz
6	System bandwidth	10 MHz
7	IN power	0 dB to 50 dB
8	Disturbance Ratio, dr	0.00135%, 0.00632% & 0.0327%

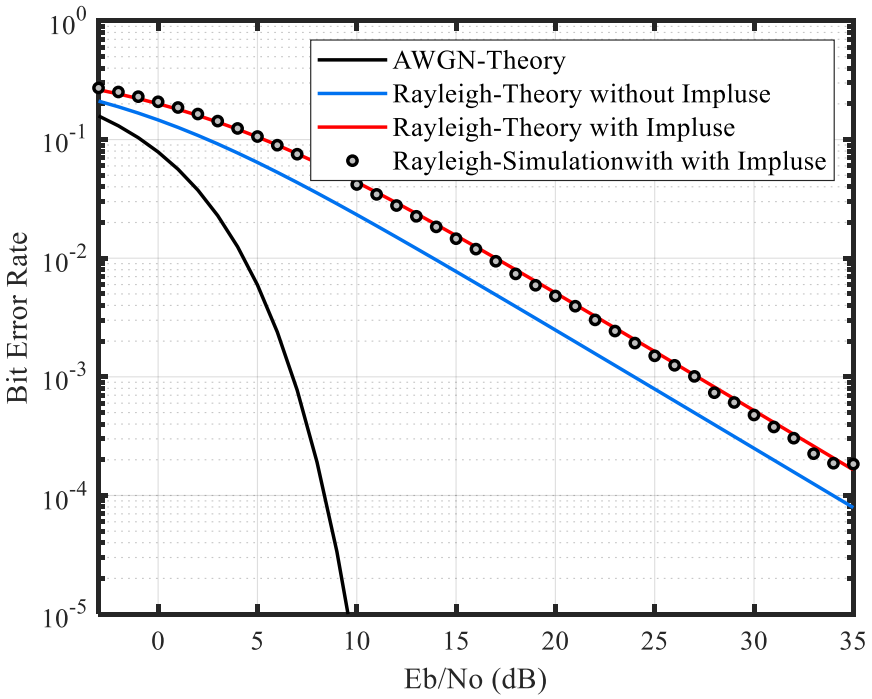

Figure 5.4:: Comparison of BER performance of the AWGN and flat fading Rayleigh channel in the presence of IN.

In the PD-NOMA scheme, knowledge of accurate SNR is essential for allocating power to different users. Fig. 5.4 shows the comparison of BER performance of the proposed scheme over flat fading Rayleigh channel and AWGN channel in the presence of IN. This is very helpful for defining the SNR in presence of IN over

Rayleigh fading channel for power allocation to users. It can be observed from the graph that the effect of IN is greater at low SNR. An increase in SNR rapidly decreases the effect of IN and BER. It is because the amplitude of most of the impulses is not too high (between 0 dBm to 20 dBm) therefore by increasing SNR, the signal level becomes larger than the average impulse noise level. Furthermore, in PD-NOMA, several users' signals are superimposed, other users' signals are considered as noise. Therefore, it is also noticeable that the increase in SNR of one user increases the interuser interference of other users' signals.

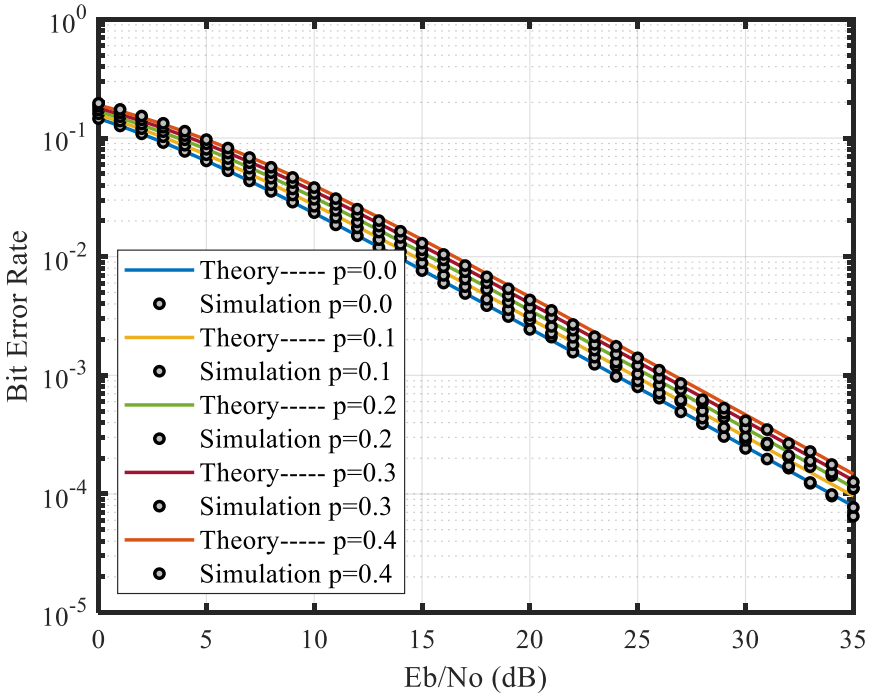

Figure 5.5:: Average BER performance with probability of IN, $p = \{0 - 0.5\}$.

The BER performance of the proposed scheme with the different probability of IN is illustrated in Fig. 5.5. The plot shows how much error-free data can be transmitted with an impulse probability of p over Rayleigh fading channel. It is observed from the plot that the increase in the probability of impulse decreases the BER. Therefore, SNR is required to be improved to keep the BER of the PD-NOMA system constant. With the change in probability of the impulse by 0.1, there is a difference of about 1 dB in the SNR for the same value of BER. The higher value of

BER is more affected by an increase in the probability of IN compared to the low value of the BER. At 15 dB SNR, changing the probability of impulse from 0.1 to 0.5 increases the value of BER from 0.01 to 0.02. The more the impulsivity of noise (higher value of p) is the more degradation of the BER performance will be.

The instantaneous value of impulse does not define the actual loss because impulse occurs for a very short period and increases the level of noise up to 50 dB and then disappears. At the time of occurrence of impulse, a considerable level of noise power increases. The study of the time domain of IN shows that usually widths of impulses rarely exceed a few hundred microseconds but sometimes exceed 10 milliseconds. There is a always probability of burst errors. Burst errors affect many consecutive bits, especially in high-speed data transmission. Therefore, dr can better define the actual loss. $dr = \frac{\sum_{i=1}^{l} t_{w,i}}{T_{total}}$, where $t_{w,i}$ is the width of the i_{th} impulse in a sec and l is the total number of impulses occurring in time $T_{tot}(sec)$ [142].

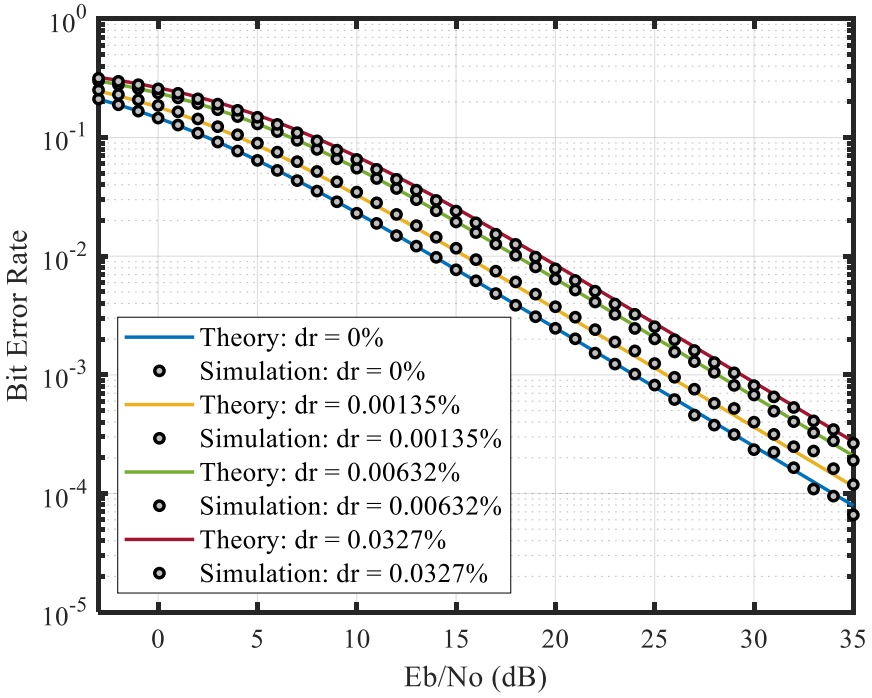

Figure 5.6:: Average BER with dr = 0.00135%, dr = 0.00632% & dr = 0.0327%.

Fig. 5.6 illustrates a comparison of BER performance of the proposed scheme

between the three IN scenarios i.e. heavily disturbed, medium disturbed, and weakly disturbed. Selecting signal power in PD-NOMA is crucial because PD-NOMA utilizes power domain multiple access. Any ambiguity in the selection of power can affect SIC decoding. The reason behind this is that SIC decodes the desired signal from a superimposed signal on the basis of their power difference. The results help in choosing the SNR in relevant real-life impulse scenarios for the preferred value of BER.

5.4.2 Performance of Deep Learning Approaches for IN Mitigation

As discussed earlier, the presented DNN methods are implemented for PD-NOMA downlink system in presence of IN over Rayleigh fading channel. Since the emphasis of this research work lies in IN detection and classification, BPSK modulation technique has been chosen for computational convenience. The proposed DNN based IN mitigation performance is compared with blanking, clipping, and blanking/clipping methods respectively for a range of BER values. Furthermore, the performance of the deep learning approach for IN classification is also evaluated.

5.4.2.1 Simulation Setup

The key simulation parameters which are common in training both the DNNs are set to the following optimal values: Learning Rate η, a hyper-parameter for fine-tuning the DNN = 0.01; $\lambda = 0.1$; Number of bit samples $(n_0) = 5$; The number of neurons in the three layers are set as $n_1 = 20,\ n_2 = 20$ and $n_3 = 10$ in the first, second and the third hidden layers, respectively. These simulation parameters are also reported in Table 5.2 for a better understanding.

The size of $W^{[1]},\ W^{[2]},\ W^{[3]}$ and $W^{[4]}$ parameter matrices are (20×3), (20×20), (10×20) and (10×1) respectively. The dimensions of bias vectors $q^{[1]}, q^{[2]}, q^{[3]}$ and $q^{[4]}$ are (20×1), (20×1), (10×1) and (1×1) respectively. The

Table 5.2:: Simulation parameters for DNN-based IN mitigation.

S.No.	Parameter	Value
1	α_1	0.333
2	α_2	0.667
3	T_1	1.5
4	T_2	1.8
5	T_B	1.6
6	T_C	1.5
7	η	0.01
8	λ	0.1
9	n	5
10	n_1	20
11	n_2	20
12	n_3	10
13	Data size	5×10^6
14	Training data	80%
15	Testing data	20%

Xavier initialization [171, 172] is used to select the initial values of all the above chosen parameters since gradient descent method was observed to suffer from poor performance when randomly initialized.

The input to the DNN for IN mitigation is a set of three features i.e. incoming sample value, difference median output feature, and ROAD statistic feature. Moreover, the input to the DNN for IN classification also contains three features i.e. incoming sample value, difference median output feature, and average occurrence probability output. An activation function (af) at each layer enables connection

from the preceding layer to the following layer using parameter matrix and bias vector. The parameter matrix W and bias vector q connect the hidden layers with each other and to the output layer using the number of neurons (n_r) selected for the R_{th} layer. The output is represented by o/p' and has one layer which generates a binary sequence of 0 or 1.

5.4.2.2 Computer Complexity

In the hidden layer, each input feature is linked to a neuron, and the total number of connections is equal to the product of the hidden layer size (n) and the input feature size (m). Because each link has a weight parameter, the total number of weight parameters is $m \times n$. Because each output neuron has one bias parameter, the total number of bias parameters is n. Therefore $m \times n + n =$ total number of trainable parameters.

In proposed DNN, the output dimension of the first dense/hidden layer is 20Âăneurons. In the model summary, this appears as the second output argument, against the first hidden layer. The succeeding dropout layer has no effect on the output dimension. It just affects the neuron weights. The second hidden layer has 20Âăoutput neurons, followed by 10. There is only one neuron in the last output layer. Let us check the model's total trainable parameters.

- First hidden layer $(m = 3, n = 20) : 3 \times 20 + 20 = 80$
- Second hidden layer $(m = 20, n = 20) : 20 \times 20 + 20 = 420$
- Third hidden layer $(m = 20, n = 10) : 20 \times 10 + 10 = 210$
- Output layer $(m = 20, n = 1) : 10 \times 1 + 1 = 11$
- Total trainable parameters $= 80 + 420 + 210 + 11 = 721$

5.4.2.3 DNN Performance for IN Detection

The proposed DNN is trained using 10^6 NOMA-based BPSK symbols defined in equations (5.1) and (5.2) which are contaminated by IN and represented by Bernoulli-Gaussian noise model in equation (3.14). In Fig. 5.7, BER performance of proposed DNN-based IN mitigation approach is evaluated for average probability of impulse occurrence.

Fig. 5.7 shows a comparison of BER performance of DNN based mitigation with blanking, clipping, and blanking/clipping for IN detection. In general, BER performance is observed to improve with an increase in the SNR. It is evident that DNN outperforms conventional methods in terms of BER improvement. The results depicted in Fig. 5.7 show that blanking and clipping are very susceptible to noise at low levels of SNR and finding a suitable threshold to distinguish between desired and contaminated signals has been a tough task. On the contrary, the proposed DNN has successfully detected IN even at low levels of signal. This phenomenon can be seen at 5 dB SNR, where the proposed DNN method has detected approximately 0.1 Mbits more true symbols out of 1 Mbits compared to conventional methods. At high SNRs, the DNN identified 700 more true symbols compared to conventional methods. This is due to the reason that conventional methods perform better detection at high SNR, therefore the performance difference between proposed DNN and conventional methods decreases.

It is noteworthy that the performance degradation level depends upon the user order in the PD-NOMA-based system. Higher-order users perform less SIC operation compared to others and are strengthened by better received power. However, they experience interference from the lower-order users. According to power allocation scheme, a power coefficient α determines the transmit signal power of the lower-order user (user 1) as α_1 and that of the higher-order user (user 2) as $\alpha_2 = 1 - \alpha_1$. Therefore, PD-NOMA users are quite sensitive to any additional noise/interference. In addition, it is observed that low IN power and low IN oc-

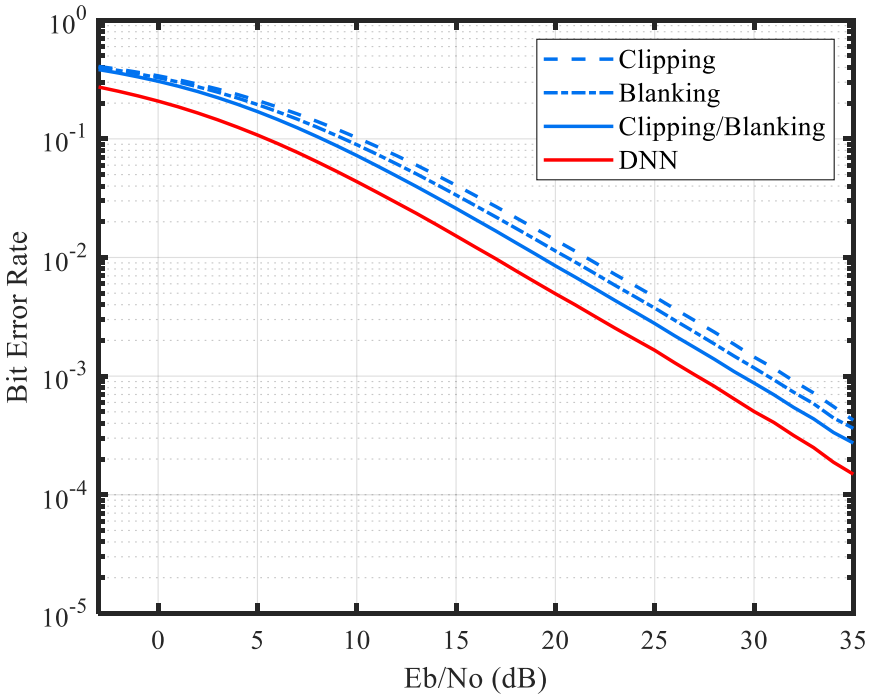

Figure 5.7:: Comparison of different IN mitigation techniques.

currence rate - which do not affect the performance of the TDMA users - have a degrading impact on PD-NOMA users. Specifically, the performance of the higher-order PD-NOMA users degrades and this degradation is expected to increase as the number of users increases. Considering the above-mentioned scenario, it is now clear that the proposed DNN based approach can efficiently eliminate the IN and has retrieved the theoretical performance of PD-NOMA user pair specifically for the higher-order user which is more sensitive to noise. In Fig. 5.8, the performance of PD-NOMA user pair using conventional method (blanking/clipping) and DNN based IN mitigation technique has been illustrated. The comparison reveals that at 5 dB SNR, the performances of user 1 and user 2 are approximately the same hence, the comparison is insignificant. At 30 dB, DNN identified 700 more true symbols for user 1 and 2000 more true symbols for user 2 compared to the conventional method. Due to more contaminated symbols in the user 2 signal, the BER performance of user 2 is poorer than user 1. Due to this reason, DNN gets a better chance of performing IN mitigation for user 2.

The DNN response for low and high impulse scenarios is evaluated by testing

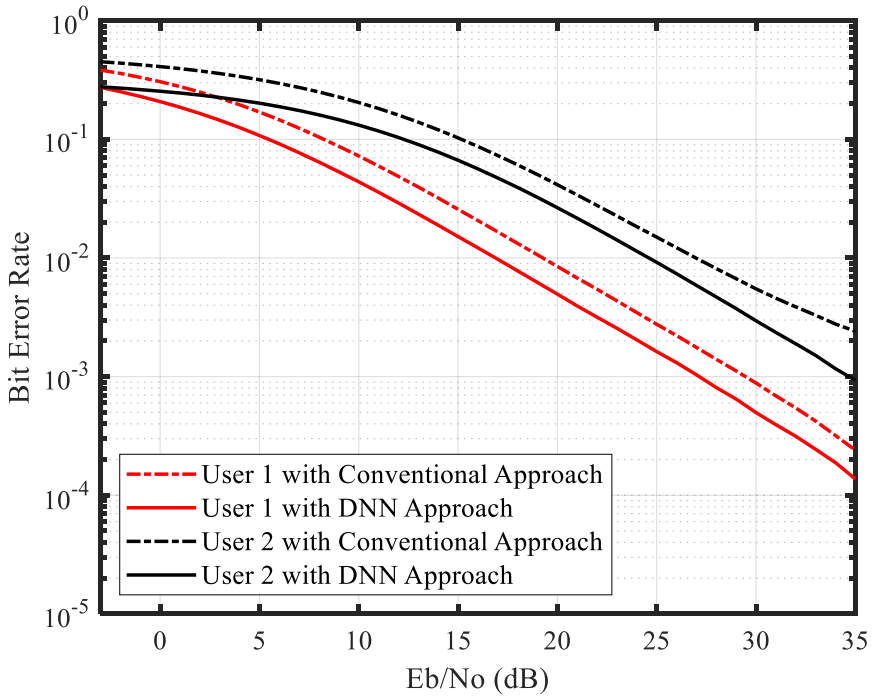

Figure 5.8:: Performance of PD-NOMA users pair using proposed DNN based technique.

the DNN on the PD-NOMA user pair in Fig. 5.9. A relatively high IN (50 dB) and low IN (20 dB) scenarios have been considered. Overall, there is less effect of high or low IN on user 1 and user 2 for SNRs less than 10 dB. As the SNR increases, the performance of DNN is observed to be improved. This is due to the fact that in low IN scenario at high SNR, the ratio of signal versus IN improves, leading the signal level to become traceable for successful IN detection.

In Fig. 5.10, DNN responses for different values of parameter p are evaluated by testing the DNN on the PD-NOMA user pair. The test scenario includes high value of parameter ($p = 0.5$) for strong likelihood of impulse occurrence and low value of parameter ($p = 0.2$) for weak likelihood of impulse occurrence.

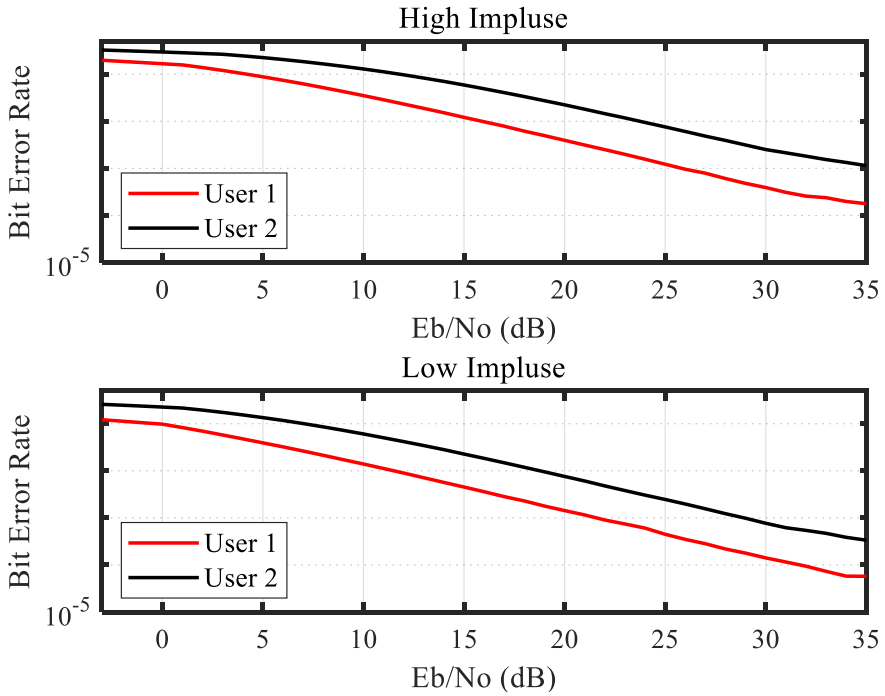

Figure 5.9:: DNN performance for high and low IN scenarios for PD-NOMA user pair.

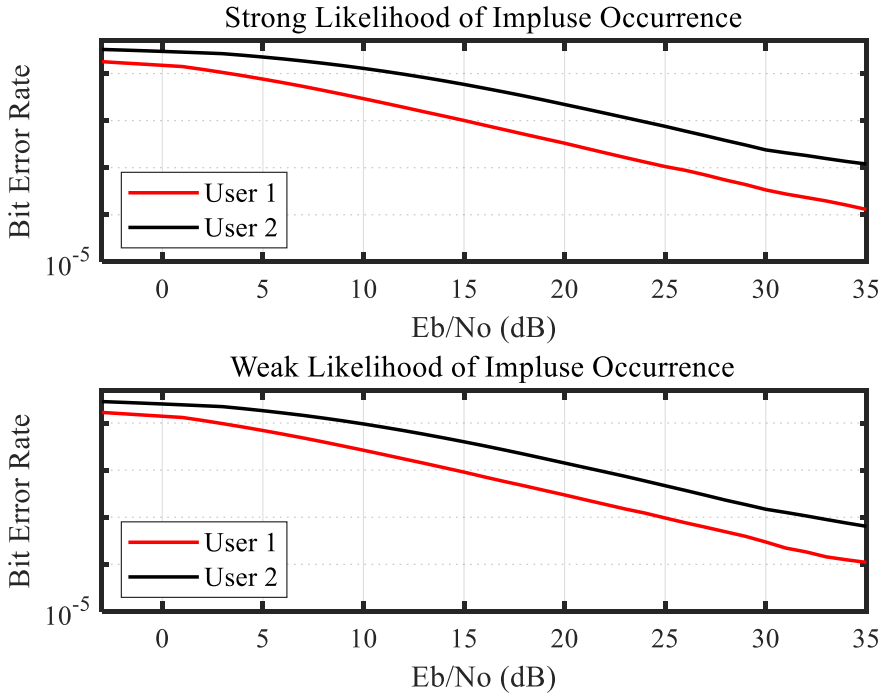

Figure 5.10:: DNN performance for strong and weak likelihood of IN occurrence for PD-NOMA user pair.

It is observed that the effect of the impulse probability parameter is very low

because the DNN gets trained more efficiently on high or low impulse as compared to the occurrence probability of impulse. The training of DNN is performed on 1 Mbits of data samples that is why the effect of probability is minimum on the result.

5.4.2.4 DNN Performance for IN Classification

The training set consists of 10^6 PD-NOMA symbols with a range of E_b/N_0 that can enable the performance evaluation under various noise interference scenarios. The performance of DNN is evaluated at 5 dB SNR and $p = 0.5$ for IN classification as high IN and low IN for 100 noise-contaminated PD-NOMA symbols. A numerical value of 2 is considered as the normalized threshold level for IN classification. Since IN arrival is random, the proposed DNN has classified the IN based on the probability of arrival and the median amplitude deviation from the neighboring samples as input features.

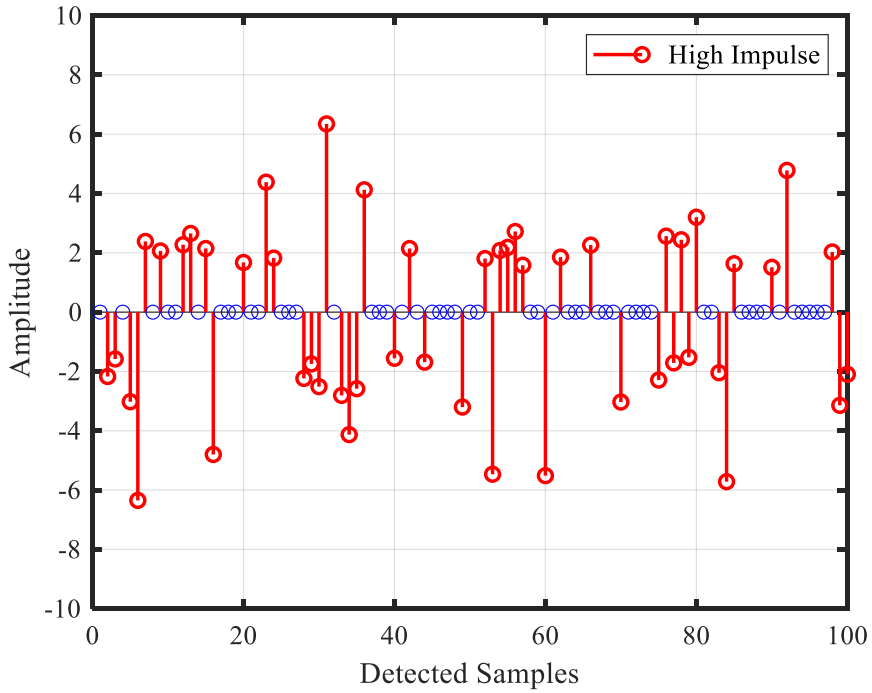

Figure 5.11:: High impulse detection using DNN.

In Fig. 5.11, high impulse detection using DNN is shown. High impulses are represented by red stems and low impulses which are removed using DNN are

represented by blue circles on the x-axis. The x-axis represents 100 random IN samples and the y-axis represents the normalized amplitude of impulses. In Fig. 5.12, low impulse detection is demonstrated where low IN is represented by blue stems, and high impulses which are removed using DNN are represented by red circles on the x-axis. It is evident from Fig. 5.11 that all identified high impulses are higher than the normalized threshold level of 2. In Fig. 5.12, all identified low impulses are shorter than the normalized threshold level of 2 which shows the robust performance of DNN. The classification of impulse gives information about the nature of impulses which depends upon the type of source of IN. It is clearly visible from Fig. 5.11 and Fig. 5.12 that most of the impulses are either low or high amplitude impulses and only two impulses are in the very high amplitude category. This type of information is valuable to set parameters of DNN for IN detection.

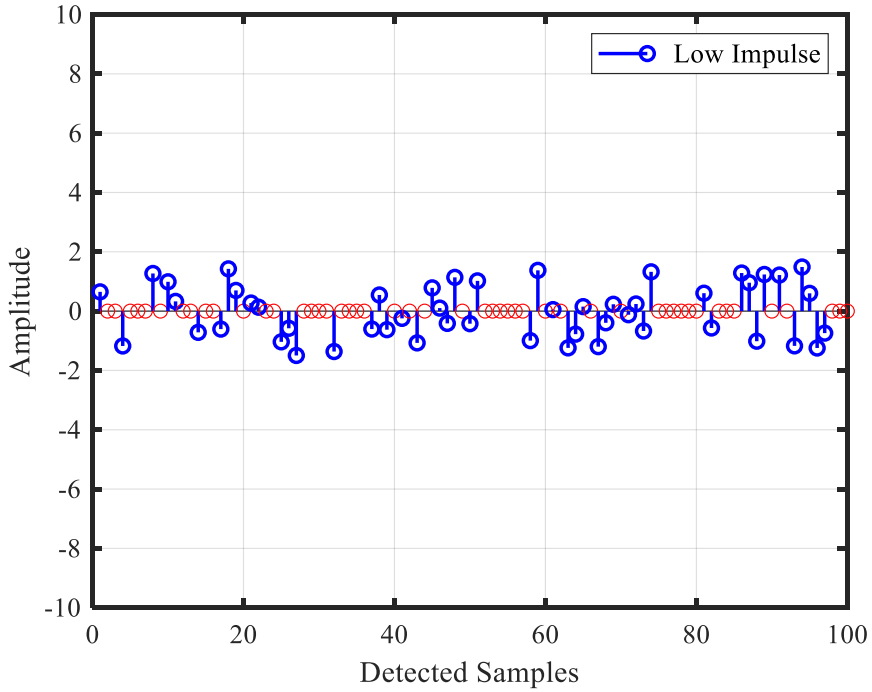

Figure 5.12:: Low impulse detection using DNN.

The DNN has identified high IN in the incoming noisy PD-NOMA symbols with an accuracy of 99% and low impulses with an accuracy of 87% respectively. However, DNN classified a few noiseless PD-NOMA symbols as low IN instances. This has been due to the random IN peakedness which is similar to the amplitude

of noiseless PD-NOMA symbols and cannot be accurately determined. Overall, the proposed DNN classified a sufficient number of IN instances accurately. The IN classification in PD-NOMA symbols using the deep learning approach has been carried out for the first time according to the authors' best knowledge in this research and is a significant contribution.

5.5 Summary

The first part of the chapter examined the performance of the proposed scheme in presence of IN. Hence, a combined statistical noise model has been used which includes the impact of IN and background noise in system capacity expression. The Bernoulli-Gaussian model and the Laplacian-Gaussian model are the prime choices for IN as the distribution curve is close to the actual IN scenario. Furthermore, the characteristics of these models have been investigated in terms of PDF, CDF, the arrival rate of impulse, and probability parameter p in order to derive instantaneous SNR and BER.

Statistical formation i.e. the PDF and CDF have been formulated for the channel to estimate the effect of IN. Moreover, two closed-form expressions have been derived i.e. instantaneous SNR by using the PDF and CDF for IN-contaminated wireless channel and BER by using instantaneous SNR for IN-contaminated PD-NOMA-based system. This will be useful for the designer to predict the performance of wireless links over the IN-contaminated Rayleigh fading channel. The performance of the proposed scheme over the IN-contaminated Rayleigh fading channel has been evaluated in terms of BER, the effect of dr, and the effect of probability parameter p on BER.

In the second part of the chapter, novel IN mitigation and classification techniques have been presented using deep learning approaches for NOMA-based communication systems. The IN detection has been performed by first identifying

the IN occurrences using a DNN which learns statistical traits of noisy samples, followed by removal of the harmful effect of IN in the detected occurrences. The proposed DNN offered higher BER performance as compared to the existing IN detection methods. The proposed method has been further validated for high and low IN, and weak and strong IN occurrence probabilities. Moreover, another deep learning network has been proposed in this research to effectively distinguish between high IN and low IN in the IN-contaminated PD-NOMA symbols to improve the performance of IN detection models. The proposed DNN method has detected approximately 0.1 Mbits more true symbols out of 1 Mbits compared to conventional methods. Both of the deep learning methods proposed in this study showed strong potential to address IN problem faced by the PD-NOMA scheme. Future research involving the DNN-based approach for IN detection should consider the impact of the nature of IN to obtain better DNN capabilities.

CHAPTER 6

SUMMARY OF DISSERTATION AND DIRECTION OF FUTURE RESEARCH

6.1 Summary of Dissertation

In this dissertation, the analysis of the design of the communication networks and associated mechanisms for NGNs such as SG, IoT, VANET, etc. has been presented and discussed. The major contributions of the research performed in the thesis are revisited and concluded as followed.

- A new composite multiple access scheme has been presented based on OBF and PD-NOMA for exchanging information between SG, SMs, and other communication units in the presence of IN. In the proposed scheme a cell is divided into sectors and OBF is implemented between sectors to reduce inter beams interference using orthogonalization. Within these sectors, the PD-NOMA scheme is implemented to utilize maximum bandwidth with the help of the SIC scheme. Furthermore, Gaussian and Laplacian models with Bernoulli arrival rate were adopted to find the effect of IN on the performance of the proposed scheme. According to the simulation and numerical findings, the proposed scheme offers a 3 Mbit/sec higher data rate than the traditional OFDMA scheme leading to better system capacity in the case of 10 SMs/users in a sec-

tor of a cell. Another significant achievement of the proposed scheme is that it does not cause inter beam interference and provides 17 Mbit/sec higher data rate by using OBF compared to CBF in the case of 60 SMs/users in 12 sectors of a cell.

- In addition, this research proposed the first algorithm for the user ordering strategy for the PD-NOMA downlink system. Also, the power and bandwidth optimization has been presented, under ergodic user-rate constraints and total transmission power constraints. As a result of the optimization, the optimum power allocation scheme achieved a higher sum-rate, by identifying the users with greater influence on system capacity. On the basis of the optimization results, the second algorithm has been presented for the optimum power allocation scheme. The purpose of the optimum power allocation scheme is to ensure that each user gets a minimum data rate. With the help of the aforementioned contributions, the maximum possible number of users has been determined - who can employ simultaneously on the PD-NOMA scheme without degrading the sum-rate over IN-contaminated Rayleigh fading channel.

- In addition, this research has investigated and evaluated the performance degradation of SMs due to IN-contaminated SG wireless channel. By investigating Bernoulli-Gaussian model and Laplacian-Gaussian model, statistical formation about the channel i.e. the PDF and CDF has been formulated for estimation of the channel. Moreover, two closed-form expressions have been derived i.e. instantaneous SNR by using the PDF and CDF for IN contaminated wireless channel and BER by using instantaneous SNR for IN-contaminated PD-NOMA-based system. Using impulse rate and disturbance ratio, this research further discovered the actual loss of bits during impulses in different IN practical scenarios.

- A novel IN mitigation and classification technique is presented using deep learning methods for PD-NOMA-based communication systems. The IN de-

tection is performed by first identifying the IN occurrences using a DNN that learns statistical traits of noisy samples, followed by removal of the harmful effect of IN in the detected occurrences. Compared to the existing IN detection methods, the proposed DNN provided an enhanced BER performance. The proposed method has been further tested for high and low IN and weak and strong IN occurrence probabilities. The proposed DNN method has detected approximately 0.1 Mbits more true symbols out of 1 Mbits compared to conventional methods. Moreover, this research has investigated and evaluated another relevant deep method to effectively distinguish high IN and low IN in the noise-contaminated PD-NOMA symbols that can help to improve the performance of IN detection models. In essence, the result of this study revealed that the two deep learning methods proposed in this study have strong potential to address IN problem faced by the PD-NOMA scheme.

6.2 Directions of Future Work

The rapid increase in connected devices continues to impose unprecedented challenges for the development of next generation wireless networks, such as supporting massive connectivity, improving spectral and energy efficiency, robustness in high noise environments, developing ultra-reliable low-latency communications, etc. Some of these issues have been addressed in this thesis by implementing the PD-NOMA with OBF to enhance system performance through resource allocation and novel noise mitigation schemes. However, there are some modifications, tests, and investigations that need to be addressed in the future. More performance parameters can also be used to increase the authenticity of the results, the proposed model can be tested in different fading channels, and the effect of harsh environments such as temperature, dust, humidity, etc. can also be considered with IN. Following are some major future study directions.

6.2.1 Two Deep Learning Approach

DNN is used in this research is its ability to execute feature engineering that is helpful in the mitigation of IN. Firstly, IN mitigation is performed using a DNN. Then, another DNN model is developed for IN classification. The second DNN is used to understand the nature of IN which is helpful in adjusting the parameters of the first DNN. Therefore, utilizing the result of the second DNN for the performance improvement of the first DNN should be the first priority in respect to future research.

6.2.2 Various Categories of NOMA Schemes

NOMA is generally a promising future radio access technology due to its variety of categories such as code domain and power domain. Different categories of NOMA have gained the attention of researchers such as PD-NOMA, SCMA, PDMA, and MUSA. This research presented and evaluated PD-NOMA with OBF. It would be interesting to study OBF with other NOMA's popular categories to find the most appropriate and useful NOMA scheme.

6.2.3 Different Fading Channel

Variations in received signal intensity or fading is one of the most important aspects to consider when evaluating the performance of a wireless network. This research also evaluated the performance of the proposed scheme under AWGN and Rayleigh fading channel in presence of IN. Hence, future researchers can most likely support and evaluate the proposed scheme in different fading channels.

Bibliography

[1] R. Borralho, A. Mohamed, A. U. Quddus, P. Vieira, and R. Tafazolli, "A survey on coverage enhancement in cellular networks: Challenges and solutions for future deployments," *IEEE Communications Surveys & Tutorials*, vol. 23, no. 2, pp. 1302–1341, 2021.

[2] Y. Liu, S. Zhang, Z. Ding, R. Schober, N. Al-Dhahir, E. Hossain, and X. Shen, "Special issue on next generation multiple access part i," *IEEE Journal on Selected Areas in Communications*, vol. 40, no. 4, pp. 1031–1036, 2022.

[3] M. S. Ahmed, A. N. Rashid, and S. A. Aliesawi, "Efficient scheme to suppress the disturbance of impulsive noise among iot devices," *Journal of Southwest Jiaotong University*, vol. 54, no. 3, 2019.

[4] A. Yıldız, Š. Džakmić, and M. A. Saleh, "A short survey on next generation 5g wireless networks," *Sustainable Engineering and Innovation*, vol. 1, no. 1, pp. 57–66, 2019.

[5] S. Timotheou and I. Krikidis, "Fairness for non-orthogonal multiple access in 5g systems," *IEEE Signal Processing Letters*, vol. 22, no. 10, pp. 1647–1651, 2015.

[6] Y. S. Cho, J. Kim, W. Y. Yang, and C. G. Kang, *MIMO-OFDM wireless communications with MATLAB*. John Wiley & Sons, 2010.

[7] C. Yuqing, L. Xiaoyan, S. Xixia, and P. Su, "Resource allocation in multi-user mimo-ofdm systems with double-objective optimization," *KSII Trans. Internet Inf. Syst.*, vol. 12, no. 5, pp. 2063–2081, 2018.

[8] G. Siamack, H. Jamil, S. S. Tarlochan, and P. Serguei, "Effect of impulse noise on wireless relay channel," *Wireless Sensor Network*, vol. 2012, 2012.

[9] S. V. Zhidkov, "Analysis and comparison of several simple impulsive noise mitigation schemes for ofdm receivers," *IEEE Transactions on Communications*, vol. 56, no. 1, pp. 5–9, 2008.

[10] Y. Yan, Y. Qian, H. Sharif, and D. Tipper, "A survey on smart grid communication infrastructures: Motivations, requirements and challenges," *IEEE communications surveys & tutorials*, vol. 15, no. 1, pp. 5–20, 2012.

[11] Y. Chen, A. Bayesteh, Y. Wu, B. Ren, S. Kang, S. Sun, Q. Xiong, C. Qian, B. Yu, Z. Ding, S. Wang, S. Han, X. Hou, H. Lin, R. Visoz, and R. Razavi, "Toward the standardization of non-orthogonal multiple access for next generation wireless networks," *IEEE Communications Magazine*, vol. 56, no. 3, pp. 19–27, 2018.

[12] N. Parekh and R. Joshi, "Non orthogonal multiple access techniques for next generation wireless networks: A review," in *Proceedings of the International e-Conference on Intelligent Systems and Signal Processing.* Springer, 2022, pp. 171–188.

[13] N. Framework, "Roadmap for smart grid interoperability standards, release 2.0," *NIST special publication 1108R2*, pp. 1–225, 2012.

[14] M. Hussain, H. Rasheed, N. Ali, and N. Saqib, "Roadside infrastructure transmission of vanet using power line communication," in *2017 International Conference on Communication, Computing and Digital Systems (C-CODE).* IEEE, 2017, pp. 139–143.

[15] M. Hussain and H. Rasheed, "Performance of orthogonal beamforming with noma for smart grid communication in the presence of impulsive noise," *Arabian Journal for Science and Engineering*, pp. 1–15, 2020.

[16] M. Hussain and H.Rasheed, "Communication infrastructure for stationary and organized distributed smart meters," in *2019 2nd International Conference on*

Communication, Computing and Digital systems (C-CODE). IEEE, 2019, pp. 17–22.

[17] M. Hussain and HRasheed, "A computational power allocation scheme for fair noma downlink system," *Journal of Information Communication Technologies and Robotic Applications*, pp. 73–79, 2018.

[18] M. Hussain, H. Shakir, and H. Rasheed, "Deep learning approaches for impulse noise mitigation and classification in noma-based systems," *IEEE Access*, vol. 9, pp. 143 836–143 846, 2021.

[19] M. Hussain and H. Rasheed, "Nonorthogonal multiple access for next-generation mobile networks: A technical aspect for research direction," *Wireless Communications and Mobile Computing*, vol. 2020, 2020.

[20] P. Wongchampa and M. Uthansakul, "Orthogonal beamforming for multiuser wireless communications: Achieving higher received signal strength and throughput than with conventional beamforming." *IEEE Antennas and Propagation Magazine*, vol. 59, no. 4, pp. 38–49, 2017.

[21] R. Addaci, K. Haneda, A. Diallo, P. Le Thuc, C. Luxey, R. Staraj, and P. Vainikainen, "Dual-band wlan multiantenna system and diversity/mimo performance evaluation," *IEEE transactions on antennas and propagation*, vol. 62, no. 3, pp. 1409–1415, 2013.

[22] P. Krishna, T. A. Kumar, and K. K. Rao, "Multiuser mimo systems: Spectral and energy efficiencies, estimations and capacity limits," in *2015 Twelfth International Conference on Wireless and Optical Communications Networks (WOCN)*. IEEE, 2015, pp. 1–6.

[23] P. J. Smith, P. A. Dmochowski, M. Chiani, and A. Giorgetti, "On the number of independent channels in multi-antenna systems," *IEEE transactions on wireless communications*, vol. 13, no. 1, pp. 75–85, 2013.

[24] P. Rayi, M. Prasad, and P. Kishore, "Modelling, simulation of multi-user grouping considering channel states in mimo systems," in *2015 International*

Conference on Signal Processing and Communication Engineering Systems. IEEE, 2015, pp. 231–235.

[25] O. Shmuel, A. Cohen, and O. Gurewitz, "Performance analysis of opportunistic distributed scheduling in multi-user systems," *IEEE Transactions on Communications*, vol. 66, no. 10, pp. 4637–4652, 2018.

[26] M. Maros and J. Jaldén, "Admm for distributed dynamic beamforming," *IEEE Transactions on Signal and Information Processing over Networks*, vol. 4, no. 2, pp. 220–235, 2017.

[27] E. Park, H. Kim, H. Park, and I. Lee, "Feedback bit allocation schemes for multi-user distributed antenna systems," *IEEE Communications Letters*, vol. 17, no. 1, pp. 99–102, 2012.

[28] P. Sriploy and M. Uthansakul, "Nonfeedback distributed beamforming using spatial-temporal extraction," *International Journal of Antennas and Propagation*, vol. 2016, 2016.

[29] A. Benjebbour, K. Saito, and Y. Kishiyama, "Experimental trials on non-orthogonal multiple access," in *Multiple Access Techniques for 5G Wireless Networks and Beyond*. Springer, 2019, pp. 587–607.

[30] H. Nikopour and H. Baligh, "Sparse code multiple access," in *2013 IEEE 24th Annual International Symposium on Personal, Indoor, and Mobile Radio Communications (PIMRC)*. IEEE, 2013, pp. 332–336.

[31] Z. Yuan, G. Yu, and W. Li, "Multi-user shared access for 5g," *Telecommun. Network Technology*, vol. 5, no. 5, pp. 28–30, 2015.

[32] R. Hoshyar, F. P. Wathan, and R. Tafazolli, "Novel low-density signature for synchronous cdma systems over awgn channel," *IEEE Transactions on Signal Processing*, vol. 56, no. 4, pp. 1616–1626, 2008.

[33] X. Dai, Z. Zhang, B. Bai, S. Chen, and S. Sun, "Pattern division multiple access: A new multiple access technology for 5g," *IEEE Wireless Communications*, vol. 25, no. 2, pp. 54–60, 2018.

[34] L. Dai, B. Wang, Z. Ding, Z. Wang, S. Chen, and L. Hanzo, "A survey of non-orthogonal multiple access for 5g," *IEEE Communications Surveys Tutorials*, vol. 20, no. 3, pp. 2294–2323, 2018.

[35] H. Tataria, M. Shafi, A. F. Molisch, M. Dohler, H. Sjöland, and F. Tufvesson, "6g wireless systems: Vision, requirements, challenges, insights, and opportunities," *Proceedings of the IEEE*, vol. 109, no. 7, pp. 1166–1199, 2021.

[36] A. Benjebbour, K. Saito, A. Li, Y. Kishiyama, and T. Nakamura, "Non-orthogonal multiple access (noma): Concept, performance evaluation and experimental trials," in *2015 International Conference on Wireless Networks and Mobile Communications (WINCOM)*. IEEE, 2015, pp. 1–6.

[37] J.-B. Kim, J. Lee, D. Kim, and Y. Choi, "System-level performance evaluation for non-orthogonal multiple access in coordinated direct and relay transmission," in *2017 International Conference on Information and Communication Technology Convergence (ICTC)*. IEEE, 2017, pp. 1296–1298.

[38] Z. Ding, P. Fan, and H. V. Poor, "Impact of user pairing on 5g nonorthogonal multiple-access downlink transmissions," *IEEE Transactions on Vehicular Technology*, vol. 65, no. 8, pp. 6010–6023, 2015.

[39] H. Xing, Y. Liu, A. Nallanathan, Z. Ding, and H. V. Poor, "Optimal throughput fairness tradeoffs for downlink non-orthogonal multiple access over fading channels," *IEEE Transactions on Wireless Communications*, vol. 17, no. 6, pp. 3556–3571, 2018.

[40] S. Arzykulov, T. A. Tsiftsis, G. Nauryzbayev, and M. Abdallah, "Outage performance of cooperative underlay cr-noma with imperfect csi," *IEEE Communications Letters*, vol. 23, no. 1, pp. 176–179, 2018.

[41] P. Yang, Y. Xiao, M. Xiao, and Z. Ma, "Noma-aided precoded spatial modulation for downlink mimo transmissions," *IEEE Journal of Selected Topics in Signal Processing*, vol. 13, no. 3, pp. 729–738, 2019.

[42] S. Li, S. Li, and Y. Sun, "Power allocation for full-duplex noma relaying based underlay d2d communications." *TIIS*, vol. 13, no. 1, pp. 16–33, 2019.

[43] A. Li, A. Benjebbour, X. Chen, H. Jiang, and H. Kayama, "Uplink non-orthogonal multiple access (noma) with single-carrier frequency division multiple access (sc-fdma) for 5g systems," *IEICE Transactions on Communications*, vol. 98, no. 8, pp. 1426–1435, 2015.

[44] B. Xia, J. Wang, K. Xiao, Y. Gao, Y. Yao, and S. Ma, "Outage performance analysis for the advanced sic receiver in wireless noma systems," *IEEE Transactions on Vehicular Technology*, vol. 67, no. 7, pp. 6711–6715, 2018.

[45] S. Riaz, J. Kim, and U. Park, "Evolutionary game theory-based power control for uplink noma." *KSII Transactions on Internet & Information Systems*, vol. 12, no. 6, 2018.

[46] B. Makki, K. Chitti, A. Behravan, and M.-S. Alouini, "A survey of noma: Current status and open research challenges," *IEEE Open Journal of the Communications Society*, vol. 1, pp. 179–189, 2020.

[47] H. Tabassum, E. Hossain, and J. Hossain, "Modeling and analysis of uplink non-orthogonal multiple access in large-scale cellular networks using poisson cluster processes," *IEEE Transactions on Communications*, vol. 65, no. 8, pp. 3555–3570, 2017.

[48] "Study on Non-Orthogonal Multiple Access (NOMA) for NR," 3GPP, Technical report (TR) TR38.812, June 2018, v0.3; Release 15.

[49] Z. Ding, M. Peng, and H. V. Poor, "Cooperative non-orthogonal multiple access in 5g systems," *IEEE Communications Letters*, vol. 19, no. 8, pp. 1462–1465, 2015.

[50] Z. Ding, F. Adachi, and H. V. Poor, "The application of mimo to non-orthogonal multiple access," *IEEE Transactions on Wireless Communications*, vol. 15, no. 1, pp. 537–552, 2015.

[51] Y. Sun, D. W. K. Ng, Z. Ding, and R. Schober, "Optimal joint power and

subcarrier allocation for full-duplex multicarrier non-orthogonal multiple access systems," *IEEE Transactions on Communications*, vol. 65, no. 3, pp. 1077–1091, 2017.

[52] F. Fang, H. Zhang, J. Cheng, and V. C. Leung, "Energy-efficient resource allocation for downlink non-orthogonal multiple access network," *IEEE Transactions on Communications*, vol. 64, no. 9, pp. 3722–3732, 2016.

[53] Y. Wu, S. Zhang, and Y. Chen, "Iterative multiuser receiver in sparse code multiple access systems," in *2015 IEEE International Conference on Communications (ICC)*. IEEE, 2015, pp. 2918–2923.

[54] C. Dong, G. Gao, K. Niu, and J. Lin, "An efficient scma codebook optimization algorithm based on mutual information maximization," *Wireless Communications and Mobile Computing*, vol. 2018, 2018.

[55] Y. Du, B. Dong, Z. Chen, J. Fang, and L. Yang, "Shuffled multiuser detection schemes for uplink sparse code multiple access systems," *IEEE Communications Letters*, vol. 20, no. 6, pp. 1231–1234, 2016.

[56] F. Wei and W. Chen, "Low complexity iterative receiver design for sparse code multiple access," *IEEE Transactions on Communications*, vol. 65, no. 2, pp. 621–634, 2016.

[57] J. Chen, Z. Zhang, S. He, J. Hu, and G. E. Sobelman, "Sparse code multiple access decoding based on a monte carlo markov chain method," *IEEE Signal Processing Letters*, vol. 23, no. 5, pp. 639–643, 2016.

[58] M. Moltafet, N. Mokari, M. R. Javan, H. Saeedi, and H. Pishro-Nik, "A new multiple access technique for 5g: Power domain sparse code multiple access (psma)," *IEEE Access*, vol. 6, pp. 747–759, 2017.

[59] Z. Yuan, C. Yan, Y. Yuan, and W. Li, "Blind multiple user detection for grant-free musa without reference signal," in *2017 IEEE 86th Vehicular Technology Conference (VTC-Fall)*. IEEE, 2017, pp. 1–5.

[60] Y. Xu, G. Wang, L. Zheng, R. Liu, and D. Zhao, "Ber performance evaluation

of downlink musa over rayleigh fading channel," in *International Conference on Machine Learning and Intelligent Communications*. Springer, 2017, pp. 85–94.

[61] R1-166404, "Receiver details and link performance for musa," *3GPPTSG RAN WG1 Meeting No. 86, Gothenbur*, vol. 86, pp. 22–26, August, 2016.

[62] N. Ye, H. Han, L. Zhao, and A.-h. Wang, "Uplink nonorthogonal multiple access technologies toward 5g: A survey," *Wireless Communications and Mobile Computing*, vol. 2018, 2018.

[63] W. Tang, S. Kang, and B. Ren, "Performance analysis of cooperative pattern division multiple access (co-pdma) in uplink network," *IEEE Access*, vol. 5, pp. 3860–3868, 2017.

[64] B. Ren, X. Yue, W. Tang, Y. Wang, S. Kang, X. Dai, and S. Sun, "Advanced idd receiver for pdma uplink system," in *2016 IEEE/CIC International Conference on Communications in China (ICCC)*. IEEE, 2016, pp. 1–6.

[65] D. Kong, J. Zeng, X. Su, L. Rong, and X. Xu, "Multiuser detection algorithm for pdma uplink system based on sic and mmse," in *2016 IEEE/CIC International Conference on Communications in China (ICCC)*. IEEE, 2016, pp. 1–5.

[66] J. Zeng, B. Liu, and X. Su, "Joint pattern assignment and power allocation in pdma," in *2017 IEEE 86th Vehicular Technology Conference (VTC-Fall)*. IEEE, 2017, pp. 1–5.

[67] B. Ren, Y. Wang, X. Dai, K. Niu, and W. Tang, "Pattern matrix design of pdma for 5g ul applications," *China Communications*, vol. 13, no. Supplement2, pp. 159–173, 2016.

[68] Y. Saito, Y. Kishiyama, A. Benjebbour, T. Nakamura, A. Li, and K. Higuchi, "Non-orthogonal multiple access (noma) for cellular future radio access," in *2013 IEEE 77th vehicular technology conference (VTC Spring)*. IEEE, 2013, pp. 1–5.

[69] A. Benjebbour, Y. Saito, Y. Kishiyama, A. Li, A. Harada, and T. Nakamura, "Concept and practical considerations of non-orthogonal multiple access (noma) for future radio access," in *2013 International Symposium on Intelligent Signal Processing and Communication Systems*. IEEE, 2013, pp. 770–774.

[70] X. Chen, A. Beiijebbour, A. Li, H. Jiang, and H. Kayama, "Consideration on successive interference canceller (sic) receiver at cell-edge users for non-orthogonal multiple access (noma) with su-mimo," in *2015 IEEE 26th Annual International Symposium on Personal, Indoor, and Mobile Radio Communications (PIMRC)*. IEEE, 2015, pp. 522–526.

[71] G. Gui, H. Sari, and E. Biglieri, "A new definition of fairness for non-orthogonal multiple access," *IEEE Communications Letters*, vol. 23, no. 7, pp. 1267–1271, 2019.

[72] B. Di, L. Song, and Y. Li, "Radio resource allocation for uplink sparse code multiple access (scma) networks using matching game," in *2016 IEEE International Conference on Communications (ICC)*. IEEE, 2016, pp. 1–6.

[73] S. Zhang, K. Xiao, B. Xiao, Z. Chen, B. Xia, D. Chen, and S. Ma, "A capacity-based codebook design method for sparse code multiple access systems," in *2016 8th International Conference on Wireless Communications & Signal Processing (WCSP)*. IEEE, 2016, pp. 1–5.

[74] Y. Zhou, H. Luo, R. Li, and J. Wang, "A dynamic states reduction message passing algorithm for sparse code multiple access," in *2016 Wireless Telecommunications Symposium (WTS)*. IEEE, 2016, pp. 1–5.

[75] K. Au, L. Zhang, H. Nikopour, E. Yi, A. Bayesteh, U. Vilaipornsawai, J. Ma, and P. Zhu, "Uplink contention based scma for 5g radio access," in *2014 IEEE Globecom workshops (GC wkshps)*. IEEE, 2014, pp. 900–905.

[76] Z. Yang, J. Cui, X. Lei, Z. Ding, P. Fan, and D. Chen, "Impact of factor

graph on average sum rate for uplink sparse code multiple access systems," *IEEE Access*, vol. 4, pp. 6585–6590, 2016.

[77] H. Kwon, J. Lee, and I. Kang, "Successive interference cancellation via rank-reduced maximum a posteriori detection," *IEEE transactions on communications*, vol. 61, no. 2, pp. 628–637, 2013.

[78] Z. Yuan, G. Yu, W. Li, Y. Yuan, X. Wang, and J. Xu, "Multi-user shared access for internet of things," in *2016 IEEE 83rd Vehicular Technology Conference (VTC Spring)*. IEEE, 2016, pp. 1–5.

[79] E. M. Eid, M. M. Fouda, A. S. T. Eldien, and M. M. Tantawy, "Performance analysis of musa with different spreading codes using ordered sic methods," in *2017 12th International Conference on Computer Engineering and Systems (ICCES)*. IEEE, 2017, pp. 101–106.

[80] X. Dai, "Successive interference cancellation amenable space–time codes with good multiplexing-diversity tradeoffs," *Wireless personal communications*, vol. 55, no. 4, pp. 645–654, 2010.

[81] X. Dai, S. Sun, and Y. Wang, "Reduced-complexity (quasi-) maximum-likelihood detectors with no performance degradation for s-qam modulated mimo systems," *Wireless Personal Communications*, vol. 66, no. 4, pp. 613–627, 2012.

[82] S. Chen, B. Ren, Q. Gao, S. Kang, S. Sun, and K. Niu, "Pattern division multiple access-a novel nonorthogonal multiple access for fifth-generation radio networks," *IEEE Transactions on Vehicular Technology*, vol. 66, no. 4, pp. 3185–3196, 2016.

[83] J. Zeng, D. Kong, X. Su, L. Rong, and X. Xu, "On the performance of pattern division multiple access in 5g systems," in *2016 8th International Conference on Wireless Communications & Signal Processing (WCSP)*. IEEE, 2016, pp. 1–5.

[84] Y. Tao, L. Liu, S. Liu, and Z. Zhang, "A survey: Several technologies of non-

orthogonal transmission for 5g," *China communications*, vol. 12, no. 10, pp. 1–15, 2015.

[85] K. Zheng, Y. Wang, L. Lei, and W. Wang, "Cross-layer queuing analysis on multihop relaying networks with adaptive modulation and coding," *IET communications*, vol. 4, no. 3, pp. 295–302, 2010.

[86] Y. Saito, A. Benjebbour, Y. Kishiyama, and T. Nakamura, "System-level performance evaluation of downlink non-orthogonal multiple access (noma)," in *2013 IEEE 24th Annual International Symposium on Personal, Indoor, and Mobile Radio Communications (PIMRC)*. IEEE, 2013, pp. 611–615.

[87] M. Al-Imari, P. Xiao, M. A. Imran, and R. Tafazolli, "Uplink non-orthogonal multiple access for 5g wireless networks," in *2014 11th international symposium on wireless communications systems (ISWCS)*. IEEE, 2014, pp. 781–785.

[88] I. Budhiraja, S. Tyagi, S. Tanwar, N. Kumar, and J. J. Rodrigues, "Tactile internet for smart communities in 5g: An insight for noma-based solutions," *IEEE Transactions on Industrial Informatics*, vol. 15, no. 5, pp. 3104–3112, 2019.

[89] I. Budhiraja, S. Tyagi, S. Tanwar, N. Kumar, and Rodrigues, "Diya: Tactile internet driven delay assessment noma-based scheme for d2d communication," *IEEE Transactions on Industrial Informatics*, vol. 15, no. 12, pp. 6354–6366, 2019.

[90] I. Budhiraja, S. Tyagi, S. Tanwar, N. Kumar, and M. Guizani, "Cross layer noma interference mitigation for femtocell users in 5g environment," *IEEE Transactions on Vehicular Technology*, vol. 68, no. 5, pp. 4721–4733, 2019.

[91] I. Budhiraja, S. Tyagi, S. Tanwar, N. Kumar, and N. Guizani, "subchannel assignment for swipt-noma based hetnet with imperfect channel state information," in *2019 15th International Wireless Communications & Mobile Computing Conference (IWCMC)*. IEEE, 2019, pp. 842–847.

[92] I. Budhiraja, S. Tyagi, S. Tanwar, N. Kumar, and M. Guizani, "Cr-noma

based interference mitigation scheme for 5g femtocells users," in *2018 IEEE Global Communications Conference (GLOBECOM)*. IEEE, 2018, pp. 1–6.

[93] X. HOU, W. LIU, J. LIU, X. WANG, L. CHEN, Y. KISHIYAMA, and T. ASAI, "Non-orthogonal physical layer (nophy) design towards 5g evolution and 6g," *IEICE Transactions on Communications*, p. 2021EBP3192, 2022.

[94] L. Dai, B. Wang, Z. Ding, Z. Wang, S. Chen, and L. Hanzo, "A survey of non-orthogonal multiple access for 5g," *IEEE communications surveys & tutorials*, vol. 20, no. 3, pp. 2294–2323, 2018.

[95] M. A. Albreem, "5g wireless communication systems: Vision and challenges," in *2015 International Conference on Computer, Communications, and Control Technology (I4CT)*. IEEE, 2015, pp. 493–497.

[96] F. Li, K.-Y. Lam, X. Li, Z. Sheng, J. Hua, and L. Wang, "Advances and emerging challenges in cognitive internet-of-things," *IEEE Transactions on Industrial Informatics*, vol. 16, no. 8, pp. 5489–5496, 2019.

[97] P. Kamalinejad, C. Mahapatra, Z. Sheng, S. Mirabbasi, V. C. Leung, and Y. L. Guan, "Wireless energy harvesting for the internet of things," *IEEE Communications Magazine*, vol. 53, no. 6, pp. 102–108, 2015.

[98] I. . W. Group *et al.*, "Ieee standard for wireless access in vehicular environments (wave) multi channel operation. ieee standards associations; new york, ny, usa: 2016," *IEEE Std*, pp. 1609–4.

[99] A. Ahamed and H. Vakilzadian, "Issues and challenges in vanet routing protocols," in *2018 IEEE international conference on electro/information technology (EIT)*. IEEE, 2018, pp. 0723–0728.

[100] K. B. Kelarestaghi, M. Foruhandeh, K. Heaslip, and R. Gerdes, "Survey on vehicular ad hoc networks and its access technologies security vulnerabilities and countermeasures," *arXiv preprint arXiv:1903.01541*, 2019.

[101] Y. Yabuuchi, D. Umehara, M. Morikura, T. Hisada, S. Ishiko, and S. Horihata,

"Measurement and analysis of impulsive noise on in-vehicle power lines," in *ISPLC2010*. IEEE, 2010, pp. 325–330.

[102] L. M. H. Shhab, A. Rizaner, A. H. Ulusoy, and H. Amca, "Impact of impulsive noise on millimeter wave cellular systems performance," in *2017 10th UK-Europe-China Workshop on Millimetre Waves and Terahertz Technologies (UCMMT)*. IEEE, 2017, pp. 1–4.

[103] P. Fan, J. Zhao, and I. Chih-Lin, "5g high mobility wireless communications: Challenges and solutions," *China Communications*, vol. 13, no. 2, pp. 1–13, 2016.

[104] S. Jaffry, R. Hussain, X. Gui, and S. F. Hasan, "A comprehensive survey on moving networks," *IEEE Communications Surveys & Tutorials*, 2020.

[105] G. W. Arnold, "Challenges and opportunities in smart grid: A position article," *Proceedings of the IEEE*, vol. 99, no. 6, pp. 922–927, 2011.

[106] H. Gözde, M. C. Taplamacıoğlu, M. Arı, and H. Shalaf, "4g/lte technology for smart grid communication infrastructure," in *2015 3rd International Istanbul Smart Grid Congress and Fair (ICSG)*. IEEE, 2015, pp. 1–4.

[107] O. Neagu and W. Hamouda, "Performance of smart grid communication in the presence of impulsive noise," in *2016 International Conference on Selected Topics in Mobile & Wireless Networking (MoWNeT)*. IEEE, 2016, pp. 1–5.

[108] M. H. Rehmani, M. Reisslein, A. Rachedi, M. Erol-Kantarci, and M. Radenkovic, "Integrating renewable energy resources into the smart grid: Recent developments in information and communication technologies," *IEEE Transactions on Industrial Informatics*, vol. 14, no. 7, pp. 2814–2825, 2018.

[109] Z. Fan, P. Kulkarni, S. Görmüs, C. Efthymiou, G. Kalogridis, M. Sooriyabandara, Z. Zhu, S. Lambotharan, and W. Chin, "Smart grid communications: Overview of research challenges, solutions, and standardization activities," *IEEE Communications Surveys & Tutorials*, vol. 15, pp. 21–38, 2013.

[110] V. C. Gungor, D. Sahin, T. Kocak, S. Ergut, C. Buccella, C. Cecati, and

G. P. Hancke, "Smart grid technologies: Communication technologies and standards," *IEEE transactions on Industrial informatics*, vol. 7, no. 4, pp. 529–539, 2011.

[111] L. de MBA Dib, V. Fernandes, M. d. L. Filomeno, and M. V. Ribeiro, "Hybrid plc/wireless communication for smart grids and internet of things applications," *IEEE internet of things Journal*, vol. 5, no. 2, pp. 655–667, 2017.

[112] S. Galli, A. Scaglione, and Z. Wang, "For the grid and through the grid: The role of power line communications in the smart grid," *Proceedings of the IEEE*, vol. 99, no. 6, pp. 998–1027, 2011.

[113] K. M. Rabie and E. Alsusae, "On improving communication robustness in plc systems for more reliable smart grid applications," *IEEE Transactions on Smart Grid*, vol. 6, no. 6, pp. 2746–2756, 2015.

[114] F. Khan, A. ur Rehman, M. Arif, M. Aftab, and B. K. Jadoon, "A survey of communication technologies for smart grid connectivity," in *2016 International Conference on Computing, Electronic and Electrical Engineering (ICE Cube)*. IEEE, 2016, pp. 256–261.

[115] P. Yi, A. Iwayemi, and C. Zhou, "Developing zigbee deployment guideline under wifi interference for smart grid applications," *IEEE transactions on smart grid*, vol. 2, no. 1, pp. 110–120, 2010.

[116] R. Merritt, "Bluetooth group explores apps in smart grid," 2011.

[117] P. P. Parikh, M. G. Kanabar, and T. S. Sidhu, "Opportunities and challenges of wireless communication technologies for smart grid applications," in *IEEE PES General Meeting*. IEEE, 2010, pp. 1–7.

[118] J. Brown and J. Y. Khan, "Performance comparison of lte fdd and tdd based smart grid communications networks for uplink biased traffic," in *2012 IEEE Third International Conference on Smart Grid Communications (SmartGridComm)*. IEEE, 2012, pp. 276–281.

[119] A. Meloni and L. Atzori, "The role of satellite communications in the smart grid," *IEEE Wireless Communications*, vol. 24, no. 2, pp. 50–56, 2017.

[120] A. Laya, K. Wang, A. A. Widaa, J. Alonso-Zarate, J. Markendahl, and L. Alonso, "Device-to-device communications and small cells: enabling spectrum reuse for dense networks," *IEEE Wireless Communications*, vol. 21, no. 4, pp. 98–105, 2014.

[121] B. Holfeld, S. Jaeckel, L. Thiele, T. Wirth, and K. Scheppelmann, "Smart grid communications: Lte outdoor field trials at 450 mhz," in *2015 IEEE 81st Vehicular Technology Conference (VTC Spring)*. IEEE, 2015, pp. 1–5.

[122] E. Shafter, A. Noorwali, and R. K. Rao, "Ofdm systems with cpm mappers for smart grid applications," in *2015 IEEE Electrical Power and Energy Conference (EPEC)*. IEEE, 2015, pp. 424–428.

[123] A. Maneerung, S. Sittichivapak, and K. Hongesombut, "Application of power line communication with ofdm to smart grid system," in *2011 Eighth International Conference on Fuzzy Systems and Knowledge Discovery (FSKD)*, vol. 4. IEEE, 2011, pp. 2239–2244.

[124] G. Al-Juboori, A. Doufexi, and A. R. Nix, "Feasibility study of ofdm-mfsk modulation scheme for smart metering technology," in *2017 IEEE PES Innovative Smart Grid Technologies Conference Europe (ISGT-Europe)*. IEEE, 2017, pp. 1–6.

[125] C. Müller, M. Putzke, and C. Wietfeld, "Traffic engineering analysis of smart grid services in cellular networks," in *2012 IEEE Third International Conference on Smart Grid Communications (SmartGridComm)*. IEEE, 2012, pp. 252–257.

[126] G. C. Madueno, Č. Stefanović, and P. Popovski, "Reengineering gsm/gprs towards a dedicated network for massive smart metering," in *2014 IEEE International Conference on Smart Grid Communications (SmartGridComm)*. IEEE, 2014, pp. 338–343.

[127] F. Aalamifar and L. Lampe, "Optimized wimax profile configuration for smart grid communications," *IEEE Transactions on Smart Grid*, vol. 8, no. 6, pp. 2723–2732, 2016.

[128] C.-C. Tseng, L. Wang, and C.-H. Kuo, "Application of hybrid mixing cdma/idma/ocdma/oidma for smart grid integration of renewable-energy resources," in *2016 International Symposium on Computer, Consumer and Control (IS3C)*. IEEE, 2016, pp. 878–882.

[129] N. Alamatsaz, A. Boustani, M. Jadliwala, and V. Namboodiri, "Agsec: Secure and efficient cdma-based aggregation for smart metering systems," in *2014 IEEE 11th Consumer Communications and Networking Conference (CCNC)*. IEEE, 2014, pp. 489–494.

[130] M. Jaradat, M. Jarrah, A. Bousselham, Y. Jararweh, and M. Al-Ayyoub, "The internet of energy: smart sensor networks and big data management for smart grid," 2015.

[131] A. Balcı and R. Sokullu, "Massive connectivity with machine learning for the internet of things," *Computer Networks*, p. 107646, 2020.

[132] C. Yan, A. Harada, A. Benjebbour, Y. Lan, A. Li, and H. Jiang, "Receiver design for downlink non-orthogonal multiple access (noma)," in *2015 IEEE 81st vehicular technology conference (VTC Spring)*. IEEE, 2015, pp. 1–6.

[133] X. Song, L. Dong, J. Wang, L. Qin, and X. Han, "Energy efficient power allocation for downlink noma heterogeneous networks with imperfect csi," *IEEE Access*, vol. 7, pp. 39 329–39 340, 2019.

[134] S. Hu, X. Chen, W. Ni, X. Wang, and E. Hossain, "Modeling and analysis of energy harvesting and smart grid-powered wireless communication networks: A contemporary survey," *IEEE Transactions on Green Communications and Networking*, vol. 4, no. 2, pp. 461–496, 2020.

[135] A. Dubey, R. K. Mallik, and R. Schober, "Performance of a plc system in im-

pulsive noise with selection combining," in *2012 IEEE Global Communications Conference (GLOBECOM)*. IEEE, 2012, pp. 3508–3512.

[136] A. Dubey, D. Sharma, R. K. Mallik, and S. Mishra, "Modeling and performance analysis of a plc system in presence of impulsive noise," in *2015 IEEE Power & Energy Society General Meeting*. IEEE, 2015, pp. 1–5.

[137] S. Prakash, A. Bansal, and S. K. Jha, "Performance analysis of narrowband plc system under gaussian laplacian noise model," in *2016 International Conference on Electrical, Electronics, and Optimization Techniques (ICEEOT)*. IEEE, 2016, pp. 3597–3600.

[138] S. Niranjayan and N. C. Beaulieu, "Analysis of wireless communication systems in the presence of non-gaussian impulsive noise and gaussian noise," in *2010 IEEE Wireless Communication and Networking Conference*. IEEE, 2010, pp. 1–6.

[139] S. Habib and A. Haque, "Impulsive noise mitigation in wireless communication systems using emd technique," in *2012 7th International Conference on Electrical and Computer Engineering*. IEEE, 2012, pp. 291–294.

[140] J. Zheng, D. W. Gao, and L. Lin, "Smart meters in smart grid: An overview," in *2013 IEEE Green Technologies Conference (GreenTech)*. IEEE, 2013, pp. 57–64.

[141] A. Bodonyi, "Effects of impulse noise on digital data transmission," *IRE Transactions on Communications Systems*, vol. 9, no. 4, pp. 355–361, 1961.

[142] K. S. Al-Mawali, A. Z. Sadik, Z. M. Hussain *et al.*, "Time-domain techniques for impulsive noise reduction in ofdm-based power line communications: a comparative study," in *International Conference on Communication, Computer and Power (ICCCP 2009)*, 2009, pp. 368–372.

[143] B. Selim, M. S. Alam, J. V. Evangelista, G. Kaddoum, and B. L. Agba, "Noma-based iot networks: impulsive noise effects and mitigation," *IEEE Communications Magazine*, vol. 58, no. 11, pp. 69–75, 2020.

[144] C.-H. Yih, "Iterative interference cancellation for ofdm signals with blanking nonlinearity in impulsive noise channels," *IEEE Signal Processing Letters*, vol. 19, no. 3, pp. 147–150, 2012.

[145] D.-F. Tseng, Y. S. Han, W. H. Mow, L.-C. Chang, and A. H. Vinck, "Robust clipping for ofdm transmissions over memoryless impulsive noise channels," *IEEE Communications Letters*, vol. 16, no. 7, pp. 1110–1113, 2012.

[146] N. Rožić, P. Banelli, D. Begušić, and J. Radić, "Multiple-threshold estimators for impulsive noise suppression in multicarrier communications," *IEEE Transactions on Signal Processing*, vol. 66, no. 6, pp. 1619–1633, 2018.

[147] G. Ndo, P. Siohan, and M.-H. Hamon, "Adaptive noise mitigation in impulsive environment: Application to power-line communications," *IEEE Transactions on Power Delivery*, vol. 25, no. 2, pp. 647–656, 2010.

[148] H. Oh and H. Nam, "Design and performance analysis of nonlinearity preprocessors in an impulsive noise environment," *IEEE Transactions on Vehicular Technology*, vol. 66, no. 1, pp. 364–376, 2016.

[149] R. Barazideh, B. Natarajan, A. V. Nikitin, and R. L. Davidchack, "Performance of analog nonlinear filtering for impulsive noise mitigation in ofdm-based plc systems," in *2017 IEEE 9th Latin-American Conference on Communications (LATINCOM)*. IEEE, 2017, pp. 1–6.

[150] R. Barazideh, A. V. Nikitin, and B. Natarajan, "Practical implementation of adaptive analog nonlinear filtering for impulsive noise mitigation," in *2018 IEEE International Conference on Communications (ICC)*. IEEE, 2018, pp. 1–7.

[151] R. Barazideh, B. Natarajan, A. V. Nikitin, and S. Niknam, "Performance analysis of analog intermittently nonlinear filter in the presence of impulsive noise," *IEEE Transactions on Vehicular Technology*, vol. 68, no. 4, pp. 3565–3573, 2019.

[152] R. Barazideh, S. Niknam, B. Natarajan, and A. V. Nikitin, "Intermittently

nonlinear impulsive noise mitigation and doppler shift compensation in uwa-ofdm systems," *IEEE Access*, vol. 7, pp. 36 590–36 599, 2019.

[153] K. Al-Mawali, A. Z. Sadik, and Z. M. Hussain, "Joint time-domain/frequency-domain impulsive noise reduction in ofdm-based power line communications," in *2008 Australasian Telecommunication Networks and Applications Conference*. IEEE, 2008, pp. 138–142.

[154] R. Amiri, H. Mehrpouyan, D. Matolak, and M. Elkashlan, "Joint power allocation in interference-limited networks via distributed coordinated learning," in *2018 IEEE 88th Vehicular Technology Conference (VTC-Fall)*. IEEE, 2018, pp. 1–5.

[155] R. Barazideh, S. Niknam, and B. Natarajan, "Impulsive noise detection in ofdm-based systems: a deep learning perspective," in *2019 IEEE 9th Annual Computing and Communication Workshop and Conference (CCWC)*. IEEE, 2019, pp. 0937–0942.

[156] G. Kaliraj and S. Baskar, "An efficient approach for the removal of impulse noise from the corrupted image using neural network based impulse detector," *Image and Vision Computing*, vol. 28, no. 3, pp. 458–466, 2010.

[157] H. Purwins, B. Li, T. Virtanen, J. Schlüter, S.-Y. Chang, and T. Sainath, "Deep learning for audio signal processing," *IEEE Journal of Selected Topics in Signal Processing*, vol. 13, no. 2, pp. 206–219, 2019.

[158] R. Amiri, H. Mehrpouyan, L. Fridman, R. K. Mallik, A. Nallanathan, and D. Matolak, "A machine learning approach for power allocation in hetnets considering qos," in *2018 IEEE International Conference on Communications (ICC)*. IEEE, 2018, pp. 1–7.

[159] Y. Zhou, Q.-h. Tang, and W.-d. Jin, "Adaptive fuzzy median filter for images corrupted by impulse noise," in *2008 Congress on Image and Signal Processing*, vol. 3. IEEE, 2008, pp. 265–269.

[160] L. Ying-hui, G. Kun, and N. Guo-qiang, "An improved trilateral filter for

gaussian and impulse noise removal," in *2010 The 2nd International Conference on Industrial Mechatronics and Automation*, vol. 2. IEEE, 2010, pp. 385–388.

[161] M. Taherzadeh, H. Nikopour, A. Bayesteh, and H. Baligh, "Scma codebook design," in *2014 IEEE 80th Vehicular Technology Conference (VTC2014-Fall)*. IEEE, 2014, pp. 1–5.

[162] X. Dai, S. Chen, S. Sun, S. Kang, Y. Wang, Z. Shen, and J. Xu, "Successive interference cancelation amenable multiple access (sama) for future wireless communications," in *2014 IEEE International Conference on Communication Systems*. IEEE, 2014, pp. 222–226.

[163] N. Instruments, "3gpp release 15 overview," Sep 6, 2018. [Online]. Available: https://spectrum.ieee.org/3gpp-release-15-overview

[164] A. Alkhateeb and R. W. Heath, "Gram schmidt based greedy hybrid precoding for frequency selective millimeter wave mimo systems," in *2016 IEEE International Conference on Acoustics, Speech and Signal Processing (ICASSP)*. IEEE, 2016, pp. 3396–3400.

[165] K. Matsumura and T. Ohtsuki, "Orthogonal beamforming using gram-schmidt orthogonalization for multi-user mimo downlink system," *Eurasip journal on wireless communications and networking*, vol. 2011, no. 1, pp. 1–10, 2011.

[166] M. Zimmermann, *Energieverteilnetze als Zugangsmedium für Telekommunikationsdienste*. Shaker, 2000.

[167] T. Manglayev, R. C. Kizilirmak, and Y. H. Kho, "Comparison of parallel and successive interference cancellation for non-orthogonal multiple access," in *2018 International Conference on Computing and Network Communications (CoCoNet)*. IEEE, 2018, pp. 74–77.

[168] L. Lei, D. Yuan, C. K. Ho, and S. Sun, "Power and channel allocation for non-orthogonal multiple access in 5g systems: Tractability and computation,"

IEEE Transactions on Wireless Communications, vol. 15, no. 12, pp. 8580–8594, 2016.

[169] P. Liu, K.-K. R. Choo, L. Wang, and F. Huang, "Svm or deep learning? a comparative study on remote sensing image classification," *Soft Computing*, vol. 21, no. 23, pp. 7053–7065, 2017.

[170] H. Tao and X. Lu, "On comparing six optimization algorithms for network-based wind speed forecasting," in *2018 37th Chinese Control Conference (CCC)*. IEEE, 2018, pp. 8843–8850.

[171] W. Boulila, M. Driss, E. Alshanqiti, M. Al-Sarem, F. Saeed, and M. Krichen, "Weight initialization techniques for deep learning algorithms in remote sensing: Recent trends and future perspectives," *Advances on Smart and Soft Computing*, pp. 477–484, 2022.

[172] P. Nanda and N. Duraipandian, "An efficient algorithm for multi class classification in deep neural network," in *IoT Based Control Networks and Intelligent Systems*. Springer, 2023, pp. 381–394.